National University of Lesotho

Integration of solar heating systems in the textile industry: A case study for Vishan Clothing Laundry

Litheba Catherine Leseeka 201401302

A dissertation submitted in partial fulfilment of
the requirements for the degree of

Master of Science in Sustainable Energy

Offered by the

Energy Research Centre
Faculty of Science & Technology

1

Table of Contents

List of figures

List of tables

ABSTRACT

Currently, fossil fuels are the mostly used source of thermal energy in the industrial sector in Lesotho. They provide the necessary heat for different industrial processes across a range of temperatures. Within the sector, the textile industry is a significant consumer of thermal energy, particularly for the wetting processes that require large amounts of hot water. As global concerns about climate change and global warming intensify, industries are required to reduce their carbon footprint and transition to cleaner and sustainable energy sources. This study investigated the techno-economic viability of integrating solar water heating systems at the Vishan Clothing Laundry facility in Maseru, Lesotho, using T*SOL simulation software. The study focused on three main points: solar thermal system design, performance analysis and evaluating the economic aspects of the proposed system. To determine the most efficient system for meeting the laundry's hot water needs, six separate simulations were conducted for a comprehensive comparative analysis. From the simulations, the optimally designed system consists of Dimas SA RADIANT RSV 25 flat-plate collectors at 30° inclination angle with a collector area of 1,980 m^2 and a storage tank with a capacity of 130 m^3. This configuration achieves an efficiency of 54%, and a solar fraction of 89%, indicating a significant contribution from solar energy to the overall hot water production. The economic analysis under two different financing approaches shows that the system is economically viable. The proposed system under equity financing has a capital return time of 7 years, a positive net present value (NPV) of M 13,981,755, an internal rate of return (IRR) at 16.88% and cost of solar energy at M 0.831/kWh. Under equity-debt financing, the proposed system has a capital return time of 7.9 years, and amortization period of 10.3 years, a positive NPV of M 12,983,854, an IRR at 18.78% and cost of solar energy at M 0.872/kWh. These financial indicators demonstrate the economic feasibility and potential profitability of integrating solar heating systems in the textile industry. The study further highlights the need for further research to refine the system design and improve its performance. Most importantly, the study emphasizes the necessity of conducting in-depth energy audits to accurately determine the thermal energy demand of the

facility. Such audits can probably provide more precise data, ensuring that the designed system can adequately meet the thermal energy demand of the laundry facility.

1 INTRODUCTION

1.1 Background

The industrial sector is a major global energy consumer, accounting for approximately 166 exajoules (EJ) of energy, which represents 37% of the world's total energy consumption of 442 EJ [1]. Within the industrial sector, fossil fuels dominate the energy mix, contributing to 65% of the energy consumed, as shown in Figure 1 [1]. The energy consumption in industries is primarily driven by the need for heat generation, with temperatures often reaching up to 500°C. Notably, the energy demand for heating in industrial processes is approximately three times greater than the demand for electricity [2]. To fulfil the demand, traditional heating methods are still used, which rely heavily on fossil fuels, such as coal, oil, and natural gas, contributing to air pollution and climate change [3]. In 2022, the industrial sector was directly responsible for emitting 9.0 gigatonnes (Gt) of CO_2 [4]. The figure represents around 25% of the global CO_2 emissions associated with energy systems [4].

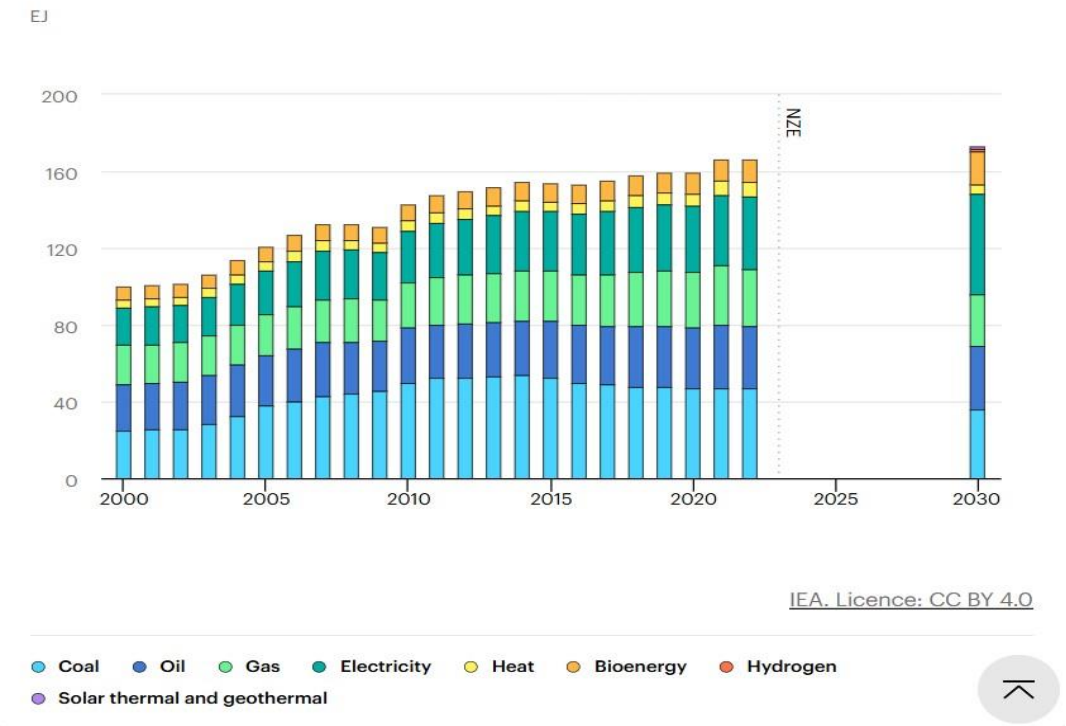

Figure 1: Industrial energy consumption by fuel [4]

A significant number of industrial processes need thermal energy within the temperature range of 50 to 500 °C [5]. To generate these temperatures, fossil fuels have commonly been used resulting in substantial greenhouse gas emissions [6]. Approximately 66.66% of the total

industrial energy demand pertains to heat energy, and, roughly 75% of this required heat energy is for industrial processes operating at temperatures below 400 °C [7]. Forecasts show that global industrial thermal energy demand is expected to increase by approximately 40% from its current level of 2250 Mtoe, which presently constitutes around 20% of global energy demand, to reach 3250 Mtoe by 2040 [7]. The demand for heat can be categorized according to the desired temperature levels: roughly 50% of the demand is for high-temperature heat (exceeding 400 °C), while approximately 25% is for medium-temperature heat (ranging from 100 to 400 °C), and the remaining 25% is for low-temperature heat (below 100 °C) [7]. According to the International Renewable Energy Agency (IRENA), most of the heating requirements for industrial purposes, specifically about 60%, fall below 250 °C and can be met using solar thermal energy. Thermal energy can be delivered in various forms, such as hot water, hot air, or hot steam [8].

The textile industry is one of the industries within the industrial sector. The textile industry, like many other industries, consumes a significant amount of electricity and fossil fuels [9]. However, the amount of energy consumed depends on the structure of the industry in each particular country [10]. It is expected that the demand for textiles in the coming years will increase, thus indicating an increase in energy demand [11]. Electrical energy in the industry is mostly used in cutting, weaving, air conditioning, lighting, and humidification, while heat energy is used in wet processes, steam production, and ironing, as shown in Figure 2. The share of electricity and fuels within the total final energy use of any one country's textile sector depends on the structure of the textile industry in that country [9], [12].

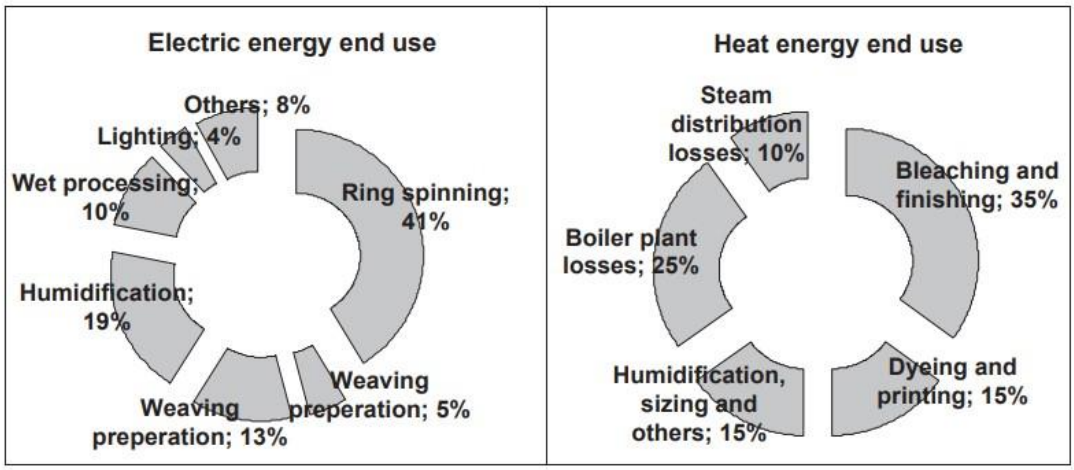

Figure 2: Electrical energy and heat energy use in the textile industry [9].

1.2 Textile industry in Lesotho

The textile industry in Lesotho serves as the largest employer within the nation's private sector, employing more than 33964 people as of December 2022 [13]. The industry is the largest

women employer, accounting for 80% of the total employees [14]. However, this current level of employment fell short of its peak in early 2003, when it reached approximately 54,000 workers [15]. There are 41 apparel firms in the country, and they produce approximately 90 million knitted garments and 26 million pairs of jeans [16]. The industry is set in two main areas, Maseru and Maputsoe. The Maseru industrial areas are at Maseru West, Tikoe and Thetsane, while the Maputsoe industrial areas include Maputsoe and Nyenye. The textile firms in Maseru are mostly Taiwanese-owned, while most of the ones in Maputsoe are South Africanowned [17].

With the implementation of the African Growth and Opportunity Act (AGOA), there was a rapid expansion in both the apparel and textile sectors, leading to significant growth in Lesotho's manufacturing industry. The sector growth rate increased from 17.7% in 2000 to 29.7% in 2002, with the textiles industry alone contributing 83% of the total exports during that year [18]. Lesotho became the top exporter to the United States under AGOA, and in 2016, the estimated total value of AGOA imports from Lesotho to the United States exceeded $295 million [18].

However, after the phase-out of the Multi-Fibre Arrangement (MFA) in 2005, which removed quantitative restrictions on imports from textile-producing countries such as India and China, the industry faced significant challenges. As a result, this led to some buyers seeking cheaper suppliers in China, resulting in the cancellation or reduction of the orders from Lesotho [19]. The global financial crisis of 2008 also added to the industry's difficulties [15].

Despite the challenges, the manufacturing sector in Lesotho grew by 34% between 2014 and 2019, primarily due to the threefold increase in textile and apparel exports to South Africa, helping to compensate for the decline in exports to the United States [14]. However, the COVID-19 pandemic further increased the decline in employment. According to a report by the Lesotho National Development Corporation, nine firms closed, resulting in the loss of 10,056 jobs [20].

1.3 Problem Statement

Considering these challenges, it becomes critical to examine specific operations within the textile industry to identify the areas for potential improvement. This study focused on the Vishan Clothing laundry facility. The laundry facility specialises in the wetting processes necessary for the final finishing of denim products. The wetting processes use a lot of hot water, which is essential for achieving the desired fabric properties. To heat the required hot water, the laundry facility uses a boiler system which burns fossil fuels to produce steam. The steam

is then used to heat the water to a certain temperature for the wetting processes. The use and reliance on fossil fuels for steam production highlights how energy intensive these processes are and points to potential areas for improving the energy efficiency and sustainability within the textile industry. The combustion of fossil fuels releases large amounts of carbon dioxide into the atmosphere, which is the primary contributor to global warming and the severe climate change challenges that the world currently faces. As the urgency to address climate change grows, industries across the globe are under immense pressure to reduce their carbon footprints and transition to more sustainable and cleaner energy sources.

1.4 Research questions

Following the challenges faced in the industry, the study will be based on the following questions:

- How will the integration of solar heating systems in industries affect energy consumption and carbon emissions?
- What are the economic and technical benefits of integrating solar heating systems in industries?
- How will the integration of solar heating systems impact the production output in industrial settings?

1.5 Research objectives

The objectives of the study are:

- To determine the energy and environmental benefits of implementing solar heating systems in industries by comparing energy consumption and greenhouse gas emissions with traditional heating methods.
- To design a solar heating system suitable to meet most of the energy demand
- To conduct a performance analysis of the designed system
- To perform an economic analysis of the designed system

1.6 Justification

The integration of solar heating systems in industries offers a great number of benefits, and Lesotho has abundant solar radiation to support the solar energy integration. There are more than 300 sunny days, and annual average irradiation levels range between 5.25 – 5.53 kWh/m^2. There are places in the Southwestern part of the country that experience average solar

irradiation of 7.2 kWh/m^2 [21]. The maximum radiation is experienced during December and January [22]. One of the benefits is the reduction of carbon emissions and environmental pollution. Solar heating systems provide a clean and renewable energy source, which contributes to climate change mitigation efforts by decreasing the reliance on fossil fuels. This transition to renewable energy sources enhances the energy security of the industries, making them less susceptible to fluctuations in coal prices and other fossil fuel markets.

Additionally, the reduced reliance on fossil fuels translates into substantial energy cost savings. This cost reduction may help industries to remain competitive and financially viable in the long term. By lowering operational costs, industries can increase their profit margins, which supports business growth and sustainability. Moreover, these savings can be reinvested into further improving the processes, adopting new technologies, or expanding operations, thereby creating more job opportunities. The adoption of solar heating systems aligns industries with sustainable practices, demonstrating a commitment to environmental stewardship and corporate social responsibility. This alignment not only enhances the industry's reputation but also attracts environmentally conscious consumers and investors.

By embracing renewable energy solutions, industries can tap into new markets and partnerships, further driving innovation and economic growth. Furthermore, the widespread adoption of solar heating systems can have a positive impact on the national economy. As industries become more energy-efficient and sustainable, the overall demand for fossil fuels decreases, leading to a reduction in the country's carbon footprint. This shift can also reduce the unemployment rate, as the growth and expansion of renewable energy industries create new job opportunities in manufacturing, installation, maintenance, research and development.

1.7 Report structure

The structure of the report is as follows: Chapter 1 provides the introduction to the study, setting the context and objectives. Chapter 2 is the literature review. It reviews the existing literature on industrial process heating and solar thermal systems for industrial applications and identifies the research gap within these topics. Chapter 3 outlines the present study research methodology, detailing the steps taken to carry out the study research process and objectives. Chapter 4 presents the results and discussion of the study, interpreting the findings of the study in detail. Chapter 5 concludes the report, summarizing the study findings, offering some recommendations, and highlighting the study's limitations.

2 LITERATURE REVIEW

2.1 Overview

This literature review explores the existing literature on the supply of thermal energy to industrial processes. The use of solar energy for thermal heating is then discussed, covering the basics while also giving an overview of how they work and their various components. The chapter also covers the literature on how solar thermal energy can be used and integrated into process heating.

2.2 Process heating systems in industries

The energy required for process heating is mainly sourced from a combination of electricity, steam, and various fuels, including natural gas, coal, biomass, and fuel oils [23]. Industrial process heating is viewed as the transfer of heat from a heat source to a substance [24]. Depending on the industrial process and the application, process heating is provided by different means [25]. The temperatures used in process heating also vary between low (≤ 150 °C), medium (≤ 400 °C), and high temperatures (≥ 400 °C) [26]. Process heating systems can be categorized into three main types: combustion-based process heating, electric process heating, and steam-based process heating. However, among these types, combustion and steam-based process heating systems are mostly used across different industrial applications due to the cost-effectiveness of their energy sources, particularly fossil fuels, high energy output and versatility. Figure 3 shows a typical process heating system used in industrial process heating.

In many industrial processes, it is important to use an enclosure to separate the heating process from the external environment [25]. The primary functions of this enclosure are diverse and important for the efficiency and safety of the process. Firstly, the enclosure serves to contain various types of radiation, such as microwave or infrared radiation, ensuring that these forms of energy are directed towards the material being processed rather than escaping into the surrounding environment [25]. This containment is crucial for maintaining the effectiveness of the heating process and protecting both equipment and personnel from potentially harmful radiation. Additionally, the enclosure plays a key role in confining combustion gases and volatile substances generated during the heating process. By trapping these by-products within the enclosure, it prevents their release into the environment, which could otherwise pose safety risks or lead to environmental pollution [27]. The enclosure also ensures that the material being processed remains contained within a controlled environment [25]. This containment is important for maintaining the consistency and quality of the material, as well as preventing contamination from external sources. Another critical function of the enclosure is to regulate the atmosphere around the material. This includes controlling factors such as temperature,

humidity, and gas composition, which can significantly impact the outcome of the heating process [28].

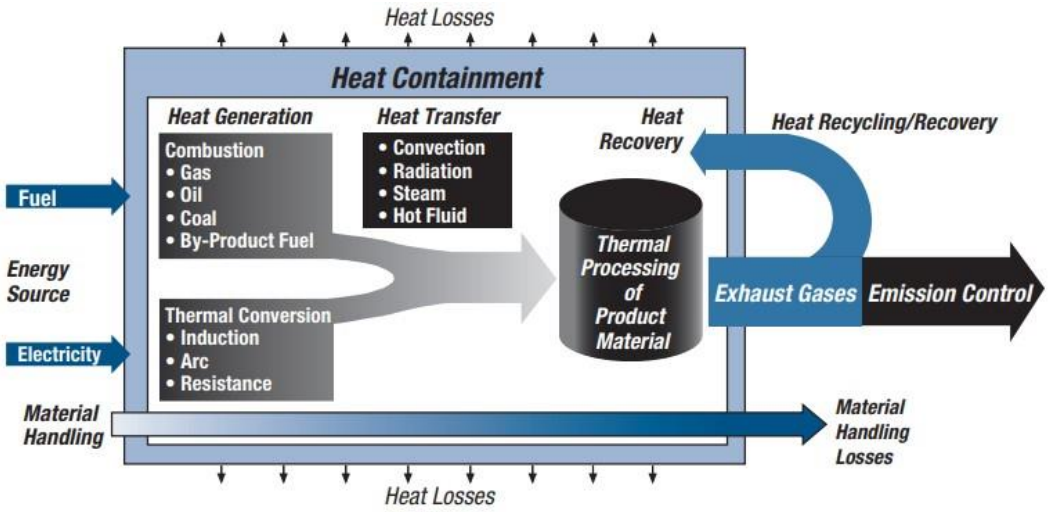

Figure 3: Typical Process Heating system [27]

2.2.1 Combustion-based process heating system

In combustion-based process heating, heat is generated through fuel combustion and subsequently transferred to the material undergoing treatment. Commonly used fuels in the combustion-based process heating include fossil fuels and biomass [28], [29]. The generated heat can be transferred either directly or indirectly to the material through conduction, convection or radiation [25]. The heat transferred to the material being processed is calculated using Equation 1.

$$Q = mc_p\Delta T \qquad \text{Equation 1}$$

Where; m- mass flowrate of the material (kg/s),

C_p- the specific heat capacity of the material (J/kg·K), and ΔT- the change in temperature (K).

In direct heating, combustion products, such as flue gases, come into contact with the materials being treated. An example of a direct heating system is a rotary kiln, as shown in Figure 4. A rotary kiln is used in cement production where required temperatures can be as high as 2000 °C [26]. The rotary kiln functions on the principle that the mass flow rate of the inputs, such as raw materials and fuel, is balanced with the mass flow rate of the outputs, which includes the produced cement and exhaust gases [28]. This mass balance is represented mathematically by the mass rate balance equation in Equation 2. In addition to maintaining a mass balance, the rotary kiln also adheres to the principles of energy conservation. This is important for ensuring

that the energy input, primarily from the combustion of fuel, is effectively converted into the thermal energy required for cement production [30]. The energy rate balance, which quantifies this energy conversion process, is outlined in Equation 5. The efficiency of the rotary kiln system is another critical factor. System efficiency is a measure of how effectively the input energy is utilized in the heating process [31]. This efficiency is calculated using **Error! Reference source not found.**Equation 6.

$$\sum \dot{m}_{in} = \sum \dot{m}_{out} \quad \text{Equation 2}$$

Where;

$\dot{m}_{in}$ - mass flowrate of the input materials for combustion $\dot{m}_{out}$

- mass flowrate of the output products

Where;

$$\sum \dot{m}_{in} = \dot{m}_{air} + \dot{m}_{fuel} + \dot{m}_{raw} \quad \text{Equation 3}$$

$$\sum \dot{m}_{out} = \dot{m}_{clinker} + \dot{m}_{dust} + \dot{m}_{gases} \quad \text{Equation 4}$$

$$\sum E_{in} = \sum E_{out} + Q_l \quad \text{Equation 5}$$

Where;

$\sum E_{in}$ -energy input

$\sum E_{out}$ -energy out

Q_l - losses during the energy conversion.

$$System\ efficiency = \frac{Energy\ in\ products\ output}{Energy\ input} = 1 - \frac{Energy\ loss}{Energy\ inputs} \quad \text{Equation 6}$$

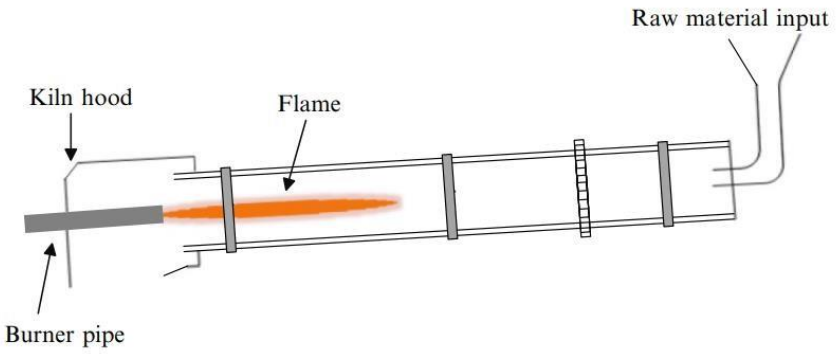

Figure 4: Rotary kiln *[28]*

In indirect heating, the heat generated from fuel combustion is transferred to the material by a heat exchanger [28]. A typical example of such system is a radiant burner tube as shown in Figure 5, it is used in heating a furnace in order not to contaminate the furnace environment with the combustion products [24]. It is used in temperature ranges of 815 °C to 1315 °C.

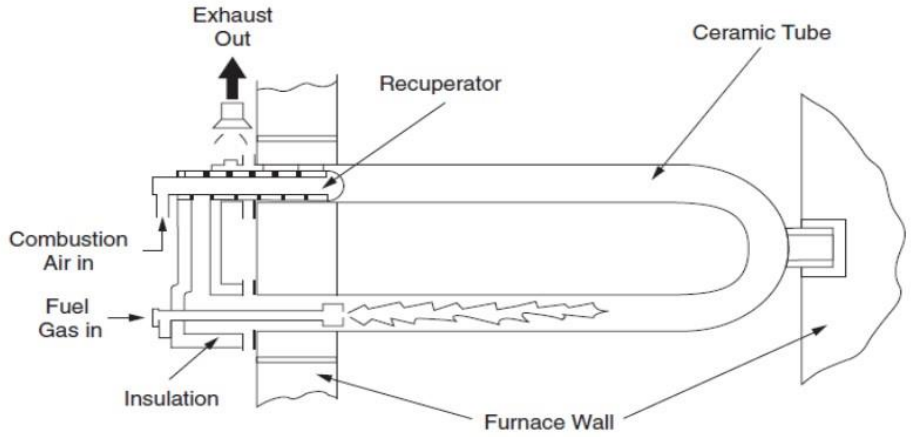

Figure 5: Radiant tube burner [32]

2.2.2 Steam based process heating system

In steam-based process heating, steam supplies the process heat [29]. The steam generated is distributed through pipes to the process, as shown in Figure 6. Steam based process heating is used in food processing, brewery and textile industries, as most of the processes in this sector require temperatures below 200 °C [33]. Steam is supplied directly or indirectly. In direct heating systems, steam is injected into the liquids or gases within the process (steam sparging). In the case of indirect heating systems, a heat exchanger is used, where steam is cooled and condensed within the tubes; the resulting heated tubes transfer heat to the liquids and gases [34]. Steam is produced using boilers, fuelled by the combustion of coal, furnace oil, or, more recently, low sulphur heavy stock oil, which is obtainable from refineries. These fuels have average calorific values of 4200, 6200, 10280, and 10700 kCal, respectively [29]. The amount of heat required to generate steam from water can be calculated using Equation 7.

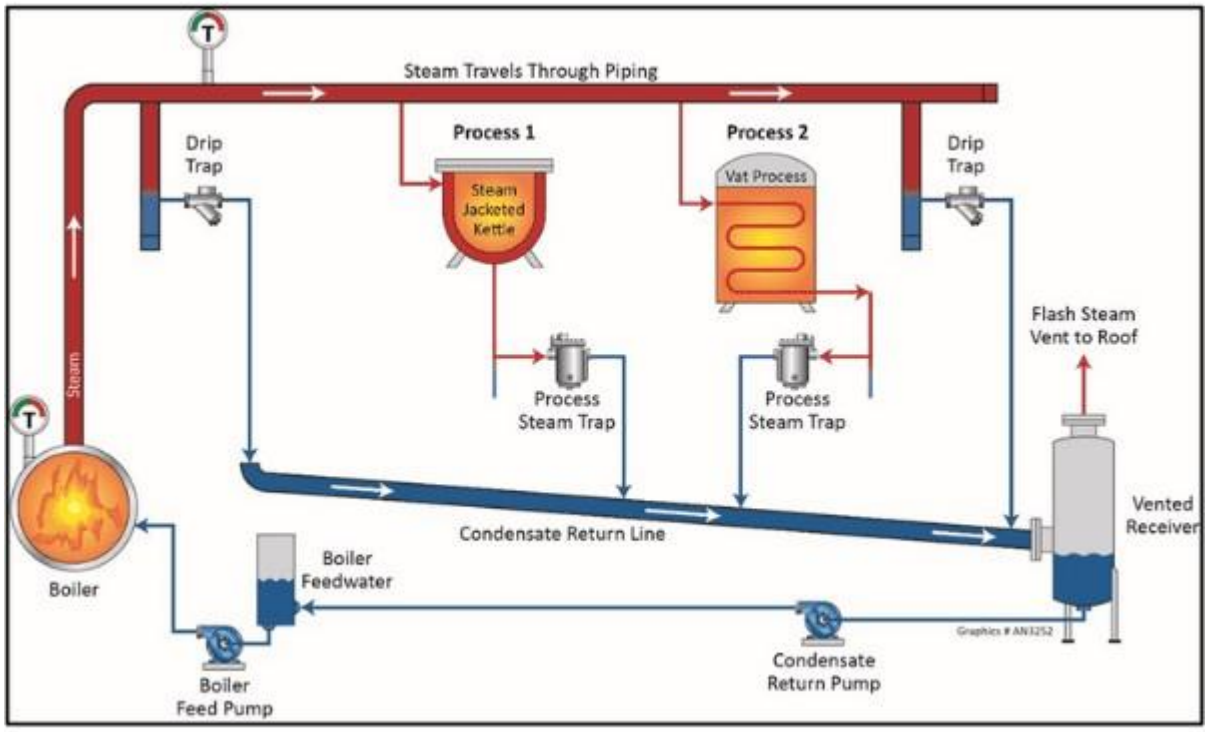

Figure 6: Steam-based process heating system [35]

$$Q = m \times (h_{fg} + c_p \times (T_s - T_w))$$ Equation 7

Where; m - mass of water h_{fg} - Latent heat of vaporization (J/kg) c_p - specific heat capacity of water (J/kg·K), T_s -steam temperature (K), and

T_w - initial water temperature (K).

The rate of heat transfer in a heat exchanger can be determined by Equation 8.

$$Q = U \times A \times \Delta T_{lm}$$ Equation 8

Where;

U - Overall heat transfer coefficient (W/m²·K),
A - Heat transfer area (m²),
ΔT_{lm} -log mean temperature difference (K).

Steam-based process heating systems are characterized by their high energy output, therefore the boiler system efficiency is given by **Error! Reference source not found.**Equation 9 [36].

$$Boiler\ efficiency = \frac{Steam\ flow \times (steam\ enthalpy - feedwater\ enthaloy)}{Fuel\ firing \times Gross\ calorific\ value} \times 100 \quad \text{Equation 9}$$

2.2.3 Electric based process heating system

Electric based process heating uses electric current or electromagnetic field to produce the heat required for industrial processes or heating the material [37]. Heating through an electric process heating can either be done directly or indirectly and is mostly used in the iron and steel industry for drying and curing [28]. One of the technologies that use electric process heating include electric arc furnace, induction and laser heating and radio frequency drying [37]. In direct electric process heating, heat is generated by using one of the techniques, which include passing the current or inducing the current into the material and using electromagnetic radiation to excite the material's atoms [34]. In indirect electric process heating, heat is still generated using the aforementioned methods, however, the generated heat is then transferred to the materials through heat transfer mechanisms, namely conduction, radiation or convection [29].

2.3 Solar thermal systems

Solar thermal energy involves converting solar radiation into heat, which can be used for various applications such as domestic hot water, space heating, and industrial process heat. [26]. This conversion is achieved through the use of solar collectors, which absorb solar radiation and convert it into heat [38]. Solar thermal systems typically consist of collectors, a heat transfer medium to transport the heat to a storage or utilization point, and a storage system to retain the heat for later use, as shown in Figure 7. Solar thermal technologies can be categorized on the basis of their working temperature into three types [39]:

- Low-temperature technologies; which operate at temperatures that are below 70°C). These are used for applications such as solar space heating, solar pond, domestic solar water heating, and solar crop drying
- Medium-temperature technologies; which operate at temperatures that range between 70°C and 200°C. These are used for solar distillation, solar cooling, industrial process heating and solar cooking.
- High-temperature technologies; which operate at temperatures above 200°C. These are used in solar thermal power generation technologies such as parabolic troughs, solar towers, and parabolic dishes.

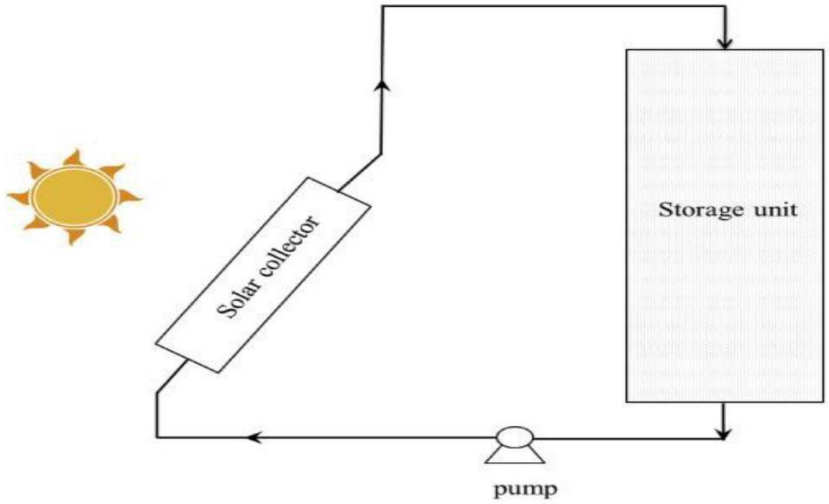

Figure 7: Solar thermal system [40]

2.3.1 Solar collectors

The temperature at which a solar thermal system operates is dependent on the type of collector used [41]. How solar thermal collection is achieved is based on the principle that when solar radiation strikes a surface, a part of it is absorbed, causing the surface temperature to increase[41]. The efficiency of the solar collector is determined by its ability to absorb solar radiation, minimize thermal losses to the surroundings and effectively transfer the useful energy to its designated purposes [42]. Solar collectors are classified by their motion (stationery, single axis or two axis tracking), concentration ratio and working temperature, and they are discussed below [43].

2.3.1.1 Flat plate collector

The flat plate solar collector is the simplest and most common type of collector, forming the basis of other solar collector types [44]. It is a non-concentrating, stationery collector primarily usually used for solar water heating and space heating. Flat plate collectors use both beam and diffuse solar radiation and do not require tracking of the sun. They are known for being lowmaintenance, affordable, and mechanically simple [45]. They are best suited for applications with temperature requirements of 30 °C to 80 °C. The main components of the flat plate collector as shown in Figure *8* are as follows:

- Glass cover: This reduces heat loss through radiation and conduction from the absorber plate to the atmosphere. Typically, one or two glass sheets are used [46].
- Heat removal passageways: This includes tubes, fins, or passages that direct the heat transfer fluid from the inlet to the outlet [38].
- Absorber plate: Is used to absorb heat and is made from materials with high conductivity, and highly absorptive like copper. The absorber plate has a selective

coating that maximizes the absorption of solar radiation while minimizing the emission of infrared radiation [47].

- Insulation: Used to minimize the heat loss from the back and sides of the collector [47].
- Casing: surrounds the aforementioned components and protects them from dust, moisture, and any other material [38].

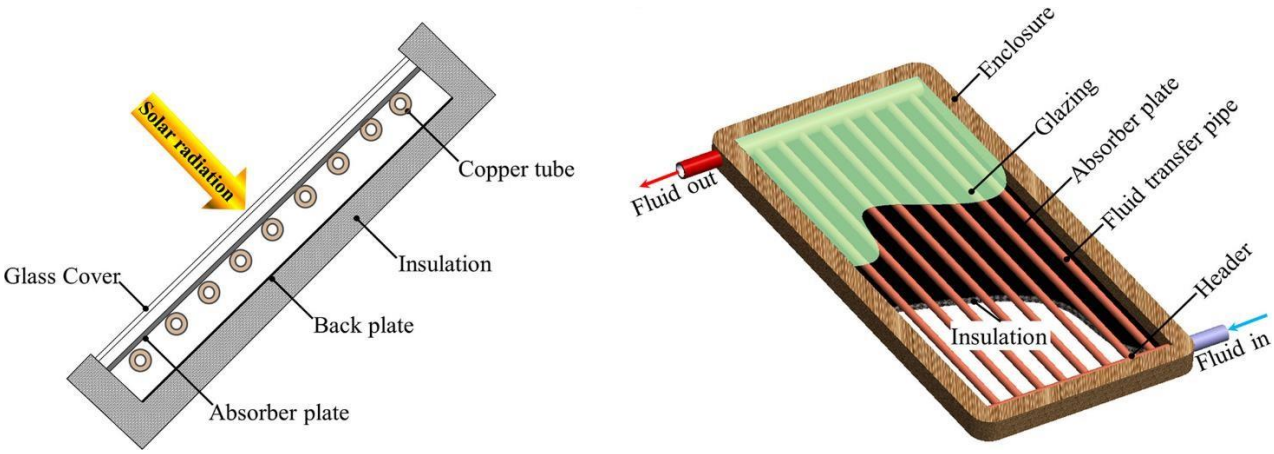

Figure 8: Flat plate collector [45]

2.3.1.2 Evacuated tube collector

The evacuated tube collector (ETC) is a non-concentrating and stationery solar collector made up of rows of parallel, translucent glass tubes as shown in Figure 9. Each tube consists of a glass outer tube and an inner tube, or absorber, which has a selective coating that absorbs solar radiation energy while minimizing radiative heat loss [48]. This collector uses air and vacuum as the insulating material to prevent heat loss through conduction and convection [49]. Similar to flat-plate collectors, evacuated tube collectors collect both direct and diffuse radiation without the need to track the movement of the sun. However, they are more efficient in low incidence angles. This characteristic gives evacuated tube collectors a performance advantage over flat-plate collectors in terms of daylong performance [38]. The operating temperature range of evacuated tube collectors (ETC) is from 50 °C to 200 °C.

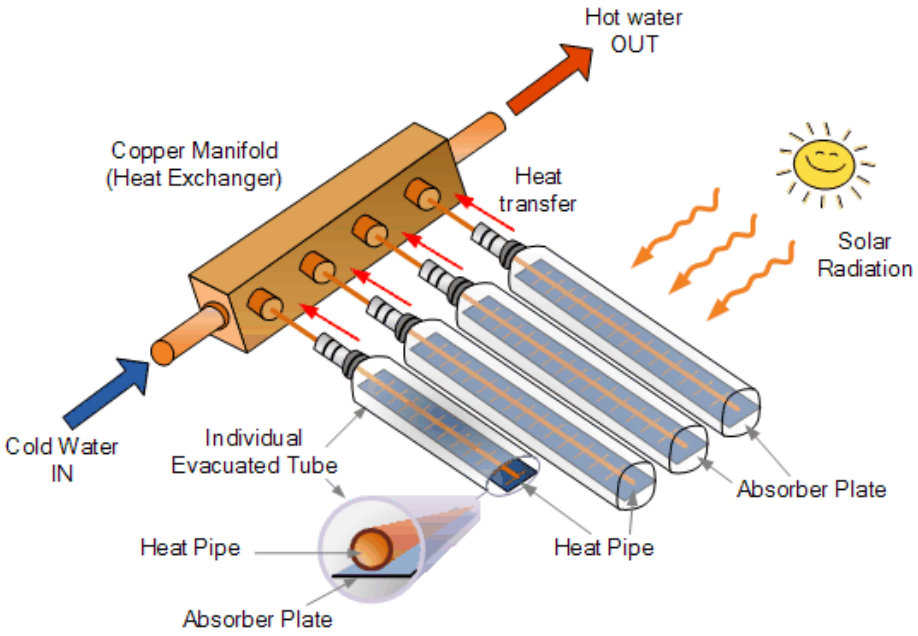

Figure 9: Evacuated tube collector *[50]*

2.3.1.3 Parabolic trough collector

The parabolic trough is a single axis tracking, concentrating solar collector that uses only beam radiation [51]. Parabolic trough collectors as depicted in Figure *10* can effectively produce heat at temperatures between 50 °C and 400 °C. The construction of parabolic trough collectors involves bending a reflective sheet of material into a parabolic shape, and a metal tube is put along the focal line of the receiver [41]. The ability of these collectors to reach such high temperatures makes them ideal for process heat applications in different industries or solar thermal electricity generation [51].

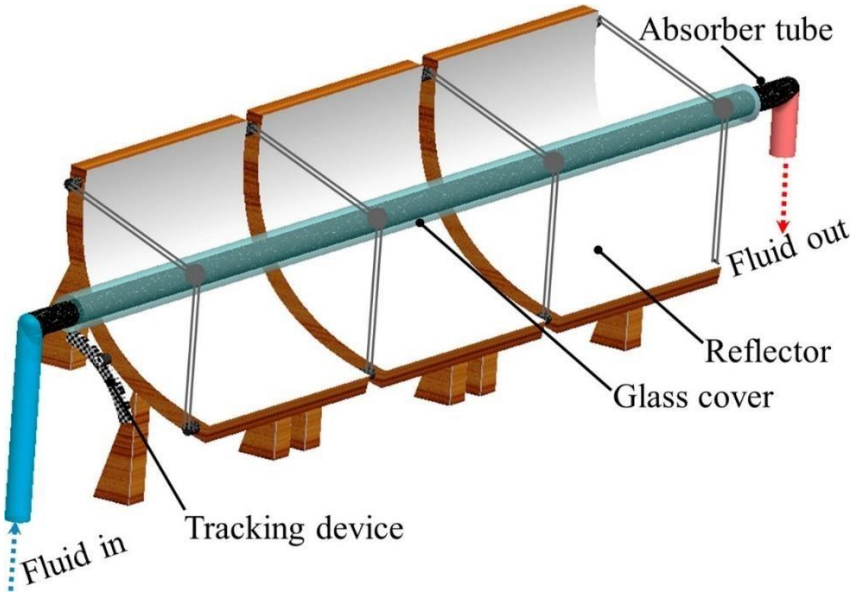

Figure 10: Parabolic trough collector *[45]*

2.3.1.4 Linear Fresnel reflector

Linear Fresnel reflector shown in Figure *11* is a concentrating solar collector with a one-axis tracking system to concentrate solar radiation and produce heat. This type of collector operates at temperatures ranging between 60 °C and 250 °C and can be used in different industries for process heating [36]. The Linear Fresnel reflector is made of an array of linear mirror strips in a parallel configuration, which concentrates the sunlight onto a fixed receiver on a linear tower [52]. Linear Fresnel reflectors are used in concentrating solar power technologies to generate electricity [42].

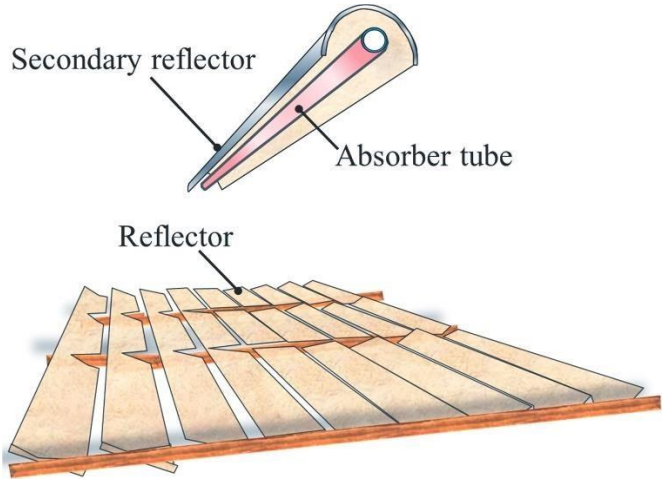

Figure 11: Linear Fresnel reflector *[45]*

2.3.1.5 Parabolic dish reflector

A parabolic dish reflector as shown in Figure *12* is a concentrating collector that uses a concave, parabolic shaped mirror to concentrate the solar radiation onto a receiver located at the focal point of the mirror [53]. The design allows the dish to concentrate a significant amount of solar radiation onto a smaller area, increasing the intensity of the radiation received from the sun [54]. Parabolic dish reflector has a two-axis tracking that ensures it continuously follows the movement of the sun throughout the sky in order to reflect sunlight onto the reflector throughout the day [26]. A parabolic dish reflector operates at a temperature that ranges from 100 °C to 1500 °C and is mostly used in parabolic dish engines. A parabolic dish engine system is described as the electric generators that use concentrated solar thermal energy to generate electricity [38].

Figure 12: Parabolic dish reflector *[53]*

2.3.1.6 Heliostat field collector

A Heliostat field collector is a concentrating collector that uses mirrors to concentrate the radiation from the sun on to a central receiver [55]. A Heliostat field collector as shown in Figure *13* uses two-axis solar tracking mechanisms which allows to track the sun's position across the sky throughout the day [38]. This type of collector operates at temperatures that range from 150 °C to as high as 2000 °C [43]. The ability to operate at these high temperatures makes them suitable for their application in industrial processes that require significant thermal energy. Heliostat field collectors are used in the production of steam at very high temperatures and pressure and electricity production [55].

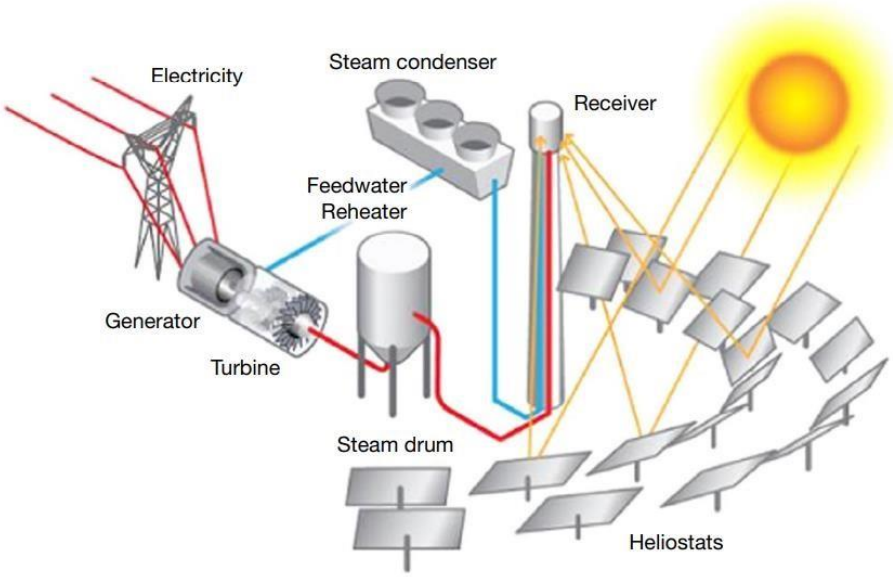

Figure 13: Heliostat field collector *[55]*

2.3.2 Solar thermal storage system

Thermal storage is a main component of solar thermal systems, since solar radiation is intermittent, the need to store thermal energy for later use is of paramount importance, especially in applications that are continuous throughout the day [42]. Hot water is the primary sensible heat storage medium for solar thermal energy [56]. This is due to the fact that water is cheap, non-toxic, and has a large storage capacity relative to its volume and weight [38]. Furthermore, the liquid state of water makes it easy to move through pumps and plumbing systems. The choice of solar thermal storage is dependent on the physical, economic, chemical and environmental factors, which include the energy density of the storage material, heat transfer and mechanical properties, thermal losses, cost and thermodynamic efficiency [57].

Since solar energy is mostly stored as hot water, liquid system thermal storage is discussed. There are two types of liquid system thermal storage, namely, pressurized and unpressurized storage systems [42]. However, there are differences between the storage systems due to the type of heat exchanger used (internal or external) and the tank configurations, which can either be single or multiple [38].

A pressurized storage system is connected to the main water supplies and is commonly used in small scale water heating systems. Additionally, pressurized storage systems can either utilize an internal or external heat exchanger and is usually placed at the collector side of the storage unit [42]. Figure 14 shows the pressurized storage systems with different heat exchangers.

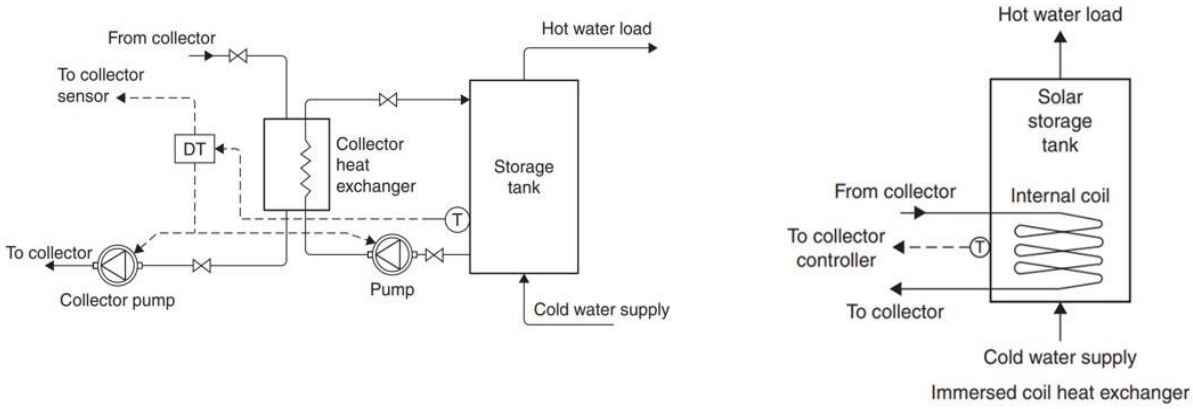

Figure 14 : Left: Pressurized storage system with external heat exchanger, Right: Pressurized storage system with internal heat exchanger *[38]*

Unpressurized storage systems similar to the pressurised storage system use both internal and external heat exchanges and are mostly used in large scale water heating systems. In this type of storage systems, the heat exchanger is placed on the load side of the storage unit [42].Figure *15* shows an unpressurized storage system with an external heat exchanger.

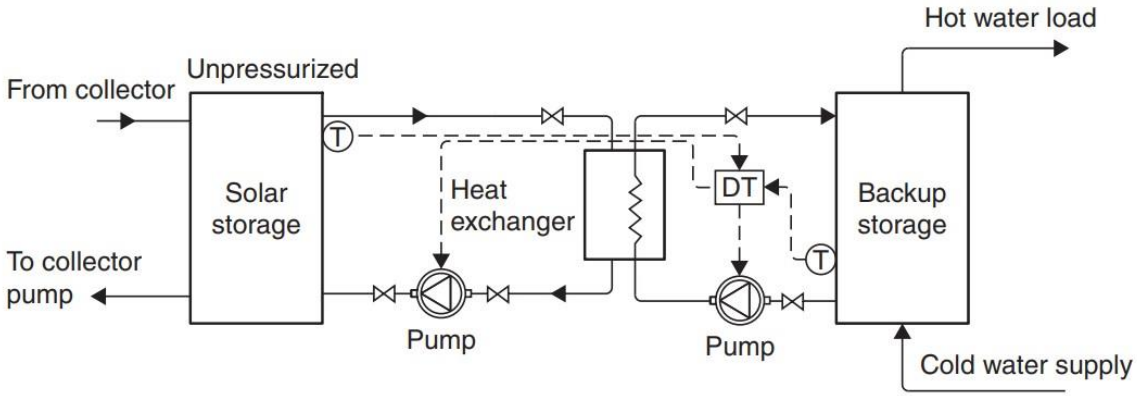

Figure 15: Unpressurized storage system with external heat exchanger *[38]*

2.3.3 Heat transfer medium

As mentioned, heat transfer medium is the main component of solar thermal systems because it improves the efficiency of such systems [58]. Heat transfer media are used to collect the heat from the collector and transfer it to the storage system either directly or indirectly with the help of a heat exchanger [48]. The commonly used heat transfer media include water, glycol water, air, hydrocarbon oils and molten salts [59]. The selection of the heat transfer medium to be used in solar thermal systems is dependent on factors such as the desired operating temperature of the designed system and cost [60]. Table *1* shows the properties of some of the heat transfer media used in solar thermal systems.

Table 1: Heat transfer medium properties *[59], [61]*

Heat transfer medium	Properties
Air	Easily available everywhere
Water	High thermal capacity Low viscosity Cheap Non-toxic Easily available
Molten salts	Found easily and cheap Non-toxic Work well for temperatures above 500 °C

Glycol water	Anti-freezing
Hydrocarbon oils	High heat transfer capability Low maintenance cost Low viscosity Works well in temperatures between 12 °C to 400°C; higher temperature difference Anti-freezing

2.4 Solar thermal system design

Designing a solar heating system requires the correct sizing of its components to ensure optimal performance and efficiency [62]. This sizing is based on the expected solar radiation and the demand for hot water. Some key considerations in the design of solar heating systems for industrial process heating include energy demand, site assessment and solar collector selection.

2.4.1 Energy demand determination

The temperatures at which industrial processes operate are important for determining the facility's energy demand [63]. Knowing these temperatures helps calculate the energy needed to keep the processes running efficiently. This information is crucial for correctly sizing a solar thermal system to meet the industry's specific energy needs. Accurate energy demand assessments consider the varying temperature requirements for different processes, the duration of these processes, and the efficiency of current thermal systems [64]. Understanding energy demand allows for the effective integration of solar thermal systems, maximizing their efficiency and cost-effectiveness while reducing reliance on traditional energy sources [64]. Properly sized solar thermal systems improve energy efficiency, reduce operational costs, and minimize the environmental impact of industrial activities [3]. Therefore, understanding the link between process temperatures and energy demand is important to the successful use of solar thermal technologies in industries [3].

2.4.2 Site assessment

Site assessment in system design is important. Site assessment helps in the identification of suitable space and location for collectors, considering factors such as shading, roof tilt and orientation, local climatic conditions [65]. Moreover, the need to do a site assessment is important because it helps analyse the energy consumption patterns and ultimately helps in determining the optimal system size that will meet the specific needs of the site [66].

2.4.3 Resource assessment

The determination of the available solar radiation on-site is another key consideration in thermal system design. Meteorological data of the site need to be known to assess whether the amount of solar radiation can be harnessed for use in solar thermal systems. Hence, it is important to have access to data on the yearly, seasonal, and daily mean global horizontal irradiance and direct normal incident radiation for a specific area of interest [63].

The amount of solar radiation hitting the solar collector holds paramount significance in the collector's sizing, with the daily global irradiance on a horizontal surface being the key parameter for the determination [5]. It is also important to know the radiation on an hourly basis since the sun's position, which is used for solar energy calculation, varies hourly.

To model the amount of radiation received on the tilted surface, several equations come into play, as shown in **Error! Reference source not found.**, **Error! Reference source not found.**, **Error! Reference source not found.**, **Error! Reference source not found.**, **Error! Reference source not found.**, **Error! Reference source not found.**, **Error! Reference source not found.**, **Error! Reference source not found.**, [49], [67], [68], [69], [70]. It is worth noting that the most commonly available solar data is in the form of monthly solar radiation.

To calculate the extraterrestrial solar radiation incident on a horizontal plane Equation 10 is used, where G_{sc} denotes solar constant, E_o is the eccentricity correction factor and θ_z is the zenith angle.

$$G_{oh} = G_{sc} E_o \cos\theta_z \qquad \text{Equation 10}$$

The extraterrestrial radiation in **Error! Reference source not found.** is integrated with respect to time from sunrise to sunset to get the daily extraterrestrial radiation on a horizontal plane as shown in **Error! Reference source not found.**

$$H_o = G_{sc} E_o \int_{t_{sr}}^{t_{ss}} \cos\theta_z \, dt \qquad \text{Equation 11}$$

$$H_o = G_{sc} E_o \int_{t_{sr}}^{t_{ss}} (\sin\varphi\sin\delta + \cos\varphi\cos\delta\cos\omega) \, dt \qquad \text{Equation 12}$$

Since solar radiation varies, the derivation of the extraterrestrial solar radiation on a horizontal plane between a time period of one hour is given by **Error! Reference source not found.**.

$$I_o = \frac{1367 \times [1 + 0.033cos(\frac{360n}{365})] \times 12 \times 3600 (\frac{\pi}{180}(\omega_2 - \omega_1)sin\varphi sin\delta + cos\varphi cos\delta[sin(\omega_2) - sin(\omega_1)])}{\pi}$$ Equation 13

Because there have been no records of diffuse radiation in various places in the developing world, there is a correlation between diffuse radiation and clearness index, K and is given by **Error! Reference source not found.**

$$K = \frac{H_d}{H_h}$$ Equation 14

The hourly fraction of daily diffuse radiation, r_d, is given by **Error! Reference source not found.**

$$r_d = \frac{I_d}{H_d} = \frac{\pi}{24}(cos\omega - cos\omega_s)\frac{}{sin\omega_s - \frac{\pi}{180}\omega_s cos\omega_s}$$ Equation 15

the hourly fraction of daily global radiation is given by **Error! Reference source not found.**

$$r_h = \frac{I_h}{H_h} = (a + bcos\omega)r_d$$ Equation 16

Where:

$$a = 0.409 + 0.5016sin(\omega_s - 60)$$ and Equation 17

$$b = 0.6609 - 0.4767sin(\omega_s - 60)$$ Equation 18

Therefore, the hourly radiation on a tilted surface is given by **Error! Reference source not found.**, where I_T is the hourly irradiation on the tilted surface; I_b is the beam radiation on a horizontal surface; R_b is the ratio of beam radiation on a tilted surface to that on a horizontal surface; and I_d is the diffuse radiation.

$$I_T = I_b R_b + \frac{I_d}{C}$$ Equation 19

$$C = \frac{A_{aperture}}{A_{receiver}}$$ Equation 20

2.4.4 Solar collector selection

The selection of a solar collector should align with the understanding of the accessible solar radiation at the specific location [63]. Other factors to be taken into consideration when selecting a suitable solar collector include the average operating temperature of the solar collector, optical efficiency and the overall heat transfer coefficient of the collector, cost and availability of space and the possibility of roof integration, energy yield and thermal efficiency at the desired temperature [5], [36]. Furthermore, the performance of a solar collector is described by an energy balance that indicates the distribution of incident solar energy into useful energy gain, thermal losses, and optical losses and is given by **Error! Reference source not found.** where the variables; Ac is the collector area, G_t the solar irradiance incident on the collector plane, 〖(τα)-the normal-incidence transmittance-absorptance product of the collector

U_L the collector heat loss coefficient, F_R-collector heat removal factor, Ta - ambient temperature, and Ti - the tank temperature, which is equivalent to the inlet temperature to determine how much useful energy is collected.

$$Q_u{}^{+} = FR\ Ac\ [G\tau\alpha - UL\ (Ti - Ta\ )] \qquad \text{Equation 21}$$

2.4.5 Simulation tools for solar thermal systems

Simulation tools are often used in the design of solar thermal systems. The following simulations: TRNSYS, T*SOL and Polysun which are commonly used in the design was discussed.

TRNSYS is a widely used simulation software for developing and analysing solar thermal systems. It is renowned for its comprehensive and flexible nature, making it the preferred choice among engineers and researchers for validating new energy concepts [71]. TRNSYS can model a range of systems, from simple residential hot water systems to complex designs involving entire buildings [49]. One of the key strengths of TRNSYS is its modular approach, which allows users to customize simulations by combining various pre-built components. This modularity facilitates the accurate simulation of thermal, electrical, and control systems, making it a versatile tool for energy systems analysis. However, TRNSYS uses traditional programming languages making it not user-friendly for those not familiar with coding [49].

T*SOL is a software tool specifically developed for the simulation, design, and optimization of solar thermal systems, with a particular focus on solar water heating systems [72]. It is designed to model various components of solar thermal systems, including collectors and storage tanks [72]. T*SOL is capable of dynamically calculating the annual performance of

solar thermal systems [26]. This allows the users to simulate the energy yield of the system throughout the year, ensuring a comprehensive understanding of its performance [73]. Furthermore, T*SOL includes tools for calculating the economic efficiency of the system, providing a complete analysis to aid in decision-making and system optimization [73].

POLYSUN is a simulation programme that simulates and optimises the solar thermal systems offering annual thermal performance simulations [26]. The programme uses features that are user-friendly, and allowing ease of use [74]. Polysun simulations run in time intervals from 1 s to 1 h, making them more stable and accurate [75]. In addition to performance simulations, Polysun does the shading and economic analysis of the designed systems [26]. Furthermore, the simulation software does the environmental analysis which includes the assessment of the greenhouse gas emissions, allowing the users to compare the emissions from the systems that use conventional fuels with those that use the solar thermal system [74].

2.5 Economics of solar heating systems

While solar energy itself, in the form of solar irradiation, is freely available, the equipment needed to harness and convert it into usable energy, either heat or electricity, comes at a cost [3]. Therefore, solar energy systems typically involve high upfront costs but low operating expenses [42]. When considering the adoption of a solar energy system, it is important to ensure that the total cost of solar collectors, additional necessary equipment, and any conventional fuel used as a backup is less than the cost of conventional energy sources for performing the same function [6]. The primary goal of economic analysis in this context is to determine the optimal size of the solar system for a specific application, achieving the lowest possible combined cost of solar and auxiliary energy [42]. The following financial indicators are commonly used for the economic assessment of solar thermal energy projects; Life cycle cost (LCC), Net present value (NPV), Internal rate of return (IRR), payback period (PB), and Levelized cost of useful thermal energy (LCUTE) [36].

2.5.1 Lifecycle cost analysis

The Life Cycle Cost approach serves as a foundational method for evaluating solar energy technologies in comparison with conventional energy technologies [38]. This method takes into consideration the comprehensive cost of the entire system over a defined time frame, typically the project's lifespan [76]. Conducting an LCC analysis provides the designer with insights into the impact of using different components with varying reliabilities and lifespans [36]. It is also a valuable tool for comparing the costs of different designs and determining whether a hybrid system may represent a cost-effective alternative [36]. The LCC analysis is given by **Error!**

Reference source not found., where C is the initial cost of installation-the present value of the cost on capital resources, M_{WP} is the aggregation of all the yearly operation and maintenance costs. It includes the wage of the operators, site access, the guarantees paid, and all the other regular maintenance costs, E_{WP} is the aggregation of all the yearly energy cost including fuel cost and its transportation to the plant site and R_{WP} is the aggregation of all the yearly replacement costs.

$$LCC = C + M_{wp} + E_{wp} + R_{wp} - S_{wp} \quad \text{Equation 22}$$

2.5.2 Net present value of solar savings

NPV is a financial metric used to evaluate the profitability of an investment. It calculates the present value of all future cash flows generated by the investment, subtracting the initial cost of the investment [77]. A positive NPV indicates that the project is expected to generate more value than the cost, making it a good investment. It is given by **Error! Reference source not found.**, where L_{annual} represents the yearly solar energy input, P_E signifies the price of electricity, η_E denotes the efficiency of converting electricity to heat, V_s represents the volume of hot water storage, C_s stands for the storage tank cost per unit volume, and C_{BOS} reflects the cost of the balance of system components.

$$NPVSS = \frac{(L_{annual} \times P_E)}{\eta_E} \quad \frac{1-(1+d)^{-w}}{d} \times - (A_C C_{area} + V_s C_s + C_{BOS}) \quad \text{Equation 23}$$

2.5.3 Internal rate of return

The internal rate of return is the annual discount rate that makes the present value of an investment equal to zero [78]. It shows the yearly growth rate of an investment. Internal rate of return helps investors determine the profitability of their investments by showing the rate at which the project is expected to generate returns [41].

2.5.4 Payback period

The payback period is the time when the cashflows of the project reach a breakeven point, or to reach the point where the net cash flow generated is equal to the initial cost of the project [36].

$$Payback\ Period = \frac{Initial\ investment}{Annual\ savings} \quad \text{Equation 24}$$

2.5.5 Levelized cost of useful thermal energy

LCUTE focuses on the cost of producing thermal energy [38]. To calculate LCUTE **Error! Reference source not found.Error! Reference source not found.** was used, where the variables, C^0_j is the unit cost of useful thermal energy delivered by the SIPH system (LCUTE) in j^{th} year of its operation, d is the discount rate and n is the useful life of the system.

$$= \left[\sum_{j=0}^{n} \frac{C\ j}{C_l}\right]\left[\frac{d(1+d\ ^{n}}{(1+d)_j}\right]^{25}_{o}\ )\qquad (1+d)_n - 1$$

Equation

The discount rate is calculated using**Error! Reference source not found.**, and the variables *i* and *j* denote the annual interest rate and annual inflation rate.

$$d = \frac{i+1}{j+1} - 1$$

Equation 26

2.6 Solar thermal energy for industrial process heating

The application of solar thermal systems for generating heat in industrial processes is an increasingly viable option that has been getting a lot of attention in recent years as part of the efforts to transition toward a net zero carbon energy future [79]. The use of solar thermal energy for industrial processes heating offers a sustainable and environmentally friendly approach to meeting the heat requirements of various industries [3]. It has proven to be effective in meeting the thermal energy demands and temperature requirements of processes operating below 200

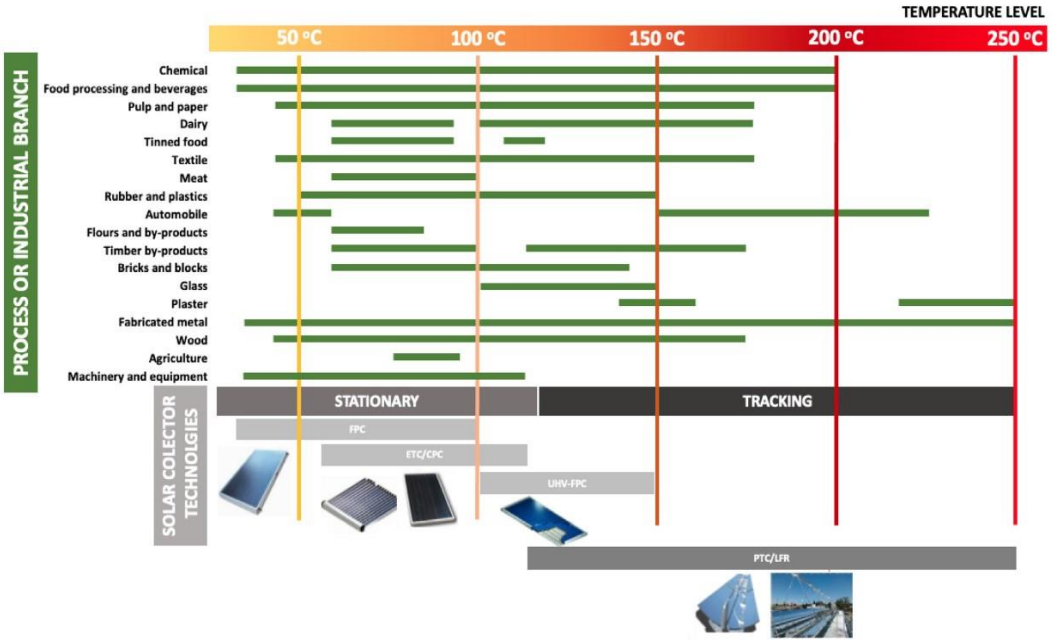

°C. As shown in Figure 16, a significant proportion of processes heating in different industries operate within these temperature ranges [80].

Figure 16: Solar collectors technologies and industrial branches as a function of the operating temperature [79]

2.6.1 Integration of solar heating systems

The integration of solar heating systems is referred to as harnessing solar energy to generate thermal energy, which can effectively be used in a wide range of industrial processes [80]. To integrate solar thermal energy into industrial process heat, various types of solar thermal collectors, as discussed in detail in the previous section, are widely used [26]. These collectors, which include flat-plate collectors, evacuated tube collectors and parabolic trough collectors, are commonly used. The integration of solar heating systems into pre-existing systems can occur either at the process level or at the supply level.

Process-level integration involves the direct supply of solar heat to specific industrial processes, as illustrated in Figure 17 [36]. This form of integration is typically employed in situations where there is a need for low-grade heat, typically up to 100°C [26]. Examples of such applications include washing, hot air drying, heating of industrial baths and cleaning. Achieving this integration effectively necessitates the implementation of a highly secure and precise control system [3]. Process level integration requires a large storage size and high collector efficiency for low temperature processes. The large storage acts as a buffer, storing excess solar energy during periods of high solar radiation and releasing it at low solar radiation

periods to ensure a continuous supply of heat to the industrial processes [3]. It also allows a low flexibility in case of process changes [81].

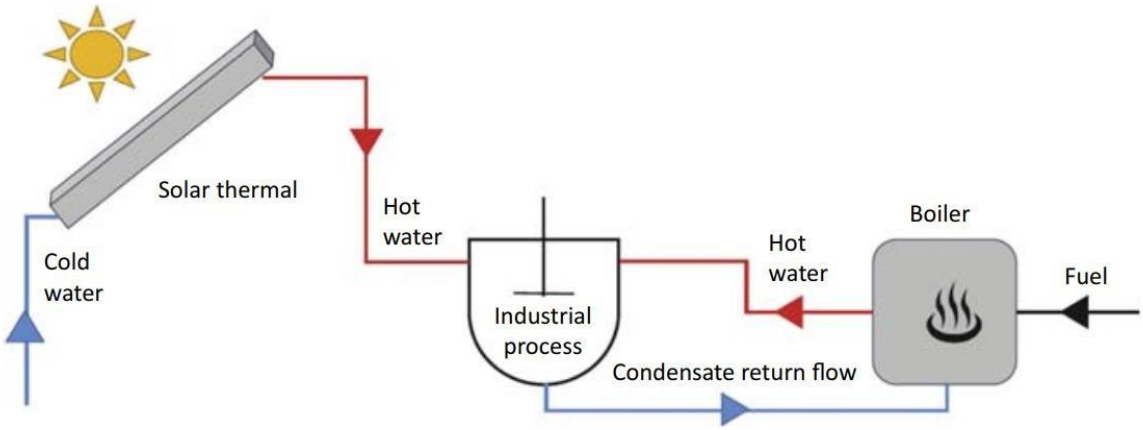

Figure 17: Process level integration *[82]*

The supply-level integration involves the supply of heat through a heat distribution network through the use of heat exchangers, as depicted in Figure 18 [63]. This integration approach is typically applied within steam networks and high-temperature networks, allowing the solar thermal system to provide preheated feed water or even direct high-temperature steam [36]. Unlike process-level integration, supply-level integration typically requires a smaller storage size because the heat is distributed more centrally and can be utilized more immediately within the network [83]. Additionally, this integration approach does not demand exceptionally high collector efficiency, except when it is used for heating the boiler makeup water, which does require more efficient collectors to reach the necessary temperatures [3].

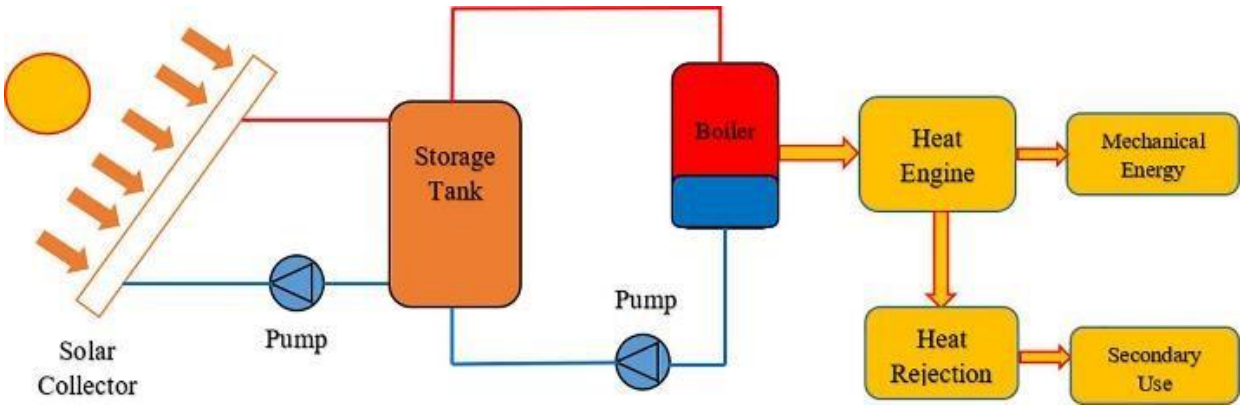

Figure 18: Supply level integration *[26]*

One of the significant advantages of the supply-level integration is its high flexibility in adapting to the changes within the industrial processes [36]. Since the heat distribution is

managed centrally, modifications in individual processes or production lines do not require extensive alterations to the solar thermal system. This flexibility ensures that the system can accommodate changes in heat demand or process parameters without substantial redesigns or additional investments [83]. A detailed comparison between these two integration techniques is presented in Table *2* for further clarity.

Table 2: Difference between process and supply level integration *[83]*

Criteria	**Process level**	**Supply level**
Accuracy of process data	High	Medium
Flexibility in case of process changes	Low	High
Collector efficiency	High (for low temperature processes)	Low (except for heating of boiler make-up water)
Solar share	Low	High
Required storage size	Large	Small
Investment cost	High	Low

2.7 Thermal processes in textile industries

In the textile industry, both electrical and thermal energy play a crucial role in driving different production processes. While electrical energy powers the machines and equipment, thermal energy is used for process heating activities such as dyeing, bleaching and the various finishing operations that are integral to textile production [6]. The processes involving heating typically operate at relatively moderate temperatures ranging from 50 to 200 °C [6]. Thermal energy consumption in textile mills is associated with two key operations: water heating and textile drying. It is also important to note that the fuel consumption in textile mills is directly proportional to the volume of the utilized water [84]. Among the different units within textile production, the wet processing unit stands out as a major consumer of both water and chemicals. Furthermore, this sector is responsible for the substantial use of thermal energy, particularly in the form of water steam generated from fossil fuels [85]. Wetting processes such

as pre-treatment, bleaching/scouring, dyeing, washing, and finishing collectively demand a significant amount of thermal energy as compared to other sectors. The energy required is often generated by heating water with fossil fuels to produce steam [85].

Wetting processes in the textile industry are important for preparing the fabrics for subsequent treatments and for achieving the desired properties and appearance. These processes can involve various chemical treatments and mechanical actions, all of which play a significant role in producing high-quality textiles for various applications [86]. The processes involved are as follows:

- Scouring is the first wetting process used to remove the natural impurities, such as waxes, pectins, and mineral matter, from raw textile materials such as cotton, wool, and silk. The scouring process typically involves the use of an alkaline solution, such as sodium hydroxide (caustic soda), to break down and remove these impurities [86].

- Bleaching: After scouring, textile materials may undergo a bleaching process to remove any remaining colour or stains. Bleaching agents like hydrogen peroxide or sodium hypochlorite are used to whiten the textile materials and to remove the natural and artificial colour from the textile material, making it suitable for dyeing. Proper wetting ensures that the bleach is evenly distributed and effective [87].

- Dyeing: Wetting is crucial in the dyeing process to ensure the even distribution of dye throughout the textile material. Whether using dye baths, dye liquor, or other dyeing methods, the textile must be adequately wet to achieve uniform and vibrant colours [88].

- Printing: In this process, the fabric is prepared for the application of dyes or pigments in specific patterns. The textile is typically wet before printing to ensure that the colours adhere uniformly to the fabric surface [89].

- Finishing: This is a wash-off process where, after dyeing or printing, fabrics are often washed to remove excess dye or chemicals, thus improving the colourfastness and overall quality [86].

- Washing and rinsing: This is a process usually used for denim and other garments where wet processes such as stone washing, acid washing, and enzyme washing are used to achieve various effects like fading and softening [86].

- Setting: This is a wet process used in some cases to set certain treatments, such as crease-resistance or flame retardants, water and stain resistance and help to remove

fuzz, pills, and surface irregularities from textiles, making them smoother and more comfortable [89]

The use of energy in the wetting processes varies according to the various factors that including the product, the type of machinery used, and the required condition of the final product [90]. Processes such as desizing, require 278 – 972 kWh of thermal energy per ton of output, while scouring consumes 1,806 kWh - 2,778 kWh per ton of output [90]. The bleaching processes require the most energy in the wetting processes [11]. The amount of energy required for dyeing is dependent on the type of machinery used. The energy demand required to dye a ton of fabric using a Jet dying machine is 972 - 4,444 kWh. The energy consumption for dyeing using a winch is between 1,667 and 4,722 (kWh) per ton of fabric [90]. When it comes to printing, the energy consumption for printing using a rotary screen is approximately 694 to 2,361 kWh per ton of output, while using stenter during the heat setting process is approximately 1,111 to 2,500 kWh per ton of output [90].

2.8 Global integration scenario in the textile industry

Solar heating for industrial process (SHIP) projects are being implemented globally [63]. As reported by the Solar Heat World Wide 2024, there are currently 1200 SHIP projects, of which 116 were installed in 2023 [91]. Nevertheless, the textile industry, in terms of solar process heat integration, is still emerging. According to the AEE-Institute of Sustainable Technologies 2020 report, there is only 26 MW thermal capacity of solar heat integration installed [92]. This accounts for only 5 % of the thermal capacity installed for the solar heat integration [63]. From the installed projects, it is observed that projects with supply level integration have flat plate collectors, while for process level integration, evacuated tube collectors, parabolic troughs and air collectors were used [63]. Table 3 and Table 4 show the installed projects for textile industries according to their integration. Flat plate collectors make up 54% of the total collectors used in solar heat integration in the textile industry, while 29% are evacuated tube collectors, 4% are air collectors, 9% are parabolic trough collectors, and the remaining 4% consist of other types of collectors [92].

Despite the extensive research and implementation of the integration of solar heating systems in textile industries in various parts of the world, there has been no study specifically focused on Lesotho's textile industry. This study aims to address this research gap by analysing the potential benefits and feasibility of implementing solar heating systems in the textile industry of Lesotho, as this industry is the largest employer after the public sector. To achieve this aim, the study used simulation software in order to model and predict the performance of solar

heating systems under local conditions. Additionally, it incorporated a range of financial indicators to provide a comprehensive financial analysis. The study also examined the environmental benefits of integrating solar heating systems, including reductions in greenhouse gas emissions and improvements in energy efficiency. By addressing these aspects, the research aims to provide a thorough understanding of the economic, environmental, and technical feasibility of solar heating systems in Lesotho's textile industry, thereby contributing valuable insights for policymakers and industry stakeholders.

Table 3: Process integration projects done [92]

Country	**Company**	**Solar collector type**	**Collector area (m^2)**	**Process temperature range (° C)**	**Installed thermal capacity (KW_{th})**	**Storage volume (m^3)**
China	Heshan Bestway Leather	Evacuated tube collector	630	70	441.0	60
China	Ruyi textile	Evacuated tube collector	9903	60	6931.2	-
Vietnam	Grammer Solar Vietnam	Air collector	480		336.0	1
Vietnam	Saigon Tantec	Evacuated tube collector	1000	70	700.0	70
India	Siddarrth Surgicals	Parabolic trough collector	263	110	184.1	-
Thailand	Ayutthaya tannery	Evacuated tube collector	1890	80	1323.0	80

Table 4: Supply level integration projects done [92]

Country	**Company**	**Solar collector type**	**Collector area (m^2)**	**Temperature range**	**Storage volume (m^3)**
Mexico	Guetermann Polygal	Flat plate	450	55-85	20
Spain	Harlequin	Flat plate	47.15	-	5.0
India	Sharman Shawls	Flat plate	360	>100	8
India	Leo Leather	Flat plate	300	15.0	15
Greece	Tripou-Katsouris Leather Treatment Factory	-	300	-	48-84
South Africa	Oudtschoorn Tannery	Flat plate	600	65	40

3 METHODOLOGY

3.1 Overview

This chapter on research methodology describes how the aim of the study, which is to assess the techno-economic viability of integrating solar water heating systems at the Vishan Clothing Laundry has been conducted. A simulation-based methodology using T*SOL simulation software was used in this study. The assessment focused on three key objectives: system design, performance analysis, and economic analysis of the designed system.

System design involves sizing of the main components, performance analysis involves how the designed will perform under normal conditions and the key parameters in this analysis are; solar collector useful energy, the solar fraction and the emissions avoided from using solar water heating systems. The economic analysis shows the financial viability of the designed system, and the financial indicators used in this analysis are from the simulation software which are NPV, IRR, Capital return time and cost of solar energy.

The T*SOL software runs a simulation based on the energy balance flows considering supply sources, with meteorological data input. The programme then performs the economic analysis of the system in terms of the life cycle savings, the total running cost, the net present value, the payback period and the cost of solar energy [73].

3.2 Present system description

Before delving into the design of the solar water heating system, the current heating system is used as shown in Figure 19 and was discussed. The current heating system at the Vishan Clothing Laundry uses a horizontal steam boiler of 6 m^3 with an energy efficiency of 85 % [93]. Coal is used to produce steam that is used to meet the thermal energy demands of the processes. It is stated that approximately four tons of coal (4,000 kg) which amounts to M86,000.00 is used monthly. The wetting processes uses hot water of temperatures between 30 and 60 °C.

However, according to the operator [93], the boiler is maintained at a pressure around 600 kPa, and from the steam graph (pressure vs temperature) depicted in Figure 20, the pressure corresponds to a temperature of 165 °C [94]. The steam production at the maintained temperature of 165 °C is a continuous process even at times with low thermal energy demand to avoid the boiler cold start. The steam is produced at a rate of 1,000 kg/hour [93]. In order to avoid the pressure build-up in pipes some of the steam is released through the pressure relief valves. It can be argued that more energy is produced than the required demand and more energy produced through coal combustion means more money spent. Studies have shown that the thermal energy demand of the processes running at low to medium temperatures of 30 °C to 200 °C can be met using solar thermal energy. The aim is to design a solar water heating system that will meet the hot water demand of the laundry. Furthermore, a performance analysis and an economic analysis was conducted to assess the viability of the designed system.

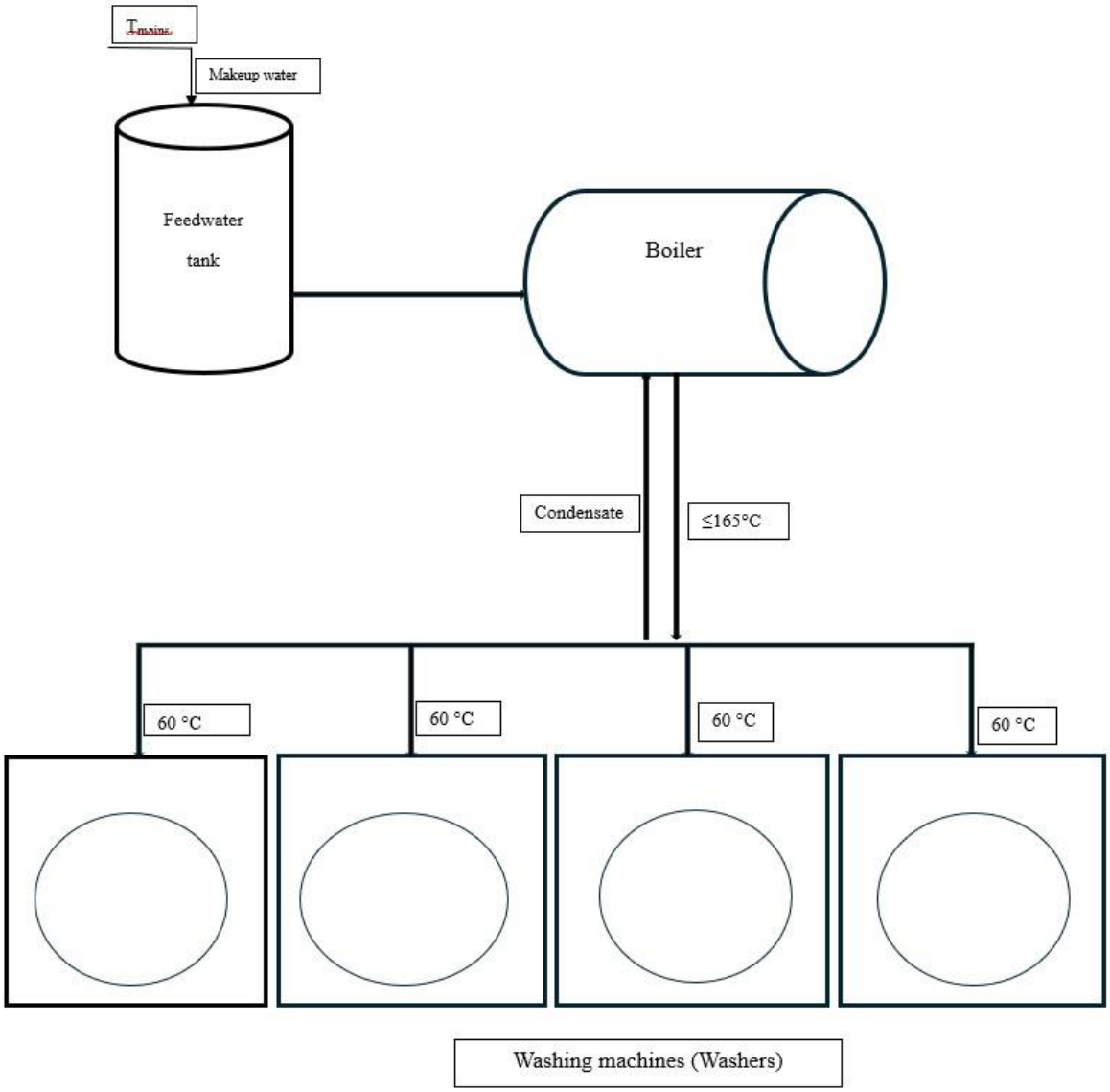

Figure 19: The present heating system

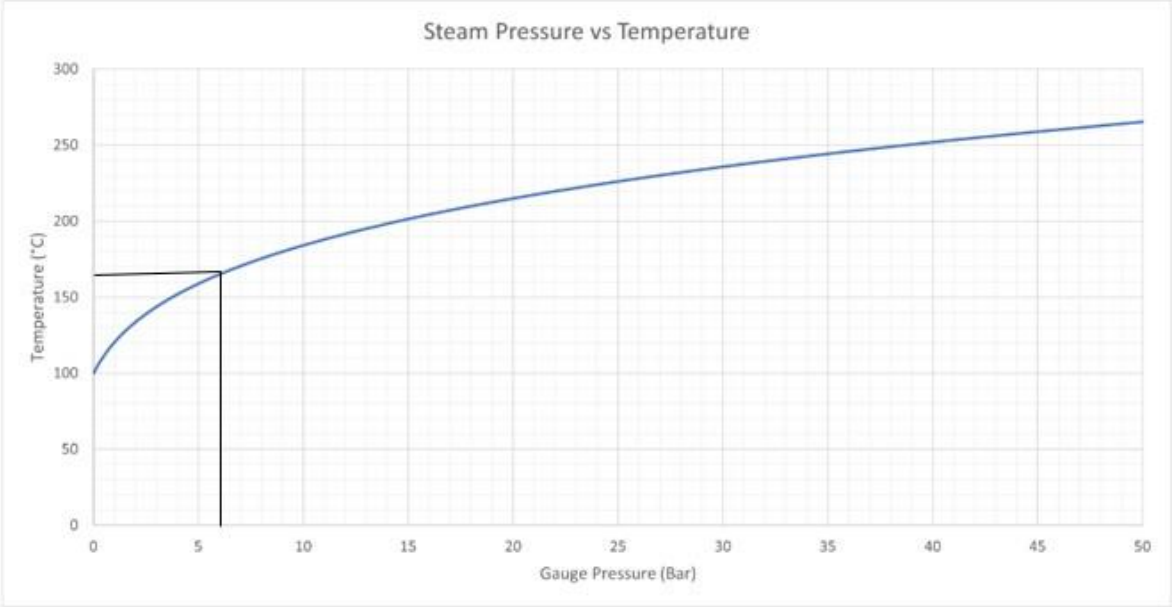

Figure 20: Steam graph (pressure vs temperature) *[94]*

3.3 System design

To design a solar heating system, the size of the main components, which are the collectors and storage tank, must be determined based on the predicted amount of solar radiation and hot water demand [95]. The amount of solar radiation is dependent on location. The main goal is to maximize the amount of solar thermal energy collected to meet the wetting process's energy demand. There may be several processes that require different temperature ranges, and it is important to choose the right collector to meet the needs of most processes. It is equally important to determine the integration point for the solar water heating system. For this study, the integration was at the supply level [36]. The design of the solar thermal system was based on Figure 21 with each factor independent of the others.

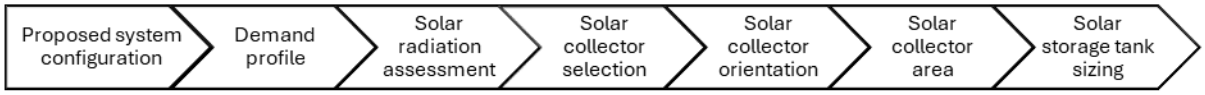

Figure 21: solar thermal system design considerations

3.3.1 Proposed solar thermal system configuration

The proposed solar water heating system design is based on the month with the least radiation, this approach plans for the worst-case scenarios in terms of solar input, during periods of low solar radiation such as during winter times [42]. This ensures reliability, as the system even in low radiation times will still be able to supply some of the thermal demand. Based on the information provided by the laundry with regard to the hot water temperatures used, the target temperature of the system to supply the processes will be at 80 °C. This is to accommodate any temperature drop when the hot water is mixed with the chemicals used in different processes. The solar water heating system that is being proposed as shown in Figure 22 is an active system. It includes a bank of solar collectors and a storage tank with a heating element. The heating element will only be used when the water temperature drops below 50 °C. The system is designed in this manner to investigate how much demand can be met from the solar supply.

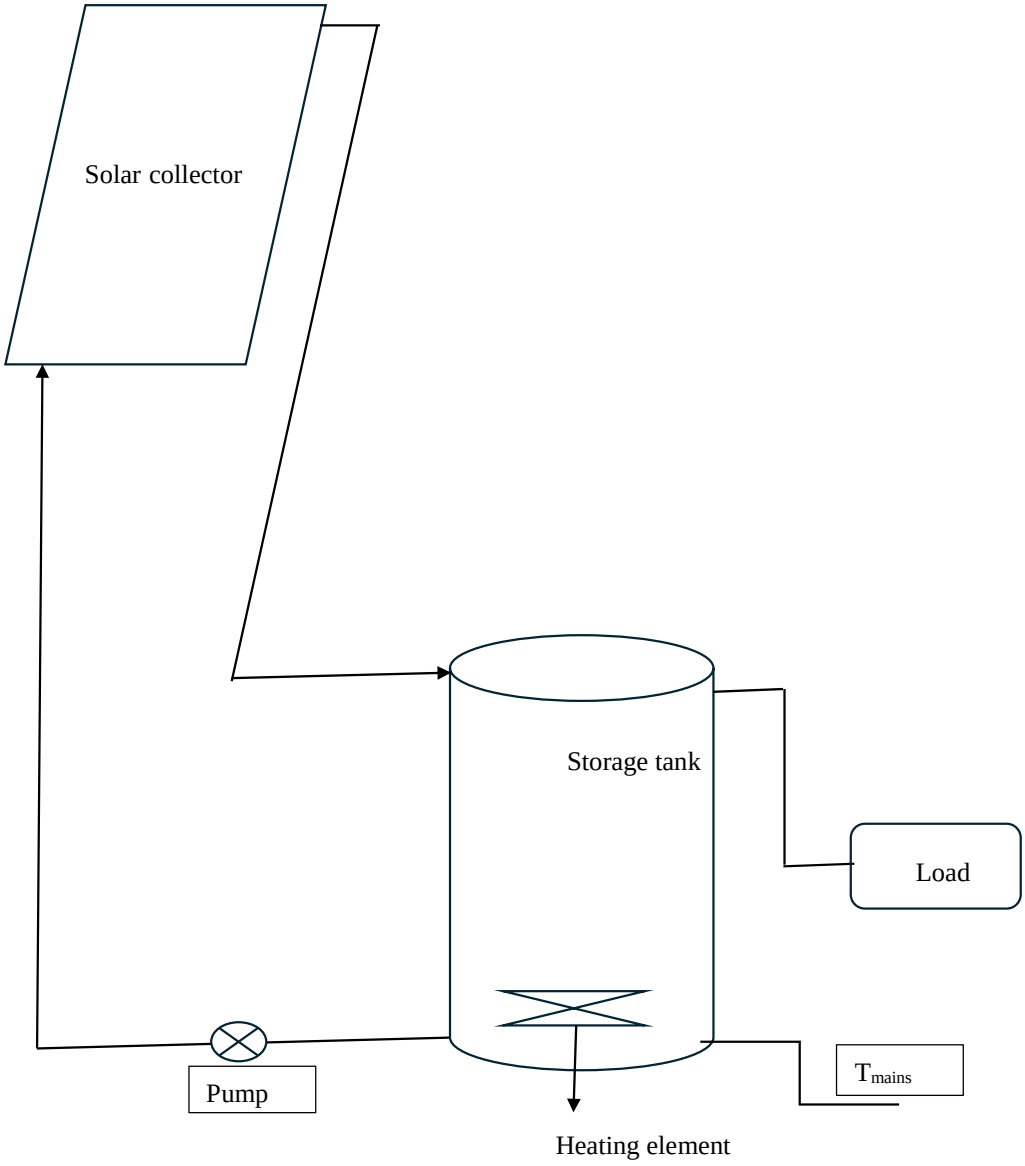

Figure 22: Proposed solar water heating system

3.3.2 Hot water demand profile

The demand profile of hot water was built based on the information provided by the laundry. There are four washing machines at the laundry, which can be programmed to perform the same processes or different processes depending on the types of orders received. The information provided by the laundry is tabulated in Table 5. It shows the typical types of processes run by washing machines, the hot water consumption, and the temperature at which the processes run. The detailed information was used to construct the hot water demand profile for the wetting processes in the laundry, as shown in Figure 23. It is worth noting that the laundry operates on double shifts, meaning it is in operation 24 hours a day. In this study, it is assumed that throughout the year, the laundry receives denim orders that typically utilize the same processes, with only the number of clothes to be processed differing.

Table 5: Laundry processes and the temperatures at which they operate

Process	Hot water consumption (L)	Temperature (°C)
Dark wash	1400	50
Enzyme	800	50
Mid bleach	1200	50
Light bleach	1400	50
Blue snow wash	1400	60
Dyeing	1200	50
Bleaching	2840	50
Enzyme II	1500	50

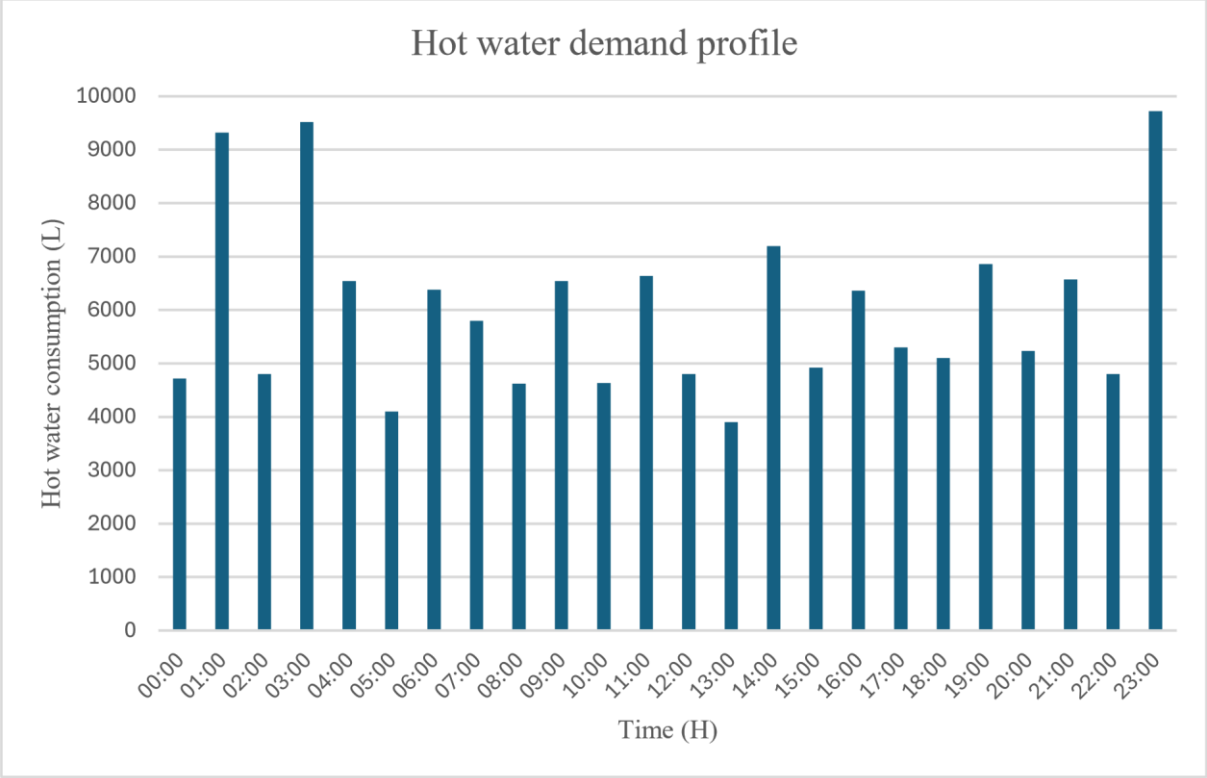

Figure 23: Hot water demand profile

The energy demand profile for the laundry wetting processes was also constructed using the hot water demand profile, as shown in Figure 24. To calculate the energy demand **Error! Reference source not found.** was used. The cold-water temperature from the main water supply differs from the ambient temperature. To find the cold-water temperature from the main water supply temperature, the relationship between ambient temperature and soil temperature is shown in **Error! Reference source not found.** was used. Since the main water supply pipes are embedded in the ground, the soil temperature was assumed to be equal to the cold water temperature [96].

$$QHWD = m \times Cp \times (T_{hot\ water} - T_{mains}) \quad \text{Equation 27}$$

Where;

Q_{HWD} denotes daily energy demand for hot water [kWh], m

is the daily hot water consumption [m^3],

Cp is the heat capacity of water [1.16 kWh/m^3K]

ΔT temperature difference - hot water temperature and cold-water temperature [K].

$$Tmains = 4.648 + 0.986\,x \quad \text{Equation 28}$$

Where;

T_{mains} is the cold-water temperature
x is the ambient temperature

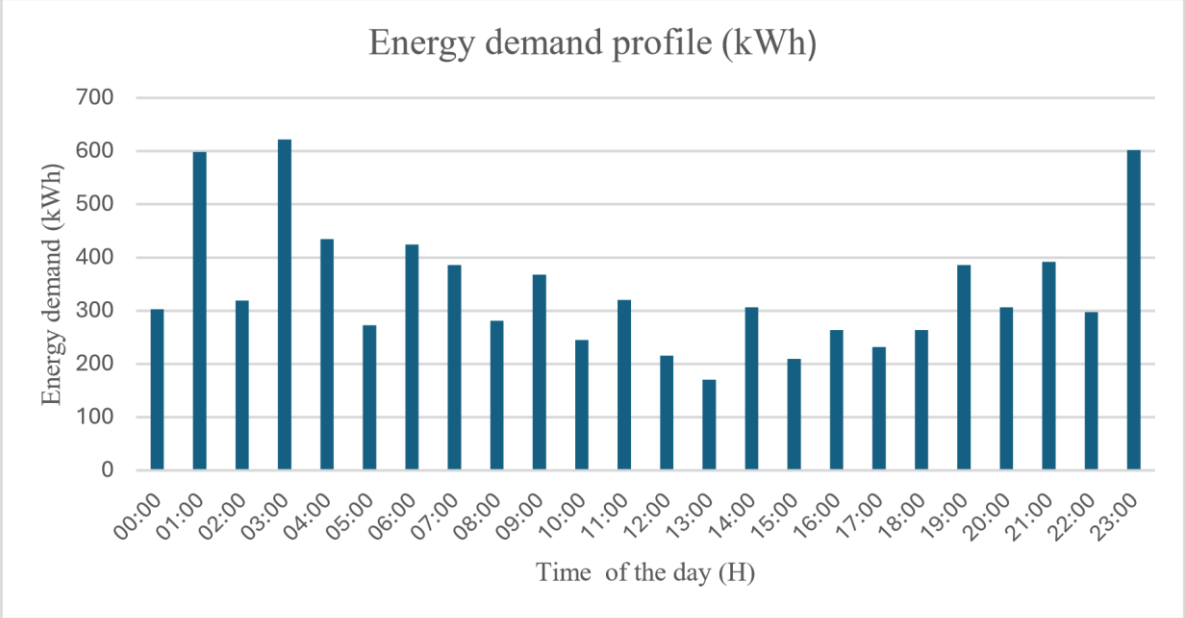

Figure 24: Energy demand profile

3.3.3 Determination of solar radiation

The geographical coordinates of the laundry, located at a latitude of -29.3° and a longitude of 27.46°, were important for determining the solar radiation data of the site. This data is crucial because the T*SOL software performs simulations using detailed meteorological inputs. By inputting the exact geographical location, the software can retrieve and utilize local solar radiation patterns, ambient temperature variations, and other weather-related factors. This information allows for the modelling of the solar water heating system's performance, ensuring that the simulations reflect the real-world conditions specific to the laundry location.

3.3.4 Solar collector selection

The collector selection is based on several key factors: the temperature required for the application, the optical efficiency of the collector, the working temperature of the collector, the annual solar irradiation at the proposed site, and the availability of roof space [4]. In this study, a flat-plate collector was chosen because the processes in the laundry require hot water at temperatures ranging between 30°C and 60°C which are within the operating temperature range of the flat-plate operate, and due to its low cost compared to the ETC and parabolic collectors.

3.3.5 Solar collector area determination

In determining the solar area, the laundry rooftop area of 1055.84 m^2 was considered to see whether the rooftop would accommodate the total collector area. It is known that the area of the solar collector field is obtained using **Error! Reference source not found.**.

$$A = \frac{Q}{\eta * Gt}$$ Equation 29

Where;

Q is the energy demand n is

the collector efficiency

G_t is the global horizontal radiation

3.3.6 Solar collector configuration

In industrial systems, many collectors are required to satisfy the heating demand. For this system, a series connection of collectors with a parallel flow, as shown in Figure *25* was incorporated because there have been many benefits associated with this configuration [42]. The parallel flow connection offers inherent balance, which ensures a uniform distribution of the fluid across all collectors, leading to consistent thermal performance. Additionally, it has a low pressure drop, which minimizes the energy required for pumping, thereby enhancing the overall efficiency of the system. Furthermore, the parallel flow setup can be easily drained, facilitating maintenance and reducing the risk of damage from freezing or stagnation [42].

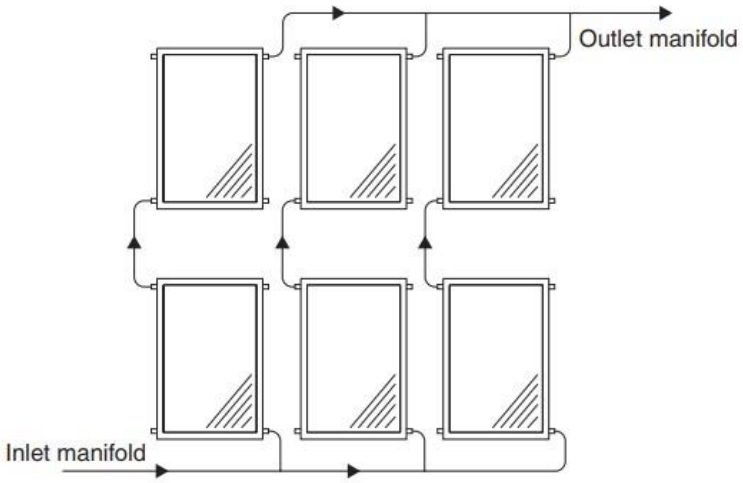

Figure 25: Series connection of collectors with parallel flow *[38]*

3.3.7 Storage tank sizing

The design of a storage tank for a solar thermal system involves considerations such as the energy demand, which is calculated using **Error! Reference source not found.**, temperature requirements, and storage duration. The volume of the storage tank (VSt) is thus calculated as follows in **Error! Reference source not found.**;

$$VSt = Hot\ Water\ Demand \times\ 1.2 \qquad \text{Equation 30}$$

3.4 Performance analysis of the designed system

To assess the performance of the system, the following performance indicators were used; solar collector useful energy, the solar fraction and the emissions avoided from using solar water heating systems.

3.4.1Solar collector useful energy

From the calculated solar collector area, the solar collector's useful energy can be calculated. The solar collector's useful energy is determined using the Hottel–Whillier–Bliss equation, and the '+' sign indicates that only the positive values of solar input Q_u are to be considered [49]. The useful solar energy is calculated using **Error! Reference source not found.**.

3.4.2 Emissions

Emissions calculations provide a broader view of the environmental benefits associated with the utilization of renewable energy technologies. These calculations help to quantify the amount of greenhouses particularly $C0_2$, that can be reduced by using the said technologies. To calculate the C_{O2} emissions**Error! Reference source not found.Error! Reference source not found.** was used.

$$Emissions\ (kg) = Coal\ consumption\ (kg) \times Emission\ factor\ (kg/t)$$ Equation 31

3.4.3 Solar fraction

The Solar Fraction describes the amount of energy provided by the solar thermal system divided by the total energy required.

$$Solar\ fraction = \frac{Energy\ supplied\ by\ the\ solar\ system}{Total\ energy\ supplied\ by\ the\ soalr\ system + auxiliary\ heating\ (Total\ energy\ required)}$$ Equation 32

3.5 Energy balance of solar water heating systems

The energy flow analysis of the solar water heating system describes the rate at which the internal energy of water changes at a given time-step, usually one hour. It is conducted to determine the long-term thermal performance and efficiency of the system, as well as to assess the impact of operation under different weather conditions [42]. The rate at which the internal energy of water changes is given by **Error! Reference source not found.**. The variables on the right side of the equation are collector useful energy as described in the solar collector performance subsection, the rate of heat losses and the storage tank losses. The rate of heat losses is given by **Error! Reference source not found.Error! Reference source not found.**. The storage tank losses describe the rate of heat loss from the storage to the surrounding environment is given by **Error! Reference source not found.**.

$$(MCp)_s = \frac{dT_s}{dt} = Q_u - L_s$$ Equation 33

$$L_s = \dot{m}_s C_P (T_s - T_{mains})$$ Equation 34

Where;

$\dot{m}_s$ is the mass flowrate of hot water from the solar storage tank

C_p is the specific heat capacity of water (4,200 J/kg/°C)

T_s is the temperature of the storage tank contents,

T_{mains} is the temperature of cold water from the main supply.

$$S_{loss} = U_s A_s (T_s - T_a)$$ Equation 35 *Where;*

U_s is the storage heat loss coefficient,

A_s is the surface area of the storage tank,

T_s is the temperature of the storage tank contents and

T_a is the temperature of the tank surroundings

3.6 Financial analysis

The economic analysis of solar energy systems is carried out to determine the least cost of meeting the energy demand. For the economic analysis, the investment cost was calculated using Equation 36, was used as input for the analysis in the software. Table *6* shows the cost of the system components. Since a simulation for the designed system was done, the economic analysis results were taken from the simulation project report.

$$Investment\ cost = C_c \times A_C + C_t \times V_t + C_p + C_i + C_{aux} \quad \text{Equation 36}$$

Table 6: Cost of system components

System components	**Price (M)**
Collector	4,695/ 2 m^2
Tank	93,000 / 2 m^3
Auxiliary heating	300,000
Piping and installation	15% of the total cost

4 RESULTS AND DISCUSSION

4.1 Overview

To identify the most efficient system for meeting the hot water demand of the wetting processes at the laundry facility, six separate simulations were performed using T*SOL. Each simulation used the same system configuration, differing only in the area of the collectors and the storage tank capacity. The storage tank capacities used were 0.9, 1.04 and 1.2 fold the hot water demand, as it is recommended that the storage capacity should be no less than 90% and no more than 120% of the calculated volume. This approach allowed for a thorough comparative analysis, helping to identify the optimal system configuration. By evaluating the performance of these simulations, it was aimed to find the best balance between the solar energy contribution and the overall system efficiency. This comparison was important in selecting the most suitable system for sustainable and cost-effective hot water production for the wetting processes at the laundry facility. The key topics in this section are simulation input parameters, system design, energy balance of the designed systems, performance analysis and financial analysis of the system.

4.2 Simulation input parameters

Figure 26, Figure 27 and Figure 28 show the input parameters used in the design of the six solar water heating systems in the T*SOL simulation software. The parameters include the annual global radiation of the location, the daily hot water consumption, the desired temperature, the collector area, the number of collectors and the type of collector used. In addition, Figure *26*, Figure 27 and Figure 28 also show the collector inclination angle and the storage tank volume used for the simulation. These parameters are essential for modelling and comparing the performance of the six systems.

Variant	Variant 1
System	A1.2
Location	Maseru
Global radiation	2091,721 kWh/m²
Site Data DHW	
Daily consumption	144,37 m³
Desired temperature	80 °C
Consumption profile	Krankenhaus (Copy) (Copy)
Collector array 1	
Number of collectors	2672,0
Total gross surface area	2 672,00 m²
Manufacturer	Dimas SA
Type	RADIANT RSV 25
Inclination (Tilt Angle)	30,0 °
Orientation	0,0 °
Tank 1	
Type	Dual coil indirect hot water tank incl. heating element (225 kW)
Manufacturer	Standard
Name	2 x Dual coil indirect hot water tank
Volume	2 x 75 m³

Variant	Variant 1
System	A1.2
Location	Maseru
Global radiation	2091,721 kWh/m²
Site Data DHW	
Daily consumption	144,37 m³
Desired temperature	80 °C
Consumption profile	Krankenhaus (Copy) (Copy)
Collector array 1	
Number of collectors	1980,0
Total gross surface area	1 980,00 m²
Manufacturer	Dimas SA
Type	RADIANT RSV 25
Inclination (Tilt Angle)	30,0 °
Orientation	0,0 °
Tank 1	
Type	Dual coil indirect hot water tank incl. heating element (150 kW)
Manufacturer	Standard
Name	3 x Dual coil indirect hot water tank
Volume	3 x 50 m³

Figure 26: Simulation input parameters for both designs with a storage capacity of 150 m^3; Left: 2672 m^2 collector area; Right: 1980 m^2 collector area

Variant	Variant 1
System	A1.2
Location	Maseru
Global radiation	2091,721 kWh/m²
Site Data DHW	
Daily consumption	144,37 m³
Desired temperature	80 °C
Consumption profile	Krankenhaus (Copy) (Copy)
Collector array 1	
Number of collectors	2672,0
Total gross surface area	2 672,00 m²
Manufacturer	Dimas SA
Type	RADIANT RSV 25
Inclination (Tilt Angle)	30,0 °
Orientation	0,0 °
Tank 1	
Type	Dual coil indirect hot water tank incl. heating element (259,87 kW)
Manufacturer	Standard
Name	2 x Dual coil indirect hot water tank
Volume	2 x 86,62 m³

Variant	Variant 1
System	A1.2
Location	Maseru
Global radiation	2091,721 kWh/m²
Site Data DHW	
Daily consumption	144,37 m³
Desired temperature	80 °C
Consumption profile	Krankenhaus (Copy) (Copy)
Collector array 1	
Number of collectors	1980,0
Total gross surface area	1 980,00 m²
Manufacturer	Dimas SA
Type	RADIANT RSV 25
Inclination (Tilt Angle)	30,0 °
Orientation	0,0 °
Tank 1	
Type	Dual coil indirect hot water tank incl. heating element (259,86 kW)
Manufacturer	Standard
Name	2 x Dual coil indirect hot water tank
Volume	2 x 86,62 m³

Figure 27: Simulation input parameters for both designs with a storage capacity of 173 m^3; Left: 2672 m^2 collector area; Right: 1980 m^2 collector area

Variant	Variant 1
System	A1.2
Location	Maseru
Global radiation	2091,721 kWh/m²
Site Data DHW	
Daily consumption	144,37 m³
Desired temperature	80 °C
Consumption profile	Krankenhaus (Copy) (Copy)
Collector array 1	
Number of collectors	2672,0
Total gross surface area	2 672,00 m²
Manufacturer	Dimas SA
Type	RADIANT RSV 25
Inclination (Tilt Angle)	30,0 °
Orientation	0,0 °
Tank 1	
Type	Dual coil indirect hot water tank incl. heating element (195 kW)
Manufacturer	Standard
Name	2 x Dual coil indirect hot water tank
Volume	2 x 65 m³

Variant	Variant 1
System	A1.2
Location	Maseru
Global radiation	2091,721 kWh/m²
Site Data DHW	
Daily consumption	144,37 m³
Desired temperature	80 °C
Consumption profile	Krankenhaus (Copy) (Copy)
Collector array 1	
Number of collectors	1980,0
Total gross surface area	1 980,00 m²
Manufacturer	Dimas SA
Type	RADIANT RSV 25
Inclination (Tilt Angle)	30,0 °
Orientation	0,0 °
Tank 1	
Type	Dual coil indirect hot water tank incl. heating element (195 kW)
Manufacturer	Standard
Name	2 x Dual coil indirect hot water tank
Volume	2 x 65 m³

Figure 28: Simulation input parameters for both designs with a storage capacity of 130 m^3; Left: 2672 m^2 collector area; Right: 1980 m^2 collector area

4.3 System design

The designed solar water heating systems, capable of meeting the hot water demand of 144.37 m^3 is a Hot water System with an electric water heater, as shown below in Figure 29, Figure 31 and Figure 34. This design was chosen to replace the boiler system, which used fossil fuels for heating the water required by the laundry wetting processes. The components of the new system include Dimas SA RADIANT RSV 25 flat-plate collectors at a 30° inclination angle, dual coil indirect hot water tank, and 150 kW electric element to meet the daily hot water demand of 144.37 m^3. The flat-plate collectors were selected for this system because they can efficiently provide hot water within the required temperature range.

The system A, as shown in Figure 29 consists of two 75 m^3 dual coil indirect hot water tanks, flat-plate collectors with a collector area of 2,672 m^2 and a 150 kW electric element. From the annual simulation results in Figure 30, the hot water system has a thermal energy demand of 3,242,724.09 kWh. However, the energy supplied to the system is 3,011,306.09 kWh, of which 2,765,858.03 kWh is the solar energy contribution and 269,932.05 kWh is the energy supplied

by the electric element. Furthermore, the system has an efficiency of 45.5% and a solar fraction of 91.1%.

As shown in Figure 29 System B consists of three 50 m^3 dual coil indirect hot water tanks, and flat-plate collectors with a collector area of 1,980 m^2. The annual simulation results are presented in Figure 30, indicate that the system has a thermal energy demand of 3,284,966.79 kWh However, the energy supplied to the system is 2,762,106.05 kWh, of which 2,462,283.46 kWh is the solar energy contribution and 318,502.5 kWh is the energy supplied by the electric element. The system has an efficiency of 54.7% solar fraction of 88.5%.

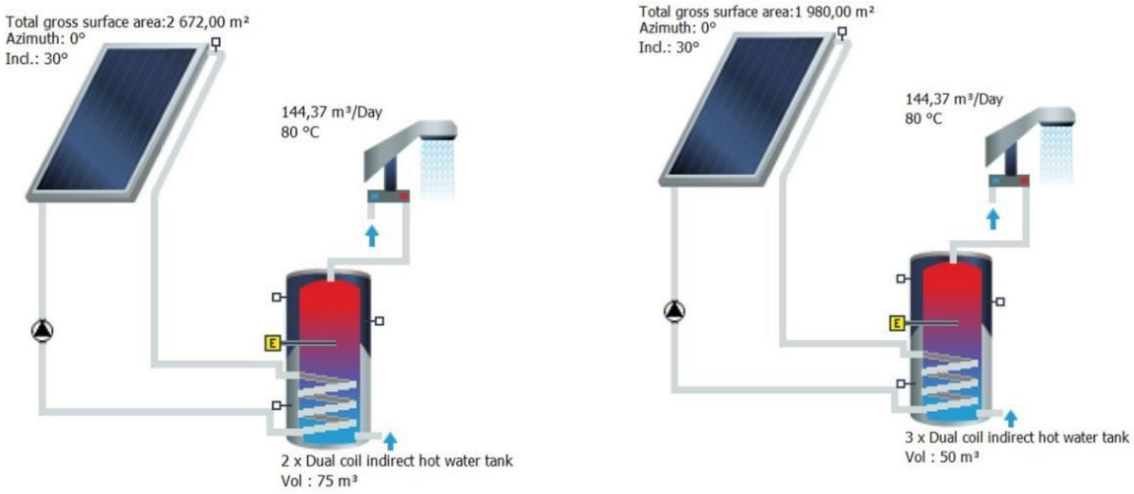

Figure 29: Hot water (HW) system with electric water heater: Left; HW system with 2672 m^2 collector area (System A). Right; HW system with 1980 m^2 collector area (System B)

DHW heating energy requirement:	3 242 724,09 kWh
DHW heating energy supply:	3 011 306,09 kWh
Solar energy contribution to DHW:	2 765 858,03 kWh
Energy from auxiliary heating:	269 932,5 kWh
Natural gas (H) savings:	**340 304,4 m³**
CO2 emissions avoided:	**719 621,79 kg**
DHW solar fraction:	**91,1 %**
Relative savings of supplementary energy (DIN EN 12977):	**91,7 %**
System efficiency:	**45,5 %**

DHW heating energy requirement:	3 284 966,79 kWh
DHW heating energy supply:	2 762 106,05 kWh
Solar energy contribution to DHW:	2 462 283,46 kWh
Energy from auxiliary heating:	318 502,5 kWh
Natural gas (H) savings:	**302 953,3 m³**
CO2 emissions avoided:	**640 637,67 kg**
DHW solar fraction:	**88,5 %**
Relative savings of supplementary energy (DIN EN 12977):	**90,3 %**
System efficiency:	**54,7 %**

Figure 30: Annual simulation results of the two systems, System A and System B

System C depicted in Figure 31, consists of two 86,65 m^3 dual coil indirect hot water tanks, flat-plate collectors with a collector area of 2,672 m^2 and a 150 kW electric element as shown in. The annual simulation results in Figure 32 also show that the system has a thermal energy demand of 3,242,724.09 kWh. However, the energy supplied to the system is 3,051,824.92 kWh, of which 2,824,482.42 kWh is the solar energy contribution and 254,696.1 kWh is the energy supplied by the electric element. The system exhibits an efficiency of 46.5% and a solar fraction of 91.7%.

Figure 31 illustrates system D, which is made up of two 86,65 m^3 dual coil indirect hot water tanks, a 150 kW electric element and flat-plate collectors with a collector area of 1,980 m^2. The annual simulation results in Figure 33 show that the thermal energy demand for the system is 3,284,966.79 kWh, and only 2,796,361.30 kWh is supplied. From the energy supplied 2,500,249.32 kWh is the solar contribution and 313,452.2 is the energy supplied by the electric element (auxiliary heater). System D has an efficiency of 55.5% and a solar fraction of 90.5%.

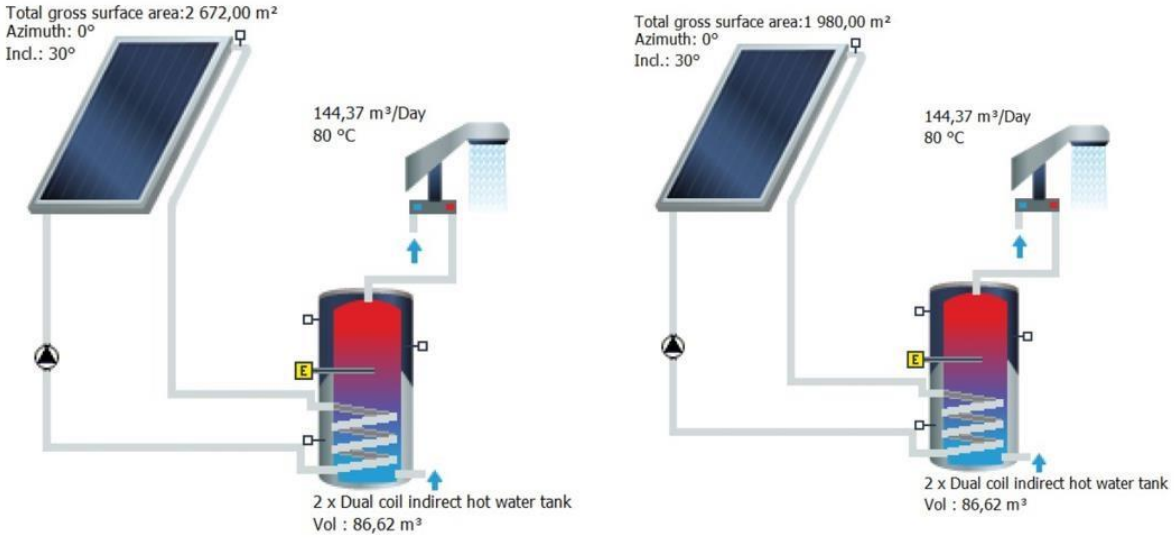

Figure 31: Hot water system with electric heater: Left; Hot water system with 2672 m^2 collector area (System C). Right; Hot water system with 1980 m^2 collector area (System D)

DHW heating energy requirement:	3 242 724,09 kWh
DHW heating energy supply:	3 051 824,92 kWh
Solar energy contribution to DHW:	2 824 482,42 kWh
Energy from auxiliary heating:	254 696,1 kWh
Natural gas (H) savings:	**347 517,4 m³**
CO2 emissions avoided:	**734 874,70 kg**
DHW solar fraction:	**91,7 %**
Relative savings of supplementary energy (DIN EN 12977):	**92,2 %**
System efficiency:	**46,5 %**

Figure 32: Annual simulation results for system C

DHW heating energy requirement:	3 284 966,79 kWh
DHW heating energy supply:	2 796 361,30 kWh
Solar energy contribution to DHW:	2 500 249,32 kWh
Energy from auxiliary heating:	313 452,2 kWh
Natural gas (H) savings:	**307 624,6 m³**
CO2 emissions avoided:	**650 515,64 kg**
DHW solar fraction:	**88,9 %**
Relative savings of supplementary energy (DIN EN 12977):	**90,5 %**
System efficiency:	**55,5 %**

Figure 33: Annual simulation results for System D

As illustrated in Figure 34, system E consists of two 65 m^3 dual coil indirect hot water tanks, flat-plate collectors with a collector area of 2,672 m^2 and a 150 kW electric element. The annual simulation results in Figure 35 show that the system has a thermal energy demand of 3,242,724.09 kWh. However, the energy supplied to the system is 2,961,506.53 kWh, of which 2,708,781.03 kWh is the solar energy contribution and 274,527.5 kWh is the energy supplied by the electric element. The system has a system efficiency of 44.6% and a solar fraction of 91.6%.

System F shown in Figure 34 is made up of two 65 m^3 dual coil indirect hot water tanks, a 150 kW electric element and flat-plate collectors with a collector area of 1,980 m^2. The annual simulation results in Figure 36 indicate that the thermal energy demand for the system is 3,284,966.79 kWh, and only 2,716,002.25 kWh is supplied. From the energy supplied 2,415,406.3 kWh is the solar contribution and 314,093.0 is the energy supplied by the electric element (auxiliary heater). Comparing all the systems, system F has the highest solar fraction of 92.2% and system D has the highest system efficiency of 55.5%. The results of the current study align closely with those of a previous study in solar water heating conducted in various cities in South Africa, which reported an average solar fraction of 95% for the designed system [97]. Similarly, the systems designed in this study demonstrate comparable performance, indicating consistency with the earlier findings.

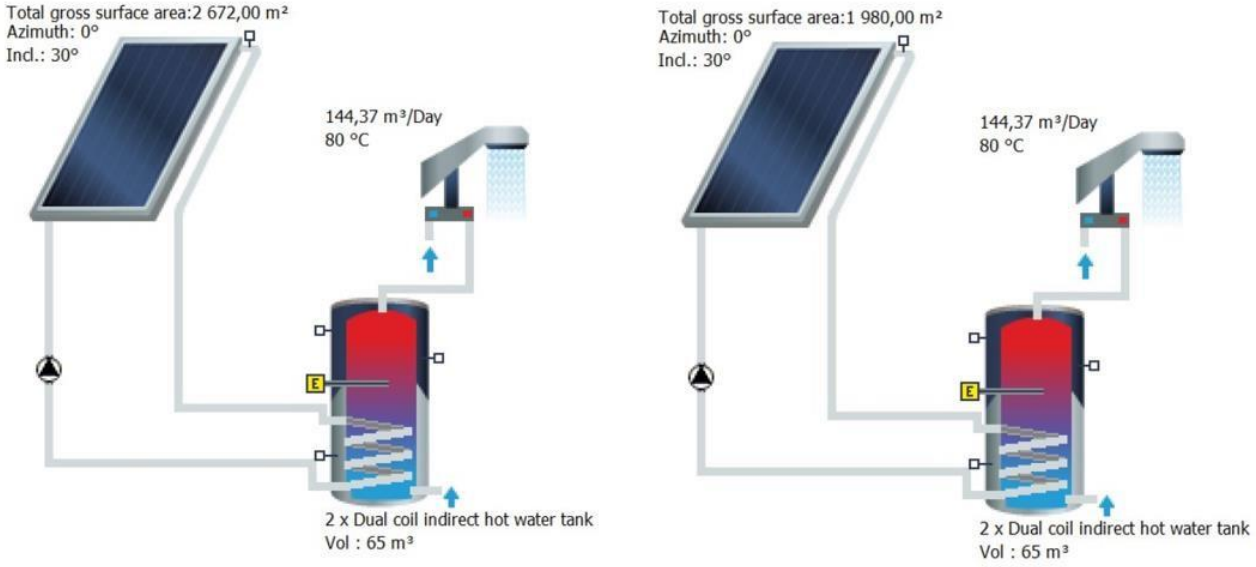

Figure 34: Hot water system with electric heater: Left; Hot water system with 2672 m^2 collector area (System E). Right; Hot water system with 1980 m^2 collector area (System F)

DHW heating energy requirement:	3 242 724,09 kWh
DHW heating energy supply:	2 961 506,53 kWh
Solar energy contribution to DHW:	2 708 781,03 kWh
Energy from auxiliary heating:	274 527,5 kWh
Natural gas (H) savings:	**333 281,8 m³**
CO2 emissions avoided:	**704 771,48 kg**
DHW solar fraction:	**90,8 %**
Relative savings of supplementary energy (DIN EN 12977):	**91,6 %**
System efficiency:	**44,6 %**

Figure 35: System E annual simulation results

DHW heating energy requirement:	3 284 966,79 kWh
DHW heating energy supply:	2 716 002,25 kWh
Solar energy contribution to DHW:	2 415 406,64 kWh
Energy from auxiliary heating:	314 093,0 kWh
Natural gas (H) savings:	**297 185,7 m³**
CO2 emissions avoided:	**628 441,24 kg**
DHW solar fraction:	**88,5 %**
Relative savings of supplementary energy (DIN EN 12977):	**90,5 %**
System efficiency:	**53,6 %**

Figure 36: System F annual simulation results

4.4 Energy balance of the systems

The energy balance analysis provides a comprehensive overview of the performance and efficiency of systems A, B, C, D, E and F. The results highlight the various stages of energy input, transfer and losses within each system, ultimately showing their overall efficiency and effectiveness in meeting the thermal energy demands.

The collectors in system A, as depicted in Figure *37* A receives 6,077,528 kWh of solar irradiation. However, due to the optical collector losses amounting to 1,454,627 kWh and the thermal collector losses of 1,828,486 kWh, the energy reaching the collector is reduced to 2,794,694 kWh. The process of transferring this solar energy to the solar tank involves further losses through convection and conduction, resulting in an actual transfer of 2,770,872 kWh. There are also internal piping losses of 647 kWh, external piping of 23,175 kWh and tank losses of 36,473 kWh. With the supplementary energy input of 269,933 kWh from the electric element, the total energy in the storage tank to meet the thermal energy demand is 3,011,306 kWh. The energy losses in System A account for 55% of the total energy input.

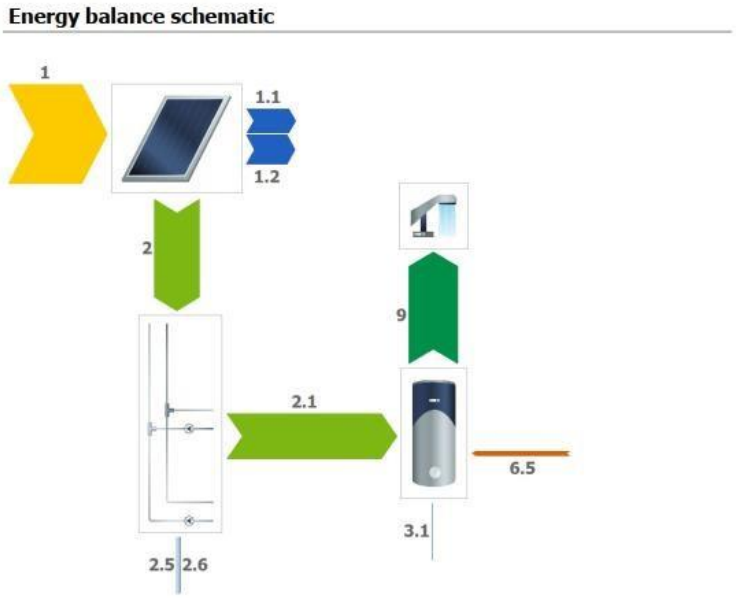

Legend		
1	Irradiation on collector surface (active)	6 077 528 kWh
1.1	Optical collector losses	1 454 627 kWh
1.2	Thermal collector losses	1 828 486 kWh
2	Energy from collector array	2 794 694 kWh
2.1	Solar energy to storage tank	2 770 872 kWh
2.5	Internal piping losses	647 kWh
2.6	External piping losses	23 175 kWh
3.1	Tank losses	36 473 kWh
6.5	Electric element	269 933 kWh
9	DHW energy from tank	3 011 306 kWh

Figure 37: Energy balance schematic for system A

Since systems C and E use the same collector area as system A, they receive the same solar radiation of 6,077,528 kWh, as shown in Figure 38 and Figure 39. In System C, optical losses of 1,456,627 kWh and thermal losses of 1,770,242 kWh reduce the collector array energy to 2,852,922 kWh. Through convection and conduction, the solar energy transferred to the solar tank is 2,829,761 kWh. There are also internal piping losses of 628 kWh, external piping of 22,533 kWh and tank losses of 40,323 kWh. With an additional energy input from the electric element of 254,696 kWh, the total energy in the storage tank to meet the thermal energy demand is 3,051,825 kWh.

Similarly, system E also incurs the optical collector losses of 1,454,627 kWh and thermal collector losses of 1,885,284 kWh, thus reducing the collector array energy to 2,737,899 kWh. Because of more heat losses, the solar energy transferred to the tank is 2,713,437 kWh. The internal piping losses of 666 kWh, external losses of 23,796 kWh and tank losses of 32,825 kWh further reduce the energy. With the supplementary energy input of 274,528 kWh from the electric element, the total energy in the storage tank to meet the thermal energy demand is 2,961,507 kWh. The energy losses in System C account for 54% of the total energy input, while the energy losses in System E account for 56% of the total energy input.

Energy balance schematic

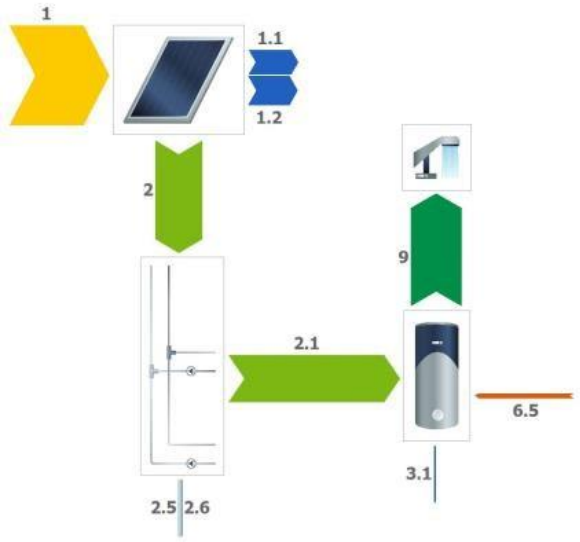

Legend		
1	Irradiation on collector surface (active)	6 077 528 kWh
1.1	Optical collector losses	1 454 627 kWh
1.2	Thermal collector losses	1 770 242 kWh
2	Energy from collector array	2 852 922 kWh
2.1	Solar energy to storage tank	2 829 761 kWh
2.5	Internal piping losses	628 kWh
2.6	External piping losses	22 533 kWh
3.1	Tank losses	40 323 kWh
6.5	Electric element	254 696 kWh
9	DHW energy from tank	3 051 825 kWh

Figure 38: Energy balance schematic for system C

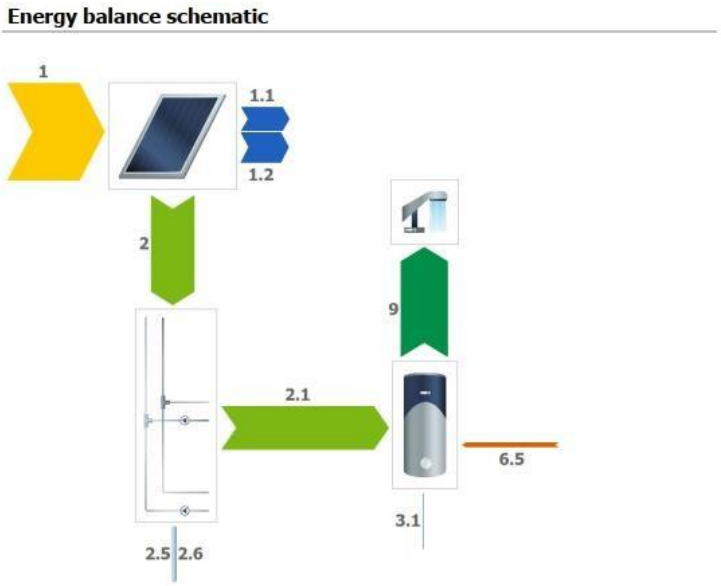

Legend		
1	Irradiation on collector surface (active)	6 077 528 kWh
1.1	Optical collector losses	1 454 627 kWh
1.2	Thermal collector losses	1 885 284 kWh
2	Energy from collector array	2 737 899 kWh
2.1	Solar energy to storage tank	2 713 437 kWh
2.5	Internal piping losses	666 kWh
2.6	External piping losses	23 796 kWh
3.1	Tank losses	32 825 kWh
6.5	Electric element	274 528 kWh
9	DHW energy from tank	2 961 507 kWh

Figure 39: Energy balance schematic for system E

The collectors in system B receive 4,503,557 kWh of solar irradiation. After accounting for optical collector losses of 1,077,905 kWh and thermal collector losses of 947,066 kWh, the energy reaching the collector in system B is reduced to 2,478,755 kWh. Through convection and conduction, the solar energy transferred to the solar tank after convection and conduction losses amount to 2,466,017 kWh. Additional losses occur which include 463 kWh from the internal piping, 12,275 kWh from external piping, and 29,955 kWh from the tank. The electric element adds 318,503 kWh, making the total energy in the storage tank to meet the thermal energy demand 2,762,106 kWh. The energy losses in System B account for 46% of the total energy input.

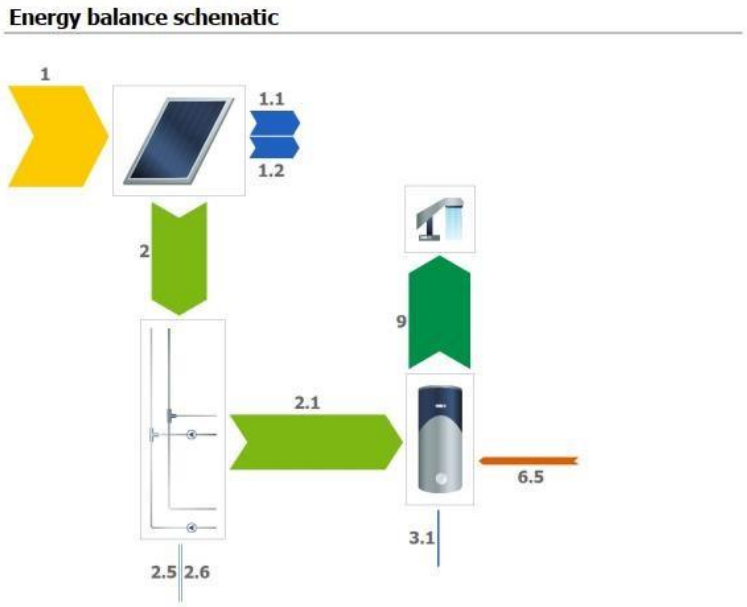

Legend		
1	Irradiation on collector surface (active)	4 503 557 kWh
1.1	Optical collector losses	1 077 905 kWh
1.2	Thermal collector losses	947 066 kWh
2	Energy from collector array	2 478 755 kWh
2.1	Solar energy to storage tank	2 466 017 kWh
2.5	Internal piping losses	463 kWh
2.6	External piping losses	12 275 kWh
3.1	Tank losses	29 955 kWh
6.5	Electric element	318 503 kWh
9	DHW energy from tank	2 762 106 kWh

Figure 40: Energy balance schematic for system B

System D and system F also receive the same amount of irradiation on the collector surface of 4,503,557 kWh as shown in Figure 41 and Figure 42. In system D, the optical collector losses of 1,077,905 kWh and thermal collector losses of 909,768 kWh reduce the collector array energy to 2,516,052 kWh. After further convection and conduction losses, the solar energy transferred to the solar tank is 2,503,775 kWh. There are also internal piping losses of 446 kWh, external piping of 11,831 kWh and tank losses of 28,467 kWh. With an additional energy input from the electric element of 313,452 kWh, the total energy in the storage tank to meet the thermal energy demand is 2,796,361 kWh. System F also incurs the optical collector losses of 1,077,905 kWh and thermal collector losses of 994,021 kWh, thus reducing the collector array energy to 2,431,801 kWh. Because of more heat losses, the solar energy transferred to the tank is 2,418,484 kWh. The internal piping losses of 485 kWh, external losses of 12,832 kWh and tank losses of 23,892 kWh further reduce the energy in the storage tank. With the supplementary energy input of 314,093 kWh from the electric element, the total energy in the storage tank to meet the thermal energy demand is 2,716,002 kWh. The energy losses in System D account for 45% of the total energy input, while the energy losses in System F account for 47% of the total energy input.

Comparing all the systems, system D has the lowest energy losses at 45% of the total energy input, followed by system B at 46%, system F at 47%, system C at 54%, system A at 55% and lastly system E with the highest energy losses of 56% of the total energy input. Systems B, D, and F, with smaller initial energy inputs, experience lower energy losses compared to Systems A, C, and E, which have larger inputs but greater losses.

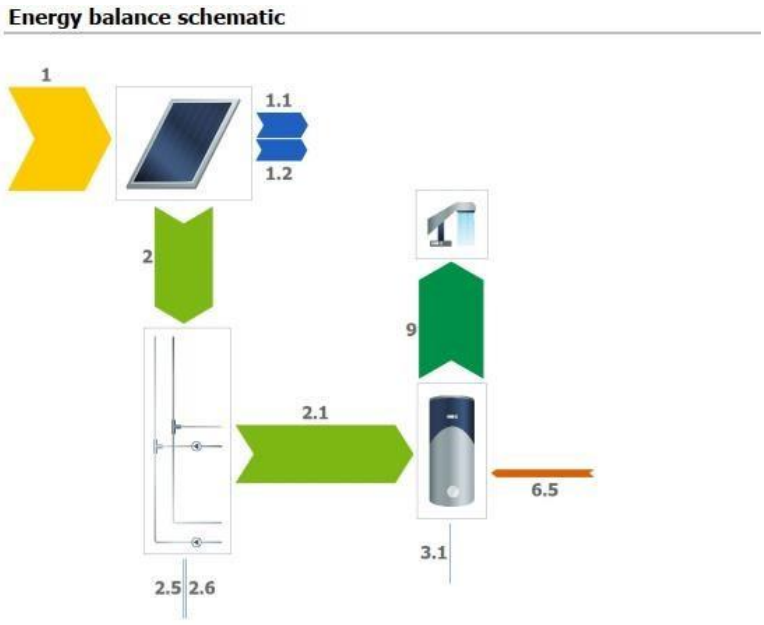

Legend		
1	Irradiation on collector surface (active)	4 503 557 kWh
1.1	Optical collector losses	1 077 905 kWh
1.2	Thermal collector losses	909 768 kWh
2	Energy from collector array	2 516 052 kWh
2.1	Solar energy to storage tank	2 503 775 kWh
2.5	Internal piping losses	446 kWh
2.6	External piping losses	11 831 kWh
3.1	Tank losses	28 467 kWh
6.5	Electric element	313 452 kWh
9	DHW energy from tank	2 796 361 kWh

Figure 41: Energy balance schematic for system D

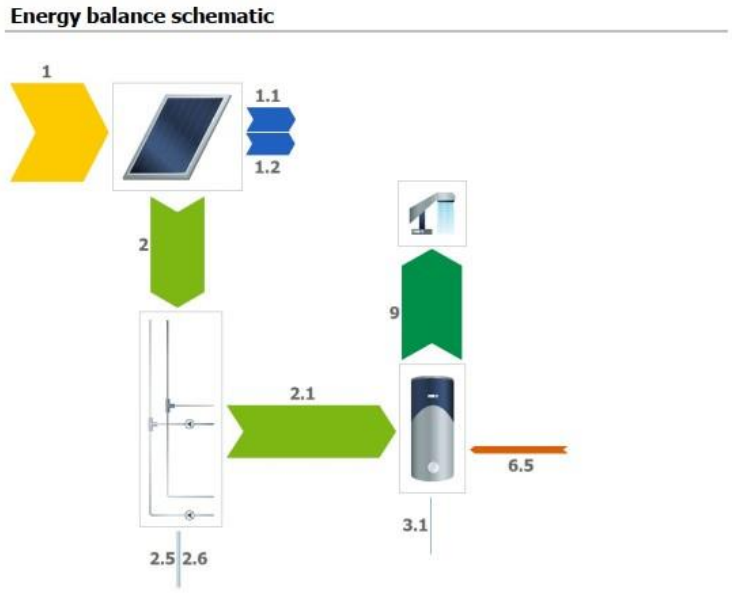

Legend		
1	Irradiation on collector surface (active)	4 503 557 kWh
1.1	Optical collector losses	1 077 905 kWh
1.2	Thermal collector losses	994 021 kWh
2	Energy from collector array	2 431 801 kWh
2.1	Solar energy to storage tank	2 418 484 kWh
2.5	Internal piping losses	485 kWh
2.6	External piping losses	12 832 kWh
3.1	Tank losses	23 892 kWh
6.5	Electric element	314 093 kWh
9	DHW energy from tank	2 716 002 kWh

Figure 42: Energy balance schematic for system F

4.5 Performance analysis of the designed systems

4.5.1 Solar energy consumption as percentage of total energy consumption

As the goal is to maximize the use of solar energy to meet the hot water demand, all the systems demonstrate a significant solar contribution. In system A, as shown in Figure *43*, the total energy consumption is 3,035,792 kWh, with 2,765,859 kWh supplied by solar energy. This means that 91.1% of the required energy to be supplied to the system comes from the solar contribution, highlighting the system's efficiency in harnessing solar power.

Similarly, as shown in Figure 44, System B's solar contribution to the total energy consumption of 2,780,787 kWh is 2,462,284 kWh, indicating that that 88.5% of the thermal demand is met by solar energy, reflecting the system's strong reliance on solar energy.

System C in Figure 45 has a total energy consumption of 3,079,181 kWh, with 2,824,483 kWh supplied by solar energy. This shows that 92% of the energy comes from solar contribution. Additionally, Figure 46 shows how much energy is contributed by solar energy by system D.

It is shown that of the total energy consumption of 2,813,957 kWh, 88.9% of the energy supplied comes from the solar contribution of 2,500,323 kWh.

Furthermore, in system E, as shown in Figure 47, the total energy consumption is 2,983,309 kWh, with 2,708,781 kWh supplied by solar energy, accounting for 91%. As shown Figure 48, System F's solar contribution to the total energy consumption of 2,729,499 kWh is 2,415,406 kWh, indicating that that 88.5% of the thermal demand is met by solar energy. All the systems have a higher solar contribution, indicating that the system can harness more solar energy.

However, seasonal variations impact the performance of these designed systems. During the months of June, July, and August, there is a decrease in solar energy contribution due to the low solar radiation. To meet the energy demand shortfall during these months, an auxiliary heater is used. This auxiliary support ensures the system's reliability and demonstrates a wellbalanced approach, integrating renewable energy while compensating for its seasonal limitations. The auxiliary heater's role, although secondary, is important in maintaining an uninterrupted energy supply, thereby enhancing the system's overall effectiveness and dependability.

For system A, 269,933 kWh is supplied by the auxiliary heater, which accounts for 8.9% of the required energy. In System B, the auxiliary heater contributes 319,503 kWh, which is 11.5% of the required energy. In system C, the auxiliary heater supplies 254,698 kWh, representing 8% of the required energy. In system D, the auxiliary heater supplies 313,634 kWh, which equates to 11.1% of the required energy. System E receives 274,528 kWh from the auxiliary heater, which accounts for 8.9% of the required energy. Lastly, system F receives 314,093 kWh from the auxiliary heater, covering 11.5% of the required energy.

Comparing the systems, systems B, D and F rely more on the auxiliary heater than systems A, C and E, indicating higher electricity consumption to meet the demand. This increased dependence on the auxiliary heater in the aforementioned systems suggests that while they may have a high solar contribution, their efficiency is slightly lower than that of System A, Cand E, particularly during the periods of reduced solar radiation.

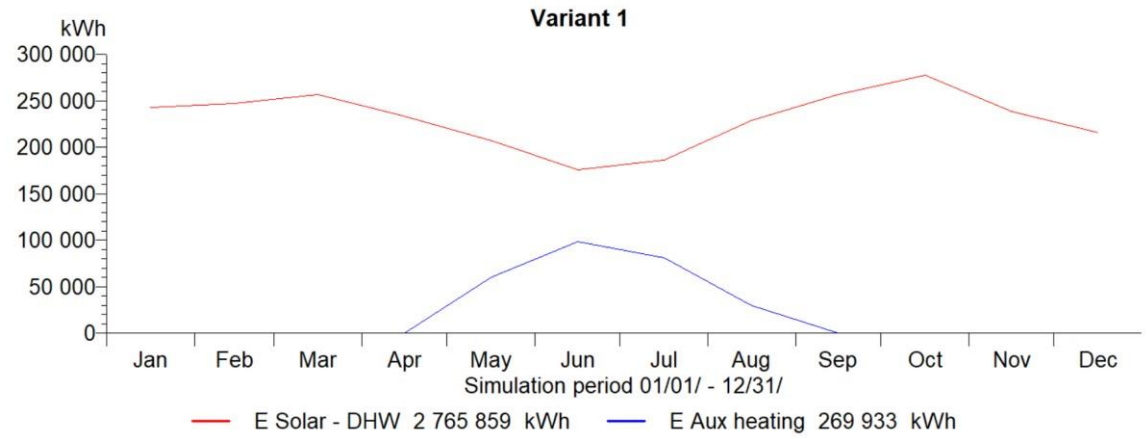

Figure 43:System A solar energy contribution vs Auxiliary heating energy

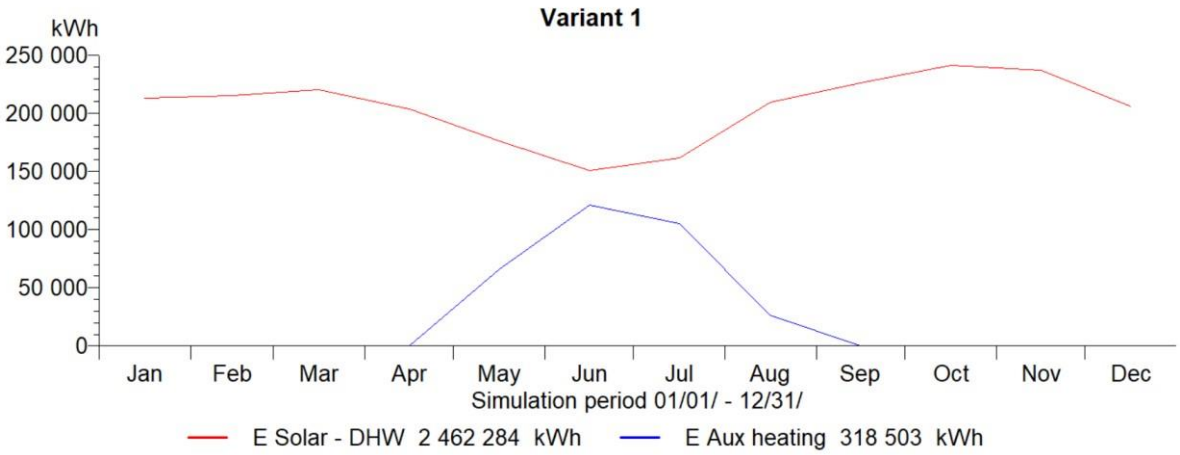

Figure 44: System B solar energy contribution vs auxiliary heating energy

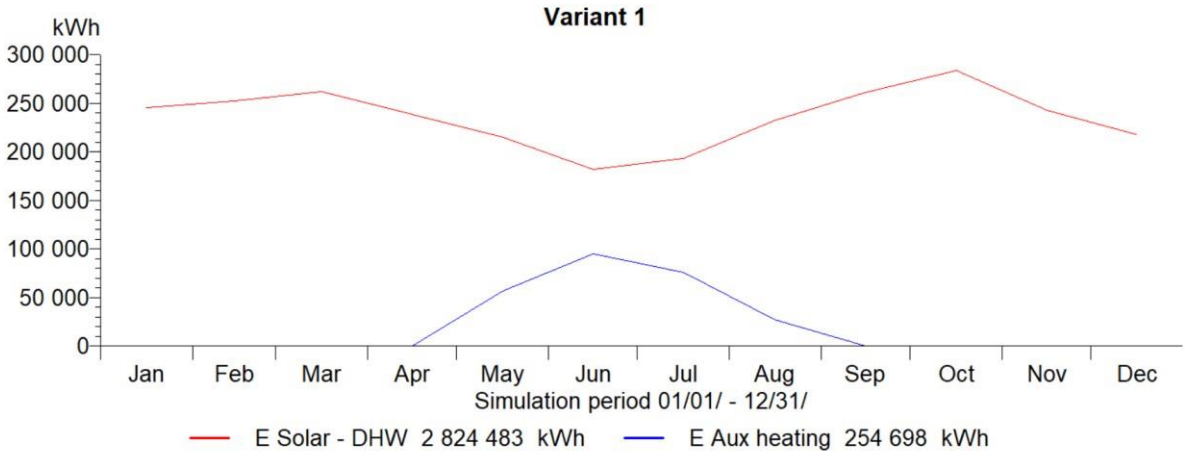

Figure 45: System C solar energy contribution vs auxiliary heating energy

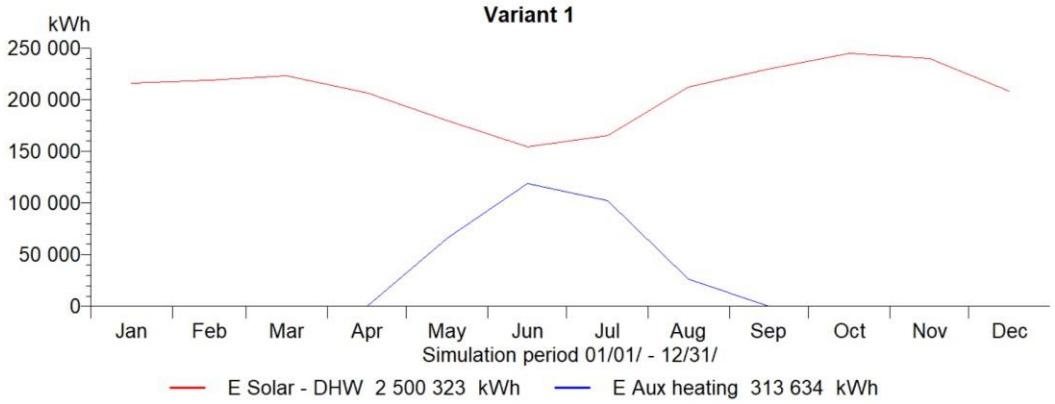

Figure 46: System D solar energy contribution vs auxiliary heating energy

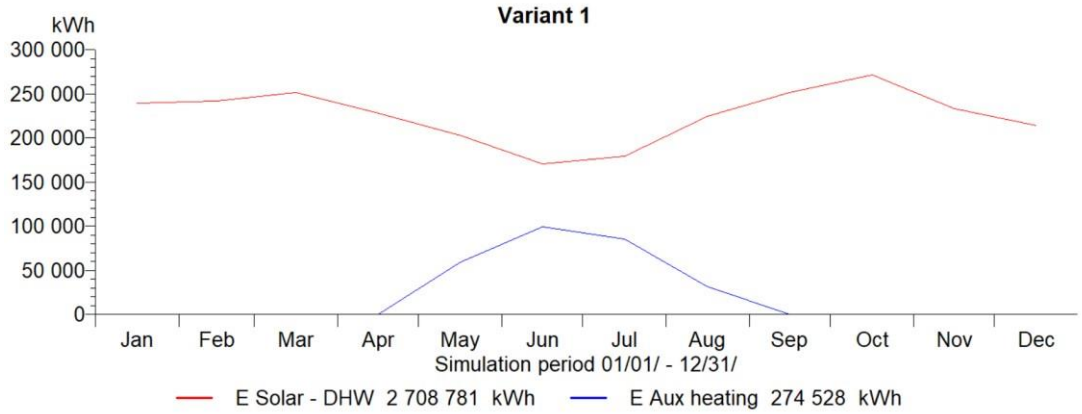

Figure 47: System E solar energy contribution vs auxiliary heating energy

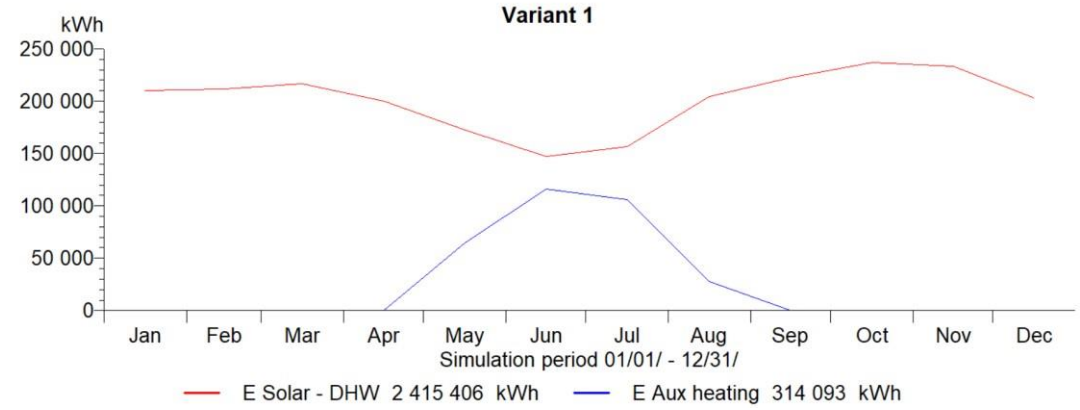

Figure 48: System F solar energy contribution vs auxiliary heating energy

4.5.2 System solar fraction and system efficiency

Systems A, C and E all use the same collector area of 2672 $m^{2,}$ but their storage tank capacities vary, leading to differences in solar fractions and overall system efficiency, as shown in Figure 49, Figure 50 and Figure 51. The solar fraction of the systems is as follows: 91% for system A,

92% for system C and 91% for system E. This high solar fraction reflects the system's strong performance in using solar energy to meet most of the required thermal energy. The systems also have a system efficiency of 46% for system A and system C and 45% for system C. System efficiency is a measure of how effectively the solar collector converts the solar irradiation it receives into useful thermal energy. It is calculated as the ratio of the energy output from the solar system to the total energy irradiation onto the collector [72]. Therefore, systems A, C and E only convert 46% and 45% of the solar energy incident on the collector into useful energy for the system.

In contrast, System B, D and F use the same collector area of 1980 m^2, but like previous systems, they also have different storage tank capacities resulting in varying solar fractions and efficiencies, as shown in Figure 52, Figure 53 and Figure 54. The solar fraction of the systems is 89% for both systems B and D and system 88% for system F. This slightly lower solar fraction compared to Systems A, C and E ,indicates that while Systems B, D and F also perform well in harnessing solar energy, they meet a marginally smaller proportion of the thermal energy demand through solar contribution. Systems B, D and F have system efficiencies of 55%, 56% and 54% respectively. These higher system efficiencies indicate that more solar energy incident on the collector is converted into useful thermal energy. Comparing the systems, system D has the highest system efficiency of 56%, and system E has the lowest system efficiency of 45%.

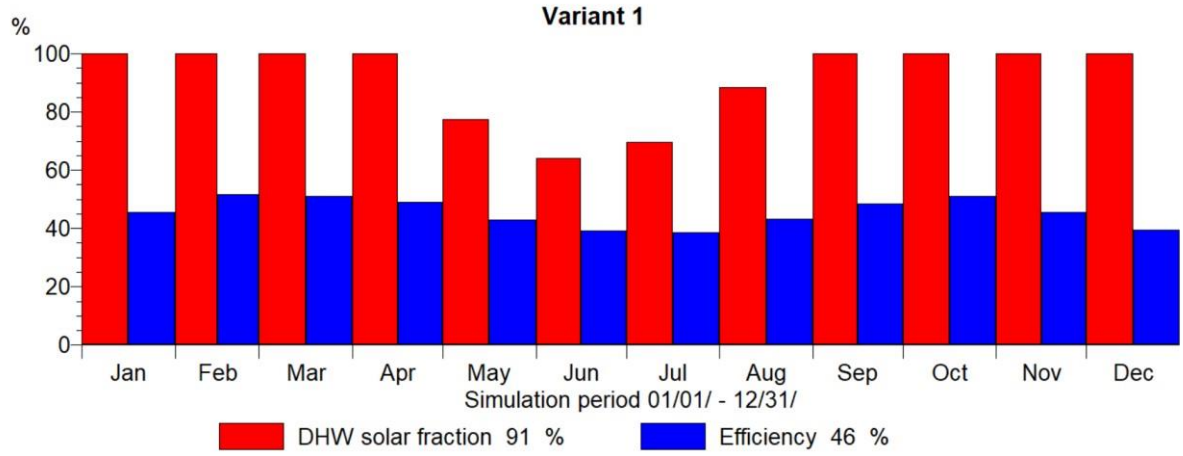

Figure 49: Solar fraction and system efficiency chart for system A

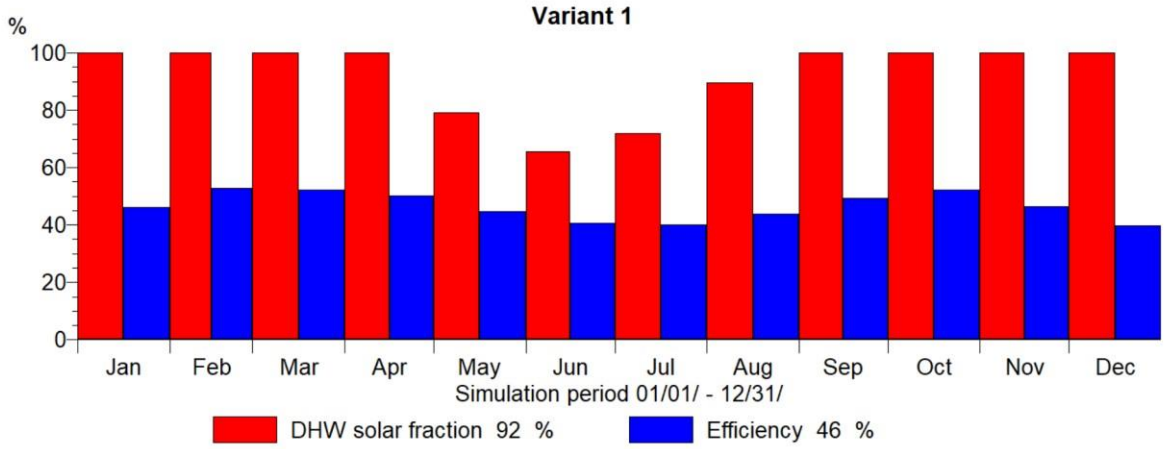

Figure 50: Solar fraction and system efficiency chart for system C

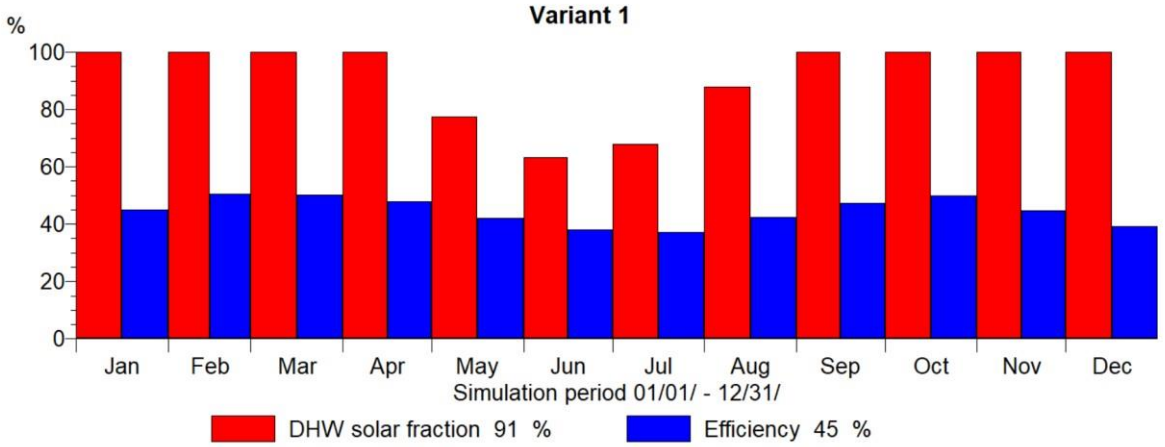

Figure 51: Solar fraction and system efficiency chart for system E

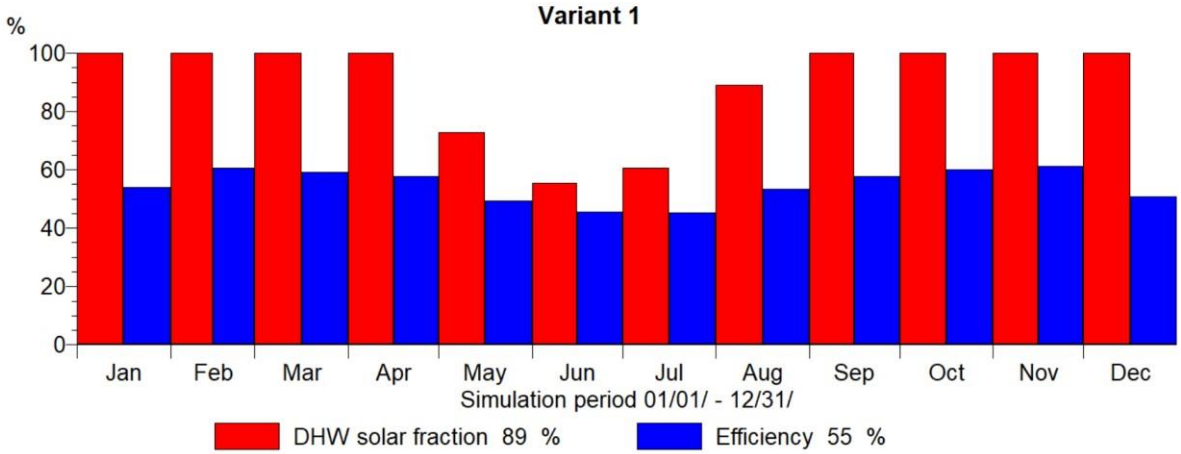

Figure 52: Solar fraction and system efficiency chart for system B

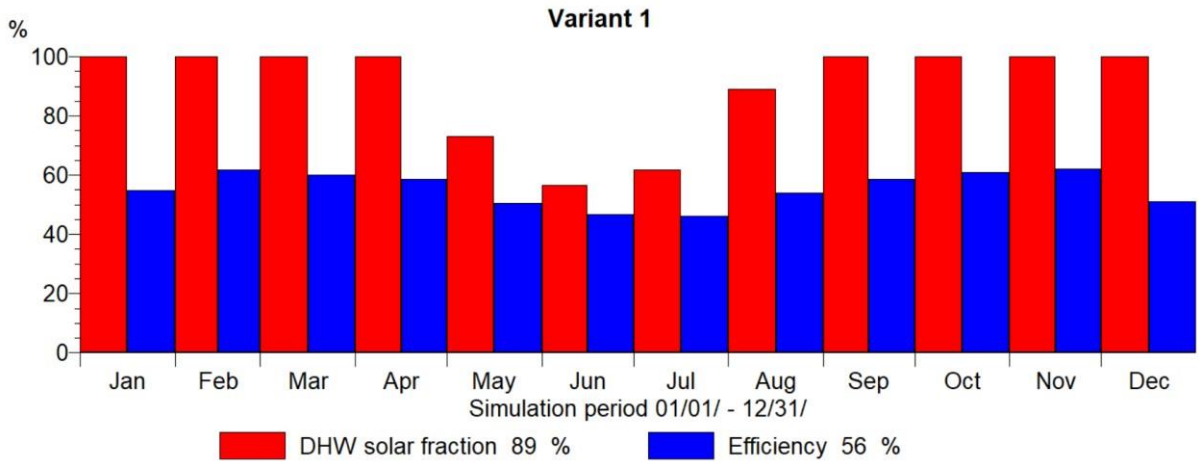

Figure 53: Solar fraction and system efficiency chart for system D

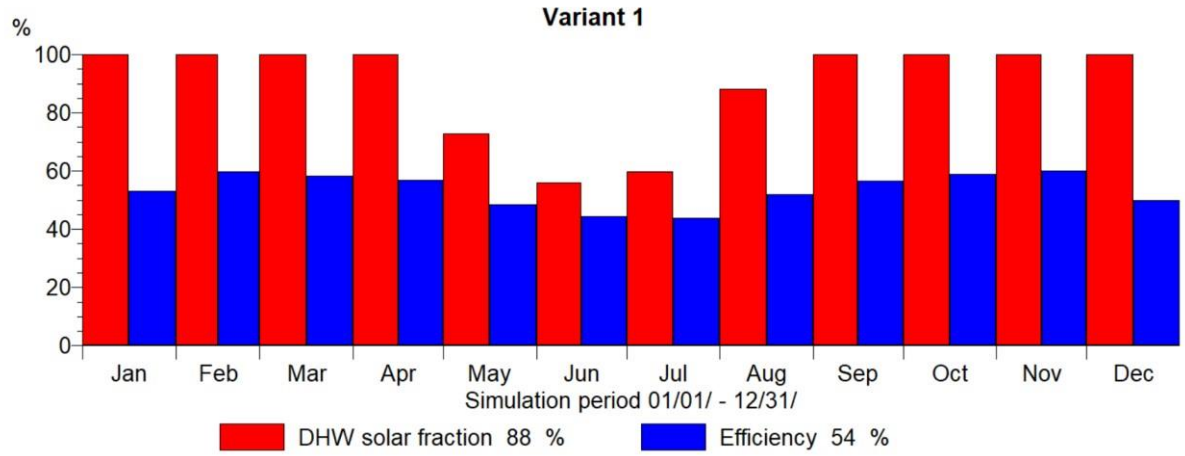

Figure 54: Solar fraction and system efficiency chart for system F

4.5.3 Emissions

The CO_2 emissions avoided in Systems A, B, C, D, E and F, as shown in Figure 55, Figure 56, Figure 57,

Figure 58, Figure 59 and Figure 60 amount to 719,622 kg, 640,638 kg, 734,875 kg, 650,535 kg, 704,771 kg and 628,441 kg, respectively. The main difference in the carbon emissions is due to the larger collector area of 2672 m^2 used in systems A, C and E, while systems B, D, and F use a smaller collector area of 1980 m^2. The larger collector area allows more solar energy to be absorbed and converted into useful energy, while smaller collector area allows less solar energy to be absorbed and converted into useful energy, resulting in a lower potential for reducing CO_2 emissions. Comparing the emissions avoided, system C has the highest amount of carbon dioxide emissions of 734,875 kg, and system F has the least amount of carbon dioxide emissions avoided of 628,441 kg.

For all the systems, there is a decrease in CO_2 emissions during the months of June, July, and August. This decrease occurs because of reduced solar radiation during these months, necessitating the use of an auxiliary heater to meet the thermal energy demand of the laundry's wetting processes. Therefore, the reliance on solar energy decreases, leading to a lower reduction in CO_2 emissions. Similar to previous studies, the current results demonstrate a significant reduction in carbon dioxide emissions, reaffirming the effectiveness of the system in achieving environmental benefits in line with established research.

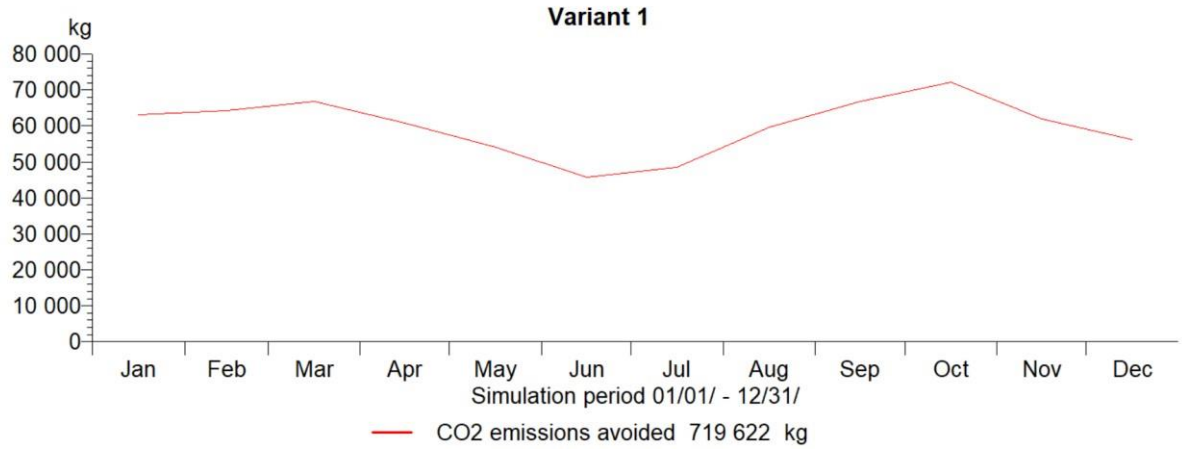

Figure 55: System A carbon dioxide emissions avoided

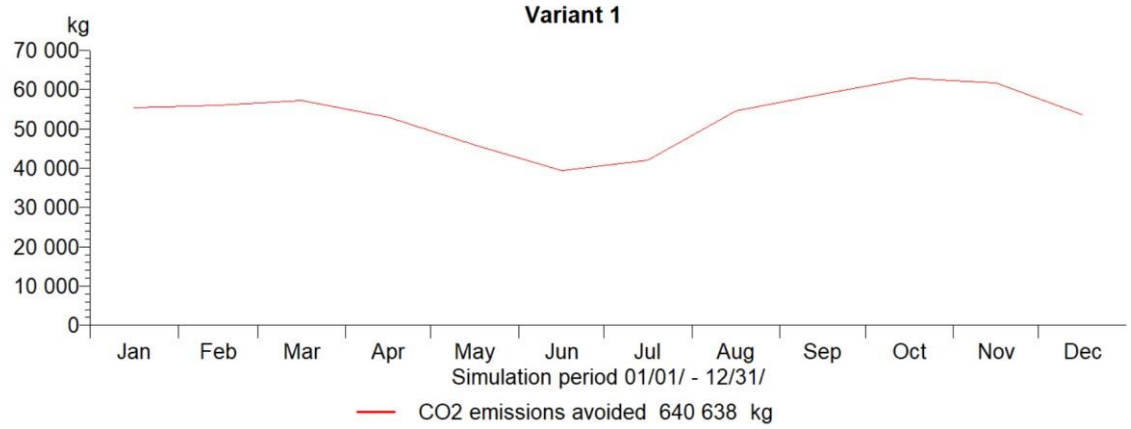

Figure 56:System B carbon dioxide emissions avoided

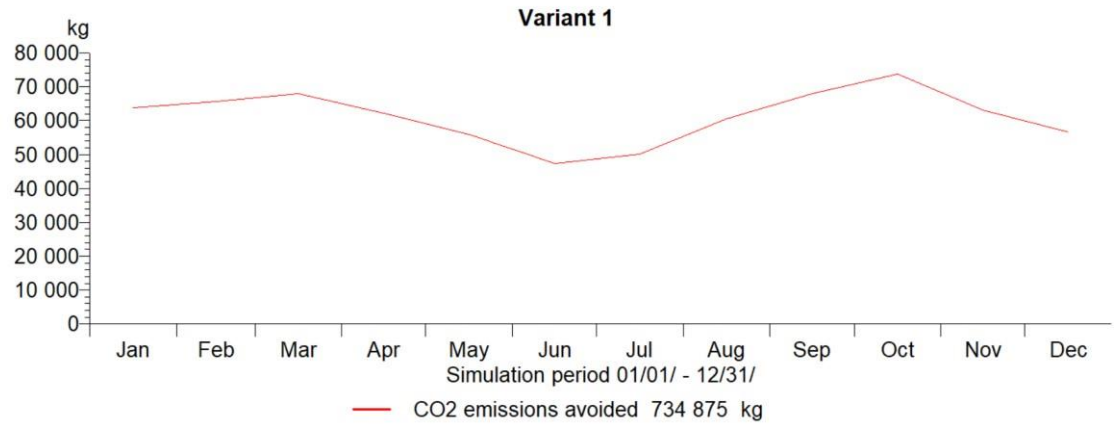

Figure 57: System C carbon dioxide emissions avoided

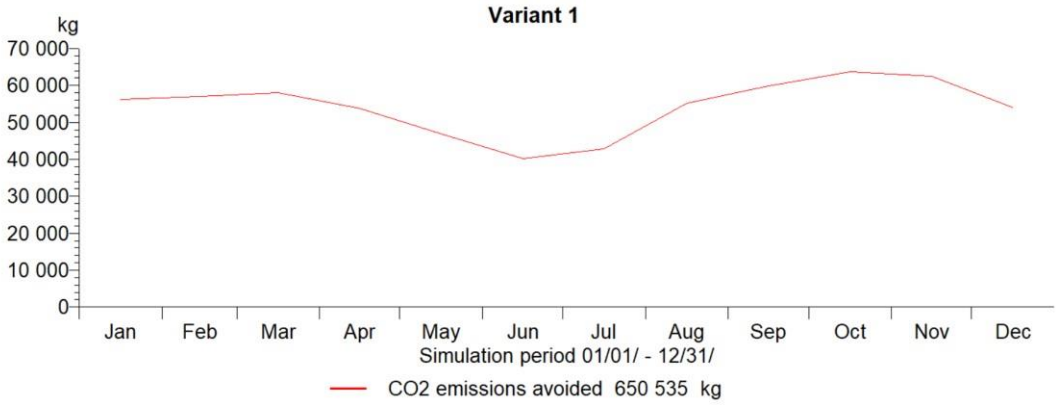

Figure 58:System D carbon dioxide emissions avoided

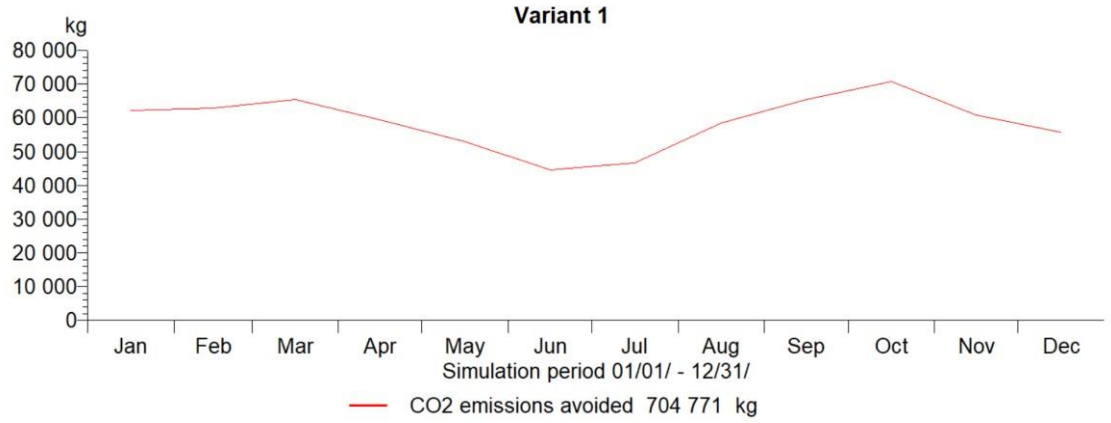

Figure 59: System E carbon dioxide emissions avoided

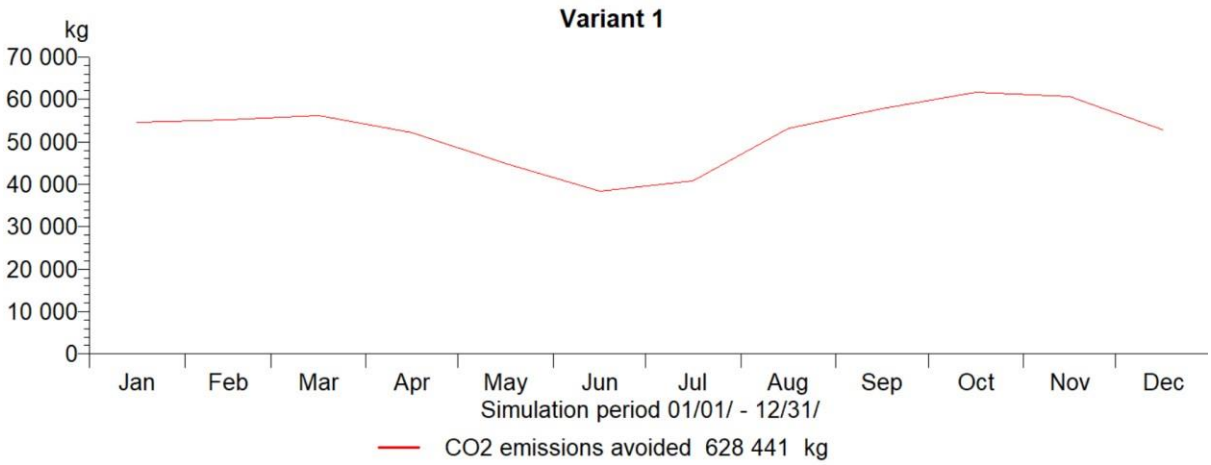

Figure 60: System F carbon dioxide emissions avoided

4.6 Financial analysis

4.6.1 Overview

The financial analysis of these systems was carried out under two different financing approaches: one where the project is funded entirely through equity, and another where the project is financed using a combination of equity and debt. This dual approach adds more rigour to the financial evaluation. In the second scenario, where both equity and debt are used, the funding was divided in a 52:48 ratio, meaning 52% of the project was financed through equity and 48% through debt. This ratio is commonly applied in industrial projects and is illustrated in Figure 61 [98]. By considering both approaches, the analysis provide a clearer understanding of the financial viability of the systems.

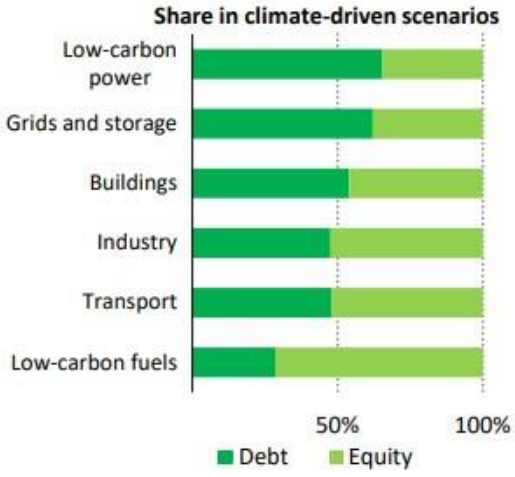

Figure 61: Debt-equity share

4.6.2 100% Equity Financing

Using Equation 36, the investment costs of the designed systems are shown in

Table *7* . The investment cost for system A is M 15,234,648; system B is 13,711,508; system C is M 16,916,523; system D is M 15,048,382; system E is M 14,510,148 and system F is M 12,642,008. The system is designed to have a lifespan of 20 years. **Error! Reference source not found.** shows the simulations' financial analysis parameters.

Table 7: Investment cost for the systems

Invest ıent cost	
System A	M 15,234,648
System B	M 13,711,508
System C	M 16,916,523
System D	M 15,048,382
System E	M 14,510,148
System F	M 12,642,008

Table 8: Financial analysis parameters for the systems

Financial analysis parameters for the systems						
System	**A**	**B**	**C**	**D**	**E**	**F**
Cost of solar energy (M/kWh)	0.929	0.863	0.973	0.899	0.919	0.831
Capital return time (Years)	7.8	7,3	8.2	7.7	7.7	7.0
Internal rate of return (IRR) (%)	15.02	15,96	13.99	15	15.33	16.88
Net present value (NPV) (M)	13,279,363	13,468,842	13,341,363	12,762,722	13,285,216	13,981,755

System A has an investment cost of M 15,234,648. The financial analysis results depicted in Table 8 show that the system has a capital return time of 7.8 years, which is the time an investment will generate enough cashflow to repay the initial investment. For the remaining years of its operation, the system is expected to generate profit. The NPV of this system is M 13,279,363. A positive NPV signifies that the investment is financially sound. The IRR for the system stands at 15.02%, which is favourable because it exceeds the current interest rate of 7.75%. The analysis further shows that the cost of generating solar energy with this system is M0.973 per unit.

System B with an investment cost of M 13,711,508 has a capital return time of 7.3 years as shown in Table 8. The system demonstrates financial viability with an internal rate of return of 15.96% higher than the current interest rate and, lastly, a positive NPV of M13,468,842. The cost of solar energy is M 0.863/ kWh.

System C, has an investment cost of M16,916,523. The financial analysis in Table 8 also shows that the system has a longer capital return time of 8.2 years due to its higher initial cost. However, it still maintains a positive NPV of M 13,341,363 an internal rate of return of 13.99%. The cost of solar energy is M 0.973/ kWh.

System D has an investment cost of M 15,048,382. The simulation financial analysis in Table 8 show a capital return time of 7.7 years and a positive NPV of M 12,762,722. The internal rate of return of the system stands at 15%. The cost of solar energy is M 0.899/ kWh.

System E has an investment cost of M 14,510,148. As shown in Table 8, the financial analysis parameters show that the capital return time for the system is 7.7 years, and the net present value is at a positive value of M 13,285,216. The internal rate of return of the system is at 15.3%. The cost of solar energy is M 0.919/ kWh.

Lastly, system F has the lowest investment cost of M 12,642,008. As shown in Table 8, the financial analysis parameters show that the system has the shortest capital return time of 7.0 years, the net present value is at a positive value of M 13,981,755. The internal rate of return of the system is at 16.88%. The cost of solar energy is M 0.831/ kWh.

Looking at the financial analysis of all the systems, it is evident all the systems are profitable because they all have a positive net present value, an internal rate of return higher than the current interest rate, and a cost of energy lower than the present cost of electricity rated at M 2.012/kWh. However, system F is the most profitable among the systems because it has the lowest cost of energy, the shortest capital return time, and the highest Net present value and internal rate of return.

4.6.3 Equity-debt financing

The equity-debt financing is done at a 52:48 split, and

Table *9* shows the financing of the systems. The borrowing interest rate is 11.25%. Table 10 also shows the simulation financial analysis results of the systems.

Table 9: Equity-debt financing for the systems

Equity-debt financing			
System	**Equity (52%)**	**Debt (48%)**	**Total Investment**
A	M 7,922,016	M 7,312,631	M 15,234,648
B	M 7,129,984	M 6,581,523	M 13,711,508
C	M 8,796,591	M 8,119,931	M 16,916,523
D	M 7,825,158	M 7,223,223	M 15,048,382
E	M 7,545,276	M 6,964,871	M 14,510,148
F	M 6,573,844	M 6,068,163	M 12,642,008

Table 10: Financial analysis parameters for the systems

Financial analysis parameters for the systems						
System	**A**	**B**	**C**	**D**	**E**	**F**
Cost of solar energy (M/kWh)	0.973	0.906	1.020	0.947	0.961	0.872
Capital return time (Years)	9.3	8.5	10.1	9.2	9.1	7.9
Amortization period (Years)	11.7	10.9	12.6	11.6	11.5	10.3
Internal rate of return (IRR) (%)	16.25	17.57	14.87	16.25	16.66	18.78
Net present value (NPV) (M)	M 12,076,811	M 12,386,520	M 11,006,052	M 11,574,873	M 12,139,853	M 12,983,854

System A has an equity share of M 7,922,016 and a debt of M 7,312,631 from the total investment of M 15,234,648. The simulation financial analysis results in Table 10 show that the system has a capital return time of 9.3 years and an amortization period of 11.7 years. The amortization period refers to how long a loan or capital investment will be repaid, mostly in equal instalments. The internal rate of return for the system is 16.25%, which is significantly higher than the current interest rate of 7.75%. The internal rate of return (IRR) being higher than the current interest rate shows that the system is profitable, and the investment is expected to yield substantial returns relative to its cost of capital. The NPV of the system is M 12,076,811, and it being positive signifies that the investment is financially viable. Moreover, the analysis shows that the cost of generating solar energy with this system is M 0.973/kWh.

This low cost of energy shows the economic benefits of adopting solar energy for this project, highlighting both cost savings and a reduction in reliance on traditional energy sources.

System B has an equity share of M 7,129,984 and a debt share of M 6,581,523 from the total investment of M 13,711,508. The financial analysis results in Table 10 show that the system has a capital return time of 8.5 years and an amortization period of 10.9 years. The system has an internal rate of return (IRR) of 17.57%, which is higher than the current interest rate. The NPV of the system is positive at a value of M 12,386,520. The cost of solar energy is M 0.906/kWh. All these parameters indicate that system B is a profitable investment.

System C also has an equity share of M 8,796,591 and a debt share of M 8,119,931 from the total investment, which amounts to M 16,916,523. The system's capital return time is 10.1 years, and the amortization period is 12.6 years. The system's internal rate of return (IRR) is 14.87% and has a positive net present value (NPV) of M 11,006,052, both of which suggest that the system is financial. The cost of solar energy for this system is rated at M 1.020/kWh making it slightly less cost-efficient than the previous systems, but still a strong investment option.

Furthermore, from the total investment of M 15,048,382, system D has an equity share of M 7,825,158 and a debt share of M 7,223,223. The system has a capital return time of 9.2 years and an amortization period of 11.6 years. The system's internal rate of return (IRR) is 16.25% and has a positive net present value (NPV) of M 11,574,873. The cost of solar energy for this system is rated at M 0.947/kWh, highlighting its profitability.

System E has an equity share of M 7,545,276 and a debt share M 6,964,871 of from the total investment of M 14,510,148. The financial analysis results in Table 10 show that the system has a capital return time of 9.1 years and an amortization period of 11.5 years. Additionally, with an internal rate of return (IRR) of 16.66% and a positive net present value (NPV) of M 12,139,853, this system is also financially viable. The cost of solar energy is M 0.961/kWh.

Lastly, system F has the lowest total investment of M 12,983,854, with an equity share of M 6,573,844 and a debt share of M 6,068,163. The system has the shortest capital return time of 7.9 years and an amortization period of 10.3 years. The system's internal rate of return (IRR) is 18.78% and has a positive net present value (NPV) of M 12,983,854 making it the highest among all systems. The cost of solar energy for this system is rated at the lowest value of M 0.872/kWh, further making it the most financially viable system. The cost of electricity in industries is charged in two ways: cost per energy consumption and cost per demand. The price of electricity based on energy consumption is M 0.2928/kWh (for high voltage) and M 0.3175/kWh (for low voltage). The cost of electricity per demand is M 324.7512 (for high voltage) and M 379.3175 (for low voltage). Normally, the price of electricity will be relatively

high because the majority of the electricity is from the demand even if the electricity consumption is low.

Looking at the financial analysis of all the systems, it is evident all the systems are financially viable because they all have a positive net present value, an internal rate of return higher than the current interest rate, and a low cost of energy. They also have amortization periods less than their life span of 20 years indicating that they will be profitable in their remaining years after the repayment period. However, system F is the most profitable among the systems because it has the least cost of energy, shortest capital return time, shortest amortization period and the highest Net present value and internal rate of return. Investing in these systems is not only beneficial in terms of cost recovery but also long-term financial savings.

5 CONCLUSION AND RECOMMENDATIONS

5.1 Concluding remarks

The aim of this study was to assess the techno-economic viability of integrating solar water heating systems at the Vishan Clothing laundry using T*SOL simulation software. To find the optimal system configuration, a comparative analysis was done on the six systems: systems A, B, C, D, E and F.

From the technical results, it is observed that all the designed systems can achieve a high solar fraction, with solar energy contributing to more than 90% of the required thermal demand for certain systems. Systems A, C, and E with solar fractions of 91% and 92% exhibit strong performance due to their larger collector areas as compared to systems B, D and F with smaller collector areas. The solar fraction for systems B, D and F are 88% and 89 %. Additionally, all the systems with a larger collector area have system efficiencies of 46% and 45% while systems with the smaller collector area have efficiencies of 54%, 55% and 56% showing that there is a higher solar energy output in these systems. Due to the lower solar fraction of systems B, D and F, these systems rely more on the auxiliary heater than systems A, C and E, indicating

higher electricity consumption to meet the demand during periods of low solar radiation. The energy losses of the systems are found to be as follows: system D has the lowest energy losses at 45% of the total energy input, followed by system B at 46%, system F at 47%, system C at 54%, system A at 55% and lastly system E with the highest energy losses of 56% of the total energy input. The carbon dioxide emissions avoided for systems A, B, C, D, E, and F amount to 719,622 kg, 640,638 kg, 734,875 kg, 650,535 kg, 704,771 kg and 628,441 kg.

The financial analysis was done under two different financing scenarios; full equity and equitydebt, showing that all the systems are financially viable. The capital return period for these systems ranges between 7 to 10.1 years for both scenarios, the amortization period ranges between 10.3 to 11.6 years. Furthermore, the internal rate of return for these systems in both financing approaches ranges between 13.99% to 18.78%. All the systems have a positive net present value of M 12,076,811, M 12,386,520, M 11,006,052, M 11,574,873, M 12,139,853 and M 12,983,854 for systems A, B, C, D, E and F. The cost of solar energy for these systems under equity financing ranges between M 0.831/kWh to M 0.97/kWh, with system F having the lowest cost and system C having the highest cost of solar energy. Under equity-debt financing, the cost of solar energy ranges between M 0.872/kWh to M 1.020/kWh, with system F again having the lowest cost and system C having the highest cost. The combination of positive NPV, high IRR, and lower energy costs contributes to the conclusion that investing in these solar energy systems is both economically beneficial and strategically advantageous for long-term sustainability and profitability. Based on both the technical and financial analyses, system F is the most optimal solution to meet the thermal energy demands of the wetting processes at the laundry facility.

These results indicate that there is significant potential to integrate solar heating systems into the textile industry since they closely align with the findings of previous studies. Despite the high initial investment costs, the long-term advantages far outweigh the financial barriers. As the world shifts toward sustainable practices in response to global warming, the integration of solar heating systems will help to reduce the energy costs, lower the carbon dioxide emissions, and to improve sustainability within the industry. The economic benefits, coupled with environmental advantages, make these solar energy systems a compelling investment for the future.

5.2 Study limitations

This study, as is the case with any other research endeavour is not without its limitations. The primary challenge was the lack of historical data at the laundry, to track the energy consumption patterns over time. Additionally, the study was constrained by the limited technical expertise

of the laundry workers. While they possessed fundamental knowledge of laundry operations, their understanding of the underlying principles, such as heat transfer and fluid dynamics, was insufficient to provide a comprehensive analysis of the system's components. Consequently, this lack of technical depth presented an obstacle to the research study. Furthermore, the estimation of thermal energy demand may have been underestimated due to the unavailability of data that accounts for thermal losses, potentially impacting the accuracy of the demand profile.

5.3 Recommendations

While this study demonstrated the feasibility of integrating solar heating systems into a laundry facility, further research is imperative to refine the system design. Specifically, in-depth energy audits are required to accurately determine thermal energy demand. A more precise understanding of thermal energy demand is essential to prevent the design of oversized or undersized systems. The findings of this study show that solar heating systems require a large collector area. It is, therefore, imperative for the textile industry corporations to prioritize the construction of industrial buildings with robust roofing capable of supporting large collector areas.

To accelerate the widespread adoption of solar heating systems within the industry, financial incentives and subsidies for system installation are important. The high upfront costs of solar thermal systems currently hinder their implementation. Additionally, targeted campaigns to educate industry stakeholders about the long-term benefits of integrating solar heating systems are important, given the prevailing knowledge gap in this area. By addressing these factors, the textile industry can effectively leverage solar energy and achieve substantial environmental and economic advantages.

REFERENCES

[1] L. Cozzi *et al.*, 'World Energy Outlook 2023', *International Energy Agency*, 2023, [Online]. Available: https://www.iea.org/reports/world-energy-outlook-2023

[2] S. H. Farjana, N. Huda, M. A. P. Mahmud, and R. Saidur, 'Solar process heat in industrial systems – A global review', *Renewable and Sustainable Energy Reviews*, vol. 82, pp. 2270–2286, Feb. 2018, doi: 10.1016/j.rser.2017.08.065.

[3] M. I. Ismail, N. A. Yunus, and H. Hashim, 'Integration of solar heating systems for lowtemperature heat demand in food processing industry – A review', *Renewable and Sustainable Energy Reviews*, vol. 147, p. 111192, Sep. 2021, doi: 10.1016/j.rser.2021.111192.

[4] 'Industry - Energy System', IEA. Accessed: Jul. 31, 2024. [Online]. Available: https://www.iea.org/energy-system/industry

[5] G. N. Kulkarni, S. B. Kedare, and S. Bandyopadhyay, 'Design of solar thermal systems utilizing pressurized hot water storage for industrial applications', *Solar Energy*, vol. 82, no. 8, pp. 686–699, Aug. 2008, doi: 10.1016/j.solener.2008.02.011.

[6] P. Kumar *et al.*, 'Economics of Implementing Solar Thermal Heating Systems in the Textile Industry', *Energies*, vol. 15, no. 12, Art. no. 12, Jan. 2022, doi: 10.3390/en15124277.

[7] 'Global Alliance German Energy'. Accessed: Oct. 25, 2023. [Online]. Available: https://www.powerfuels.org/fileadmin/gap/Publikationen/Factsheets/190612_dena_FS_Process_Heat_web.pdf

[8] 'IRENA – International Renewable Energy Agency'. Accessed: Jan. 08, 2023. [Online]. Available: https://www.irena.org/

[9] S. Palamutcu, 'Energy footprints in the textile industry', in *Handbook of Life Cycle Assessment (LCA) of Textiles and Clothing*, Elsevier, 2015, pp. 31–61. doi: 10.1016/B978-0-08-100169-1.00002-2.

[10] A. Hasanbeigi and L. Price, 'A review of energy use and energy efficiency technologies for the textile industry', *Renewable and Sustainable Energy Reviews*, vol. 16, no. 6, pp. 3648–3665, Aug. 2012, doi: 10.1016/j.rser.2012.03.029.

[11] B. Harsanto, I. Primiana, V. Sarasi, and Y. Satyakti, 'Sustainability Innovation in the Textile Industry: A Systematic Review', *Sustainability*, vol. 15, no. 2, Art. no. 2, Jan. 2023, doi: 10.3390/su15021549.

[12] P. Khude, 'A Review on Energy Management in Textile Industry', *Innovative Energy & Research*, vol. 6, p. 169, Sep. 2017, doi: 10.4172/2576-1463.1000169.

[13] U. S. D. of C. International Trade Administration, ‘Lesotho- Country Commercial guide’, Lesotho Manufacturing. Accessed: Sep. 08, 2024. [Online]. Available: https://www.trade.gov/country-commercial-guides/lesotho-manufacturing

[14] ‘Revitalizing the competitiveness of Lesotho’s export manufacturing sector’. Accessed: Aug. 07, 2023. [Online]. Available: https://blogs.worldbank.org/africacan/revitalizingcompetitiveness-lesothos-export-manufacturing-sector

[15] ‘Lesotho’s textiles, apparel and footwear manufacturing industry - tralac trade law centre’. Accessed: Sep. 25, 2023. [Online]. Available: https://www.tralac.org/news/article/11501-lesotho-s-textiles-apparel-and-footwearmanufacturing-industry.html

[16] ‘Textile and Apparel Industry - Embassy of the Kingdom of Lesotho in Ireland’. Accessed: Aug. 01, 2024. [Online]. Available: http://www.lesothoembassy.ie/tradeinvestment/15-trade-investment/trade-investment-opportunities/25-textile-and-apparelindustry.html

[17] S. Jeppesen, ‘Lesotho: The garment industry in its economic, political and social context’, *Centre for Business and Development Studies*, p. 50, 2019.

[18] (ECA) United Nations Economic Commission for Africa, ‘Country Profile-2017’, *Economic Commission for Africa*, May 2018.

[19] M. Morris and C. Staritz, ‘Industrial upgrading and development in Lesotho’s apparel industry: global value chains, foreign direct investment, and market diversification’, *Oxford Development Studies*, vol. 45, no. 3, pp. 303–320, Jul. 2017, doi: 10.1080/13600818.2016.1237624.

[20] N. Kolane, ‘JOBS BLOODBATH’, The Reporter Lesotho | Fresh News, Daily. Accessed: Aug. 13, 2023. [Online]. Available: https://www.thereporter.co.ls/2023/05/11/jobsbloodbath/

[21] Lesotho Renewable Energy Policy, ‘lesotho-renewable-energy-policy-draft-1532182953.pdf’, 2013. Accessed: Feb. 12, 2023. [Online]. Available: https://nulerc.s3.amazonaws.com/public/documents/reports/lesotho-renewable-energy-policydraft-1532182953.pdf

[22] B. Taele, L. Mokhutšoane, and H. Narayan, *Solar energy resources potential and sustainable production of biomass energy in Lesotho*. 2010. doi: 10.13140/RG.2.1.2962.0882.

[23] J. Cresko, D. Shenoy, H. Liddell, and R. Sabouni, ‘Innovating Clean Energy Technologies in Advanced Manufacturing’, 2015.

[24] T. V. Arjunan, V. Selvaraj, and M. M. Matheswaran, *Solar Thermal Conversion Technologies for Industrial Process Heating*, 1st ed. Boca Raton: CRC Press, 2023. doi: 10.1201/9781003263326.

[25] N. L. Lawrence Berkeley, ‘Improving Process Heating System Performance’: INDUSTRIAL HEATING EQUIPMENT ASSOCIATION, 2007. Accessed: Aug. 02, 2024. [Online]. Available: https://www.nrel.gov/docs/fy08osti/41589.pdf

[26] L. Kumar, M. Hasanuzzaman, and N. A. Rahim, ‘Global advancement of solar thermal energy technologies for industrial process heat and its future prospects: A review’, *Energy Conversion and Management*, vol. 195, pp. 885–908, Sep. 2019, doi: 10.1016/j.enconman.2019.05.081.

[27] E. efficiency and R. E. US Department of Energy, ‘Improving Process heating system efficincy performance’. INDUSTRIAL HEATING EQUIPMENT ASSOCIATION, 2004.

[28] I. Dincer and M. A. Rosen, ‘Industrial Heating and Cooling Systems’, in *Exergy Analysis of Heating, Refrigerating and Air Conditioning*, Elsevier, 2015, pp. 99–129. doi: 10.1016/B978-0-12-417203-6.00003-X.

[29] M. Hasanuzzaman, N. A. Rahim, M. Hosenuzzaman, R. Saidur, I. M. Mahbubul, and M. M. Rashid, ‘Energy savings in the combustion based process heating in industrial sector’, *Renewable and Sustainable Energy Reviews*, vol. 16, no. 7, pp. 4527–4536, Sep. 2012, doi: 10.1016/j.rser.2012.05.027.

[30] M. A. Rosen and I. Dincer, ‘A study of industrial steam process heating through exergy analysis’, *Int. J. Energy Res.*, vol. 28, no. 10, pp. 917–930, Aug. 2004, doi: 10.1002/er.1005.

[31] M. Al-Smairan, M. Shawaqfah, and F. AlMomani, ‘Techno-Economic Investigation of an Integrated Boiler–Solar Water Heating/Cooling System: A Case Study’, *Energies*, vol. 14, no. 1, Art. no. 1, Jan. 2021, doi: 10.3390/en14010001.

[32] Elmabrouk M Abuelbida, ‘Enhance the Heat Transfer in a Heat Treatment Furnace through Improving the Combustion Process in the Radiation Tubes’, 2012, doi: 10.13140/RG.2.2.26329.26727.

[33] ‘Advantages and disadvantages of steam systems - Bosch Steam boiler planning Industrial Heat’. Accessed: Oct. 22, 2023. [Online]. Available: https://www.boilerplanning.com/technology/steam/advantages-and-disadvantages-of-steam-systems.html [34] C. A. Schoeneberger, C. A. McMillan, P. Kurup, S. Akar, R.

Margolis, and E. Masanet, ‘Solar for industrial process heat: A review of technologies, analysis approaches, and potential applications in the United States’, *Energy*, vol. 206, p. 118083, Sep. 2020, doi: 10.1016/j.energy.2020.118083.

[35] ‘Fundamentals of Industrial Boilers and Steam Generation Systems’, ChemTreat, Inc. Accessed: Aug. 05, 2024. [Online]. Available: https://www.chemtreat.com/wateressentials-handbook-fundamentals-of-industrial-boilers-and-steam-generation-systems/

[36] M. Hasanuzzaman, Ed., *Technologies for solar thermal energy: theory, design and optimization*. London San Diego, CA Cambridge, MA Kidlington, Oxford: Academic Press, an imprint of Elsevier, 2022.

[37] A. K. Sharma, C. Sharma, S. C. Mullick, and T. C. Kandpal, ‘Solar industrial process heating: A review’, *Renewable and Sustainable Energy Reviews*, vol. 78, pp. 124–137, Oct. 2017, doi: 10.1016/j.rser.2017.04.079.

[38] S. Kalogirou, *Solar energy engineering: processes and systems*, Second edition. Amsterdam ; Boston: Elsevier, AP, Academic Press is an imprint of Elsevier, 2014.

[39] M. Asif and T. Muneer, ‘Thermal Energy: Solar Technologies’, in *Managing Air Quality and Energy Systems*, 2nd ed., B. D. Fath, S. E. Jørgensen, and M. Cole, Eds., Second edition. | Boca Raton : CRC Press, 2020. | Series: Applied ecology and environmental management: CRC Press, 2020, pp. 691–704. doi: 10.1201/9781003043461-47.

[40] R. Elbahjaoui and H. El Qarnia, ‘Performance evaluation of a solar thermal energy storage system using nanoparticle-enhanced phase change material’, *International Journal of Hydrogen Energy*, vol. 44, no. 3, pp. 2013–2028, Jan. 2019, doi: 10.1016/j.ijhydene.2018.11.116.

[41] D. Y. Goswami, *Principles of Solar Engineering, Third Edition*, 3rd ed. Boca Raton: CRC Press, 2015.

[42] S. Kalogirou, *Solar energy engineering: processes and systems*. Burlington, MA: Elsevier/Academic Press, 2009.

[43] G. Barone, A. Buonomano, C. Forzano, and A. Palombo, ‘Solar thermal collectors’, in *Solar Hydrogen Production*, Elsevier, 2019, pp. 151–178. doi: 10.1016/B978-0-12814853-2.00006-0.

[44] A. Araújo, A. C. Ferreira, C. Oliveira, R. Silva, and V. Pereira, ‘Optimization of collector area and storage volume in domestic solar water heating systems with on–off control—A thermal energy analysis based on a pre-specified system performance’, *Applied Thermal Engineering*, vol. 219, p. 119630, Jan. 2023, doi: 10.1016/j.applthermaleng.2022.119630.

[45] S. Suman, Mohd. K. Khan, and M. Pathak, ‘Performance enhancement of solar collectors—A review’, *Renewable and Sustainable Energy Reviews*, vol. 49, pp. 192–210, Sep. 2015, doi: 10.1016/j.rser.2015.04.087.

[46] C. E. Camargo Nogueira, M. L. Vidotto, F. Toniazzo, and G. Debastiani, ‘Software for designing solar water heating systems’, *Renewable and Sustainable Energy Reviews*, vol. 58, pp. 361–375, May 2016, doi: 10.1016/j.rser.2015.12.346.

[47] A. Jamar, Z. A. A. Majid, W. H. Azmi, M. Norhafana, and A. A. Razak, ‘A review of water heating system for solar energy applications’, *International Communications in Heat and Mass Transfer*, vol. 76, pp. 178–187, Aug. 2016, doi: 10.1016/j.icheatmasstransfer.2016.05.028.

[48] K. Patel, M. P. Patel, and M. J. Patel, ‘REVIEW OF SOLAR WATER HEATING SYSTEMS’, *International Journal of Advanced Engineering Technology*, 2012.

[49] J. A. Duffie and W. A. Beckman, *Solar Engineering of Thermal Processes*. John Wiley & Sons, 2013.

[50] ‘Evacuated Tube Collector for Solar Hot Water System’. Accessed: Aug. 06, 2024. [Online]. Available: https://www.alternative-energy-tutorials.com/solar-hotwater/evacuated-tube-collector.html

[51] J. Immonen and K. M. Powell, ‘Dynamic optimization with flexible heat integration of a solar parabolic trough collector plant with thermal energy storage used for industrial process heat’, *Energy Conversion and Management*, vol. 267, p. 115921, Sep. 2022, doi: 10.1016/j.enconman.2022.115921.

[52] N. Komendantova, A. Patt, L. Barras, and A. Battaglini, ‘Perception of risks in renewable energy projects: The case of concentrated solar power in North Africa’, *Energy Policy*, vol. 40, pp. 103–109, Jan. 2012, doi: 10.1016/j.enpol.2009.12.008.

[53] K. H. Kumar, A. M. Daabo, M. K. Karmakar, and H. Hirani, ‘Solar parabolic dish collector for concentrated solar thermal systems: a review and recommendations’, *Environ Sci Pollut Res*, vol. 29, no. 22, pp. 32335–32367, May 2022, doi: 10.1007/s11356-022-18586-4.

[54] K. Ravi Kumar, N. V. V. Krishna Chaitanya, and N. Sendhil Kumar, ‘Solar thermal energy technologies and its applications for process heating and power generation – A review’, *Journal of Cleaner Production*, vol. 282, p. 125296, Feb. 2021, doi: 10.1016/j.jclepro.2020.125296.

[55] I. Purohit and P. Purohit, ‘Solar Thermal Power Generation’, in *Reference Module in Earth Systems and Environmental Sciences*, Elsevier, 2019, p. B9780124095489118652. doi: 10.1016/B978-0-12-409548-9.11865-2.

[56] M. A. Hanif, F. Nadeem, R. Tariq, and U. Rashid, ‘Chapter 4 - Solar thermal energy and photovoltaic systems’, in *Renewable and Alternative Energy Resources*, M. A. Hanif, F. Nadeem, R. Tariq, and U. Rashid, Eds., Academic Press, 2022, pp. 171–261. doi: 10.1016/B978-0-12-818150-8.00007-1.

[57] J. J. C. S. Santos, J. C. E. Palacio, A. M. M. Reyes, M. Carvalho, A. J. R. Freire, and M. A. Barone, ‘Chapter 12 - Concentrating Solar Power’, in *Advances in Renewable Energies and Power Technologies*, I. Yahyaoui, Ed., Elsevier, 2018, pp. 373–402. doi: 10.1016/B978-0-12-812959-3.00012-5.

[58] M. George, A. K. Pandey, N. Abd Rahim, V. V. Tyagi, S. Shahabuddin, and R. Saidur, ‘Concentrated photovoltaic thermal systems: A component-by-component view on the developments in the design, heat transfer medium and applications’, *Energy Conversion and Management*, vol. 186, pp. 15–41, Apr. 2019, doi: 10.1016/j.enconman.2019.02.052.

[59] K. Mostakim and M. Hasanuzzaman, ‘Global prospects, challenges and progress of photovoltaic thermal system’, *Sustainable Energy Technologies and Assessments*, vol. 53, p. 102426, Oct. 2022, doi: 10.1016/j.seta.2022.102426.

[60] G. Asefi, A. Habibollahzade, T. Ma, E. Houshfar, and R. Wang, ‘Thermal management of building-integrated photovoltaic/thermal systems: A comprehensive review’, *Solar Energy*, vol. 216, pp. 188–210, Mar. 2021, doi: 10.1016/j.solener.2021.01.005.

[61] G. Alva, Y. Lin, and G. Fang, ‘An overview of thermal energy storage systems’, *Energy*, vol. 144, pp. 341–378, Feb. 2018, doi: 10.1016/j.energy.2017.12.037.

[62] A. Franco, ‘Methods for the Sustainable Design of Solar Energy Systems for Industrial Process Heat’, *Sustainability*, vol. 12, no. 12, Art. no. 12, Jan. 2020, doi: 10.3390/su12125127.

[63] N. Tasmin, S. H. Farjana, M. R. Hossain, S. Golder, and M. A. P. Mahmud, ‘Integration of Solar Process Heat in Industries: A Review’, *Clean Technologies*, vol. 4, no. 1, Art. no. 1, Mar. 2022, doi: 10.3390/cleantechnol4010008.

[64] T. P. Lima, J. C. C. Dutra, A. R. M. Primo, J. Rohatgi, and A. A. V. Ochoa, ‘Solar water heating for a hospital laundry: A case study’, *Solar Energy*, vol. 122, pp. 737–748, Dec. 2015, doi: 10.1016/j.solener.2015.10.006.

[65] Z. Awwad, A. Alharbi, A. Habib, and O. de Weck, ‘Site Assessment and Layout Optimization for Rooftop Solar Energy Generation in Worldview-3 Imagery’, *Remote Sensing*, vol. 15, p. 1356, Feb. 2023, doi: 10.3390/rs15051356.

[66] K. Bódis, I. Kougias, A. Jäger-Waldau, N. Taylor, and S. Szabó, ‘A high-resolution geospatial assessment of the rooftop solar photovoltaic potential in the European Union’,

Renewable and Sustainable Energy Reviews, vol. 114, p. 109309, Oct. 2019, doi: 10.1016/j.rser.2019.109309.

[67] W. Batayneh, A. Bataineh, I. Soliman, and S. A. Hafees, 'Investigation of a single-axis discrete solar tracking system for reduced actuations and maximum energy collection', *Automation in Construction*, vol. 98, pp. 102–109, Feb. 2019, doi: 10.1016/j.autcon.2018.11.011.

[68] T. Hove, 'Energy delivery of solar thermal collectors in Zimbabwe', *Renewable Energy*, vol. 19, no. 4, pp. 495–511, Apr. 2000, doi: 10.1016/S0960-1481(99)00080-4.

[69] T. Hove, 'Energy delivery of solar thermal collectors in Zimbabwe', *Renewable Energy*, vol. 19, no. 4, pp. 495–511, Apr. 2000, doi: 10.1016/S0960-1481(99)00080-4.

[70] T. Hove and J. Göttsche, 'Mapping global, diffuse and beam solar radiation over Zimbabwe', *Renewable Energy*, vol. 18, no. 4, pp. 535–556, Dec. 1999, doi: 10.1016/S0960-1481(98)00782-4.

[71] W. A. Beckman *et al.*, 'TRNSYS The most complete solar energy system modeling and simulation software', *Renewable Energy*, vol. 5, no. 1–4, pp. 486–488, Aug. 1994, doi: 10.1016/0960-1481(94)90420-0.

[72] 'T*SOL | Planning and simulation software for solar thermal systems'. Accessed: Oct. 28, 2023. [Online]. Available: https://valentin-software.com/produkte/tsol/

[73] O. M. Seretse, A. Agarwal, M. T. Letsatsi, O. M. Moloko, and M. S. Batlhalefi, 'Design, Modelling and Experimental Investigation of an Economic Domestic STHW System Using T*Sol® Simulation in Botswana', *MATEC Web of Conferences*, vol. 172, p. 06004, 2018, doi: 10.1051/matecconf/201817206004.

[74] R. Dħiugaite-Tumeniene and G. Streckiene, 'Solar Hot Water Heating System Analysis Using Different Software in Single Family House', in *The 9th International Conference 'Environmental Engineering 2014'*, Vilnius, Lithuania: Vilnius Gediminas Technical University Press "Technika" 2014, 2014. doi: 10.3846/enviro.2014.258.

[75] D. D. Milosavljević, T. S. Kevkić, and S. J. Jovanović, 'Review and validation of photovoltaic solar simulation tools/software based on case study', *Open Physics*, vol. 20, no. 1, pp. 431–451, Jan. 2022, doi: 10.1515/phys-2022-0042.

[76] 'Solar Energy: Renewable Energy and the Environment | Request PDF'. Accessed: Aug. 07, 2024. [Online]. Available: https://www.researchgate.net/publication/329358658_Solar_Energy_Renewable_Energy_and_the_Environment

[77] A. Abdul Malek, M. Hasanuzzaman, N. A. Rahim, and Y. A. Al–Turki, ‘Energy, economic, and environmental analysis of 10-MW biomass gasification based power generation in Malaysia’, *Energy & Environment*, vol. 32, no. 2, pp. 295–337, Mar. 2021, doi: 10.1177/0958305X20930386.

[78] H. H. Osiolo, ‘Impact of cost, returns and investments: Towards renewable energy generation in Sub-Saharan Africa’, *Renewable Energy*, vol. 180, pp. 756–772, Dec. 2021, doi: 10.1016/j.renene.2021.08.082.

[79] J. D. Gil, A. Topa, J. D. Álvarez, J. L. Torres, and M. Pérez, ‘A review from design to control of solar systems for supplying heat in industrial process applications’, *Renewable and Sustainable Energy Reviews*, vol. 163, p. 112461, Jul. 2022, doi: 10.1016/j.rser.2022.112461.

[80] P. Kumar *et al.*, ‘Economics of Implementing Solar Thermal Heating Systems in the Textile Industry’, *Energies*, vol. 15, no. 12, Art. no. 12, Jan. 2022, doi: 10.3390/en15124277.

[81] B. Schmitt, ‘Classification of Industrial Heat Consumers for Integration of Solar Heat’, *Energy Procedia*, vol. 91, pp. 650–660, Jun. 2016, doi: 10.1016/j.egypro.2016.06.225.

[82] T. jia, J. Huang, R. Li, P. He, and Y. Dai, ‘Status and prospect of solar heat for industrial processes in China’, *Renewable and Sustainable Energy Reviews*, vol. 90, pp. 475–489, Jul. 2018, doi: 10.1016/j.rser.2018.03.077.

[83] M. Haagen, ‘Using Solar Energy for Process Heating’, *Pharmaceutical Technology*, vol. 41, no. 4, Apr. 2017, Accessed: Aug. 22, 2024. [Online]. Available: https://www.pharmtech.com/view/using-solar-energy-process-heating

[84] P. P. Aravin, ‘Energy Conservation In Textile Industries & Savings’, Textiles Inside. Accessed: Jul. 19, 2023. [Online]. Available: https://textilesinside.com/energyconservation-in-textile-industries-savings/

[85] K. Farhana, K. Kadirgama, A. S. F. Mahamude, and M. T. Mica, ‘Energy consumption, environmental impact, and implementation of renewable energy resources in global textile industries: an overview towards circularity and sustainability’, *Mater Circ Econ*, vol. 4, no. 1, p. 15, Mar. 2022, doi: 10.1007/s42824-022-00059-1.

[86] S. Madhav, A. Ahamad, P. Singh, and P. K. Mishra, ‘A review of textile industry: Wet processing, environmental impacts, and effluent treatment methods’, *Environmental Quality Management*, vol. 27, no. 3, pp. 31–41, Mar. 2018, doi: 10.1002/tqem.21538.

[87] K. Amutha, ‘12 - Sustainable chemical management and zero discharges’, in *Sustainable Fibres and Textiles*, S. S. Muthu, Ed., in The Textile Institute Book Series. , Woodhead Publishing, 2017, pp. 347–366. doi: 10.1016/B978-0-08-102041-8.00012-3.

[88] M. I. bin A. Kadir, ‘Textile Wet Processing’, Textile Technology. Accessed: Aug. 07, 2024. [Online]. Available: https://textechdip.wordpress.com/contents/wet-processing/

[89] Y. Nawab, T. Vigo, and C.-W. Kan, ‘Textile Wet Processing: Stages, Flowchart and Importance’, Textile Engineering. Accessed: Aug. 08, 2024. [Online]. Available: https://textileengineering.net/textile-wet-processing-stages-flowchart-and-importance/

[90] S. S. Muthu, *Assessing the Environmental Impact of Textiles and the Clothing Supply Chain*. Elsevier, 2014.

[91] W. Weiss and M. Spörk-Dür, ‘Solar Heat Worldwide 2024’, IEA SHC, Jun. 2024. doi: 10.18777/ieashc-shww-2024-0001.

[92] ‘SHIP Plants - SHIP - AEE INTEC Energieatlas’. Accessed: Oct. 27, 2023. [Online]. Available: https://energieatlas.aeeintec.at/index.php/view/map?repository=ship&project=ship_edit

[93] ‘Dryden Combustion’. Accessed: Jun. 09, 2024. [Online]. Available: https://cochran.co.za/boilers_newsteam.html

[94] ‘Steam Tables Pressure vs Temperature’, Valvesonline. Accessed: Jun. 09, 2024. [Online]. Available: https://www.valvesonline.com.au/references/steam-tables/

[95] E. Kerme and Z. Kaneesamkandi, ‘Performance Analysis and Design of Liquid Based Solar Heating System’, *Journal of Thermal Engineering*, vol. 1, no. 5, p. 182, May 2015, doi: 10.18186/jte.02359.

[96] M. Lillane, ‘Analysis of the viability of using solar thermal energy for Maluti Mountain Brewery’, National University of Lesotho, Maseru, Lesotho, 2021. [Online]. Available: https://nul-erc.s3.amazonaws.com/public/documents/dissertations/analysis-of-theviability-of-using-solar-thermal-energy-for-maluti-mountain-brewery-1631173301.pdf

[97] A. Tang *et al.*, ‘Technical, environmental and ranking analysis of using solar heating: A case study in South Africa’, *Sustainable Energy Technologies and Assessments*, vol. 52, p. 102299, Aug. 2022, doi: 10.1016/j.seta.2022.102299.

[98] L. A. Sarazola *et al.*, ‘Financing Clean Energy Transitions in Emerging and Developing Economies’, *International Energy Agency*, p. 237, 2021.